Scholar Commons
USF University of South Florida

University of South Florida
Scholar Commons

Graduate Theses and Dissertations | Graduate School

June 2018

Additively Manufactured On-Package Multipolar Antenna Systems for Harsh Communication Channels

Ramiro A. Ramirez-Hernandez
University of South Florida, rramirezh4@gmail.com

Follow this and additional works at: https://scholarcommons.usf.edu/etd

 Part of the Electromagnetics and Photonics Commons

Scholar Commons Citation
Ramirez-Hernandez, Ramiro A., "Additively Manufactured On-Package Multipolar Antenna Systems for Harsh Communication Channels" (2018). *Graduate Theses and Dissertations.*
https://scholarcommons.usf.edu/etd/7705

This Dissertation is brought to you for free and open access by the Graduate School at Scholar Commons. It has been accepted for inclusion in Graduate Theses and Dissertations by an authorized administrator of Scholar Commons. For more information, please contact scholarcommons@usf.edu.

www.manaraa.com

Additively Manufactured On-Package Multipolar Antenna Systems for Harsh Communication Channels

by

Ramiro A. Ramirez-Hernandez

A dissertation submitted in partial fulfillment
of the requirements for the degree of
Doctor of Philosophy in Electrical Engineering
Department of Electrical Engineering
College of Engineering
University of South Florida

Major Professor: Thomas M. Weller, Ph.D.
Stephen Saddow, Ph.D.
Thomas Ketterl, Ph.D.
Gokhan Mumcu, Ph.D.
Yu Sun, Ph.D.

Date of Approval:
June 5, 2018

Keywords: 3-D printing, picosecond laser machining, MMIC packaging, multipath environments, package integrated antennas

Copyright © 2018, Ramiro A. Ramirez-Hernandez

www.manaraa.com

DEDICATION

To the memory of my mother.

www.manaraa.com

ACKNOWLEDGMENTS

I would like to express my deepest gratitude to Dr. Thomas M. Weller for his continuous guidance, patience and support throughout my graduate career. His immense knowledge and humble character made this an enjoyable experience.

I also thank the committee members for their time, recommendations and suggestions on this work. Dr. Stephen Saddow, Dr. Gokhan Mumcu, Dr. Yu Sun, Dr. Craig Lusk, with special thanks to Dr. Thomas Ketterl for his valuable assistance during my early days in the Ph.D program.

I would like to extend my sincere gratitude to Denise Lugo for her continuous and unconditional help and support throughout the realization of this work.

Many thanks go out to E. Rojas, D. Lan , M. Cordoba, E. Gonzalez, M. Grady, A. Dey, A. Menon T.J Ross, M. Hafez and other WAMI fellow students for their valuable assistance .

I would like to aknowledge the department of Electrical Engineering staff, K. Brandt, J. Hyde, J. Procko and D. Hamilton for their greatly appreciated suggestions and advice.

To the University of South Florida's Electrical Engineering Department and Nanotechnology Research and Education Center for providing excellent facilities and a high quality education.

To Dr J. Frolik and M. Golmohamadi from the University of Vermont for their valuable contributions in part of the material included in this work.

Finally, I would like to give special thanks to DJ and H. Ramirez for their continuous support.

www.manaraa.com

TABLE OF CONTENTS

www.manaraa.com

www.manaraa.com

LIST OF TABLES

www.manaraa.com

LIST OF FIGURES

www.manaraa.com

www.manaraa.com

www.manaraa.com

www.manaraa.com

ABSTRACT

Four main aspects are studied and explored throughout this dissertation: (1) On-Package Multipolar antenna system design for integration with commercial wireless sensor nodes for machine-to-machine communication applications; (2) Development of a novel MMIC packaging process and subsequent antenna integration for chip-to-chip communication applications, (3) Design and characterization of additively manufactured lumped passive elements for integration with MMIC and hybrid circuits, (4) Design and characterization of antennas for on- and off-metal radio frequency identification (RFID) applications.

This work presents the design of different 3-D printed tripolar antenna systems operating at 2.4 GHz. The antennas are designed for integration with commercial wireless nodes with the purpose of mitigating multipath and depolarization channel effects that might be present in many machine-to-machine (M2M) deployments. The antennas are fabricated utilizing an additive manufacturing (AM) approach that combines fused deposition modeling (FDM) of ABS plastic for dielectric parts and micro-dispensing of silver paste Du-Pont CB028 for conductive layers as the majority of the devices presented in this work. Over the air testing demonstrates a 1% channel improvement of up to 14 dB, achieved in a highly-reflective, Rayleigh-like fading environment by implementing selection diversity between three mutually orthogonal monopoles. This improvement leads to better bit error rate (BER) performance (as is also shown). Additionally, RSSI measurements show significant improvement when the prototype antenna system is integrated with commercial wireless sensor hardware. Implications of tripolar antenna integration on M2M systems include reduction in energy use, longer communication link distances, and/or greater link reliability.

www.manaraa.com

In order to incorporate the proposed multipolar selection diversity technique into short range wireless chip-to-chip communications, a novel and versatile 3D printed on-chip integration approach using laser machining is subsequently demonstrated for microwave and mm-wave systems in a process herein referred to as Laser Enhanced or Laser Assisted Direct Print Additive Manufacturing (LE-DPAM). The integration process extends interconnects laterally from a MMIC to a chip carrier. Picosecond laser machining is applied and characterized to enhance the 3D printing quality. Specifically, the width of micro-dispensed printed traces is accurately controlled within micrometer range (e.g. laser cuts ~12 μm wide), additionally, 150 μm probe pads are cut in order to facilitate RF measurement. The S-parameters of a distributed amplifier integrated into the package are simulated and measured from 2 to 30 GHz. It is seen how the overall performance is significantly better than a traditional wirebonded QFN package and previously reported AM MMIC interconnections. The attenuation of the microstrip line including interconnects is only 0.2 dB/mm at 20 GHz and return loss with the package is less than 10 dB throughout the operating frequency band

A 17 GHz package integrated linearly polarized patch antenna, fabricated with a multi-layer and multi-material LE-DPAM process is then introduced for vertical interconnection with a MMIC die. Performance is successfully measured and characterized achieving a return loss greater than 19 dB at the desired design frequency. Good agreement between simulated and measured radiation patterns is also obtained with a peak gain of 4.2 dBi.

Another section of this work utilizes LE-DPAM to fabricate lumped capacitors and inductors for coplanar waveguide (CPW) circuits, especially useful for filtering and matching network implementation. Laser machining is used to achieve ~12 μm slots on printed conductors, producing aspect ratios greater than 2:1, as well as to fabricate vertical interconnects or vias that allow for the fabrication of the multilayer inductors. Inductances in the range of 0.4-3 nH are achieved, with a maximum quality factor of 21, self-resonance frequencies up to 88 GHz, and an inductance per unit of area of 5.3 nH/mm^2.

www.manaraa.com

Interdigital capacitors in the range of 0.05-0.5 pF are fabricated, having a maximum quality factor of 750 and self-resonances up to 120 GHz. All the components are made on the center line of a CPW that is 836 μm wide. The results show that LE-DPAM enables the fabrication of compact passive circuits that can be easily interconnected with MMIC dies, which at the same time, can be manufactured as part of a larger component. This enables the fabrication of structural electronics that are functional into the mm-wave frequency range.

A final aspect of this work goes through antenna designs for specific RFID (radio frequency identification) applications. RFID tag design is generally focused specifically on either off-metal or on-metal configurations. In this work passive 2D and 3D RFID tags are presented which perform similarly in both configurations. The presented tags operate in the ISM RFID UHF bands that cover 864-868 MHz and 902-928 MHz. A matching loop consisting of two parallel stubs to ground is used for impedance matching to a passive integrated circuit, which has -18 dBm sensitivity. A planar 2D tag with a footprint of 13126.5 mm^2 is first introduced, showing a simulated gain of approximately 3 dBi and a measured read range of 10 m (for 31 dBm transmit power from the reader) in both on-metal and off-metal conditions. The tag is miniaturized into a 3D geometry with a footprint of 2524.25 mm^2 (520% reduction) and achieves the same broadside simulated on-metal gain. The antennas are fabricated using a DPAM process, and a meshed ground configuration is explored in order to accomplish a 50% conductive paste reduction without disrupting the performance. The proposed tags are compared with commercially available tags as well as previously published tags in terms of read range and size. The tags in this work present an improvement in terms of read range, gain, and area with respect to previous designs covering the ISM RFID UHF bands. Moreover, the performance of these tags is maintained in on- and off-metal conditions, achieving comparable performance and a reduction in volume of 11482% with respect to the best tag reported.

www.manaraa.com

CHAPTER 1: INTRODUCTION

1.1. Motivation

The Internet of Things (IoT) or Industrial Internet, generally refers to systems of electro-mechanical machines and devices interconnected to one another through embedded wireless sensors and actuators; a network that enables continuous machine-to-machine (M2M) communication is often realized autonomously without the need of any human intervention [1]. The M2M communications market is predicted to grow to a value by 2022 anywhere from US $28B to $200B [2, 3], which is why energy-efficient, small size, reliable and low-cost wireless sensor nodes are of great interest for industrial, commercial and aerospace applications. The devices that comprise the M2M networks will in most cases be expected to undergo alterations in physical temperature, pressure, moisture, etc. and will be deployed in electromagnetically harsh surroundings (e.g., non-line-of-sight (NLOS) and with severe multipath). These are environments that can weaken and depolarize a transmitted signal across all three spatial dimensions [4-6]. In such environments, several copies of the transmitted signal will show up at the receiver, such that each copy corresponds to a distinct multipath component with a distinct delay. The amplitude of these summed signals can experience fast variations over time, space, and frequency due to constructive and destructive combining [7].

To mitigate such fading effects, diversity-combining of independently fading signal paths can be applied which leverages different frequencies and/or antenna elements [7]. For M2M systems that involve multiple devices coordinating the best frequency to use is not a viable diversity approach, for it is possible that an appropriate frequency for one particular device to device link may exhibit deep fades in another. Employing multiple antennas (i.e., spatial diversity) requires elements to be located sufficiently

www.manaraa.com

far from each other (>λ/2) to guarantee uncorrelated fading effects [8]. This constraint makes spatial diversity an undesirable approach for applications (e.g. low-cost IoT systems) where the size of the antenna system is a crucial design parameter.

Along with compactness, energy consumption is an important constraint in the design of wireless sensor nodes. As noted, multi-element antenna diversity can improve link reliability thus allowing for the reduction of the transmitted RF power, but at the cost of a bulkier node design. To address this problem, in [9], a cooperative spatial diversity technique was incorporated in sensor nodes to improve link reliability. The approach utilizes several compact transmitter nodes to send a message to a single destination. The trade off in this approach is added complexity in node computation and network communications. An alternative method described in [10] employs frequency diversity to improve link quality, however it required two radios separated by 65 cm for each node and therefore is not suitable for compact installations. In the work presented herein, we leverage polarization diversity as a means to provide a compact and relatively uncomplicated approach for improving communication link quality in M2M systems.

Cross-polarized antenna systems, through their perpendicular/ orthogonal elements, provide signal paths that are weakly correlated, while keeping antenna elements colocated. Recently, a dual-polarized 2.4 GHz patch antenna has been proposed for integration into a wireless node in order to mitigate fading body shadowing effect in wearable communication systems. Implementing selection diversity has improved the 1% outage probability by 9.5 dB [11, 12].

In the presence of reflectors and retarders, an environment can lead to depolarization in all three spatial dimensions [13]. In recognition of 3D depolarization, there have been some efforts in designing antennas to leverage the extra degree of freedom [14]. For example, use of colocated antenna elements with three (one loop and two coplanar dipoles) and four elements (one loop and three mutually orthogonal dipoles) led to channel capacities greater than a single element antenna [15]. Tripolarized

www.manaraa.com

antennas have also been shown to achieve channel capacities comparable to three spatially separated single polarized antennas in a MIMO system [16]. However, to the best of our knowledge, full characterization and integration of a tripolar antenna into a sensor node has not been reported.

A comparable cluttered environment can be expected to similarly affect communication channels between integrated circuits at microwave and mm-wave frequencies, eventually causing unwanted communication link disruptions. Although in the previous decades the semiconductor industry has been driven largely by wired chip-to-chip communications, wireless buses have the potential to make a significant impact on the design of a new generation of thin and ultra-small devices. A characteristic that can enable IC packages to be minimized by removing for example I/O pads; increasing design flexibility and allowing chips to be located in the most convenient positions, either to improve aesthetics, enable better engineering or reduce the amount of overall waste

Additive Manufacturing (AM) is the proposed technology for the fabrication of the majority of the devices presented in this work, including the package integrated antenna systems. The implementation of this fabrication method for microwave and mm-wave applications has increased as enhancements in material properties and process control are made. A wide variety of options are available that involve jetting, spraying or dispensing materials into digitally-controlled patterns, followed by some post-processing for curing, surface treatment and/or metallization, e.g. through plating. These options include techniques such as binder-jetting, Polyjet, and aerosol jet. Other AM techniques with proven merits for high-frequency components include laser-based approaches such as selective laser melting and selective laser sintering[17], and Stereolithography [18]. Structures fabricated with these methods are typically all metal, all dielectric, or dielectric with a blanket metal deposition that is not patterned. In some cases, metal traces are 3D printed on substrates that are not produced with AM.

For those applications where it is desirable to use a fully-AM process for printed electronics that require both insulating and conducting layers, printing techniques that seamlessly integrate multi-

www.manaraa.com

material deposition capabilities are advantageous. One important advantage is the potential ability to deposit diverse materials without removing the structure from the printing tool. This simplifies layer-to-layer registration, and improves process control when optimizing to eliminate adhesion, delamination, or other problems. The multi-material deposition capability also provides greater freedom in building true 3D structures, rather than stacks of 2D structures which are more practical if multiple tools are in use. Both advantages naturally rely on being able to dry or cure the materials in situ, e.g. with heat, a laser or a UV source.

The inkjet technique is one multi-material AM approach that has been used to fabricate circuits such as substrate-supported antennas and microwave packaging [19]. Another multi-material method is direct print additive manufacturing (DPAM), which combines fused deposition modeling (FDM) of thermoplastics with micro-dispensing of pastes on a common platform. Whereas thin, 0.5 – 5 micron-thick layers are characteristic of the inkjet technique, the typical layer thickness with DPAM is 25-50 microns. This difference makes DPAM more useful for building up larger 3D structures, while inkjet holds the advantage in minimum feature size. Minimum feature size with inkjet and DPAM is approximately 1 and 25 microns, respectively. Pulsed picosecond laser post-processing is examined as a means to enhance the capabilities of DPAM. One immediate advantage is the ability to achieve smaller feature sizes, and thus extend the upper-frequency range for DPAM components. The ability to precisely control material removal can also be leveraged for the integration of vertical interconnects and packaging of monolithic integrated circuits (MMICs) into 3D printed structures, with low parasitic effects.

1.2. Contributions

The present work is focused on innovations related to additively manufactured (AM) package integrated multipolar antenna systems, AM MMIC packaging and interconnection, MMIC package integrated antennas , AM lumped passive elements and RFID antenna design. Systems fabricated with

www.manaraa.com

fused deposition modeling, micro-dispensing, and laser machining. The specific contributions are summarized below:

a) Development and characterization of additively manufactured microwave on-package multipolar antenna systems for harsh communication channels , including:
    - Fabrication and demonstration of conformally printed adaptive on-package tripolar antenna systems operating at 2.4 GHz
    - Integration of tripolar antenna systems onto commercially available wireless sensor nodes and performance characterization in anechoic and high multipath environments, successfully mitigating multipath and depolarization effects.

b) Development of a novel laser assisted additively manufactured (LE-DPAM) multi-material and multi-layer process for MMIC packaging, including :
    - Fabrication and demonstration of a packaged MMIC low noise amplifier and characterization up to 30GHz.
    - Demonstration and characterization of a low loss lateral interconnection from an MMIC die to an external hybrid board with a measured attenuation of 0.2 dB/mm at 20 GHz.
    - Demonstration and characterization of a cascaded lateral interconnection between MMIC dies up to 10 GHz.

c) Development of a multi-material and multi-layer LE-DPAM process for planar antenna integration with MMIC packaged devices, including:
    - Fabrication and demonstration of a vertically interconnected package integrated 17 GHz patch antenna.

d) Development and characterization of high performance LE-DPAM mm-Wave lumped passive elements, including:

www.manaraa.com

- Development, characterization and modeling of coplanar waveguide (CPW) of high-Q interdigital capacitors.
- Development of a multi-material and multilayer LE-DPAM process for fabrication of CPW spiral inductors.
- Characterization and modeling of CPW spiral inductors.

e) Development and characterization of antennas for UHF RFID systems , including:

- Fabrication and demonstration of RFID tags with enhanced read range and reduced footprint, operating at 915 MHz for on- and off-metal applications.

1.3. Dissertation Outline

This dissertation is presented in seven chapters organized as follows

a) Chapter 1 focuses on the introduction, motivation and contributions of the work

b) Chapter 2 includes a literature review of the main conditions and effects foreseen in most M2M and chip-to-chip communication channels; an overview of the additive manufacturing technologies implemented for microwave and mm-wave applications as well as the current state-of-the-art of additively manufactured MMIC packaging, package integrated antennas MMIC interconnection and lumped passive elements .

c) Chapter 3 covers the design , fabrication and characterization of three different multipolar antenna systems operating at 2.4GHz and intended for integration with commercial wireless sensor nodes; performance in anechoic as well as in highly reflective environments is presented.

d) Chapter 4 describes the fabrication process of a novel additively manufactured and laser assisted MMIC packaging process; integration with a LNA die is presented and its performance is characterized up to 30GHz. Additional package functionality is achieved by

www.manaraa.com

integrating a vertically interconnected 17 GHz linearly polarized planar patch antenna intended for chip-to-chip communications.

e) Chapter 5 presents the design, fabrication and characterization of mm-Wave lumped passive elements, specifically CPW interdigital capacitors and spiral inductors are studied, measured and modeled up to 30GHz.

f) Chapter 6 presents different antenna designs intended for UHF RFID on- and off-metal applications . Performance including radiation patterns and read range is characterized at 915MHz.

g) Chapter 7 includes a summary of the presented work and recommendations for future research.

www.manaraa.com

CHAPTER 2: BACKGROUND AND LITERATURE REVIEW

In this chapter, several concepts and previously published related work are discussed; topics that include a review on some of the most common multipath conditions foreseen in M2M wireless communications, a summary on additive manufacturing technologies as well as some of the current AM state-of-the-art microwave and mm-Wave devices specifically lumped passive elements, MMIC packaging and packaged integrated antennas.

2.1. M2M Communications in High Multi Path Environments

The anticipated growth in machine-to-machine (M2M) communications, also referred to as the Industrial Internet, has generated strong interest in new technologies for energy-efficient, reliable connectivity of low-cost wireless devices. The devices that comprise the M2M networks will often be deeply embedded, autonomous nodes with limited processing power. In many situations, the devices will also be space-constrained to accommodate retrofitting of existing machines.

One example of a M2M network is one using wireless strain/vibration/temperature sensors to monitor robotic tools on a manufacturing floor or to perform general machine diagnostics [20-22]. This example illustrates another significant factor that M2M networks may need to contend with, namely, that the installation environment can be particularly harsh for wireless communications. One can envision that there could be no line of sight (N-LOS) between two networked devices and that surfaces (e.g., the robotic tools themselves) would create severe multipath conditions that can seamlessly attenuate and depolarize propagated waves across all three spatial dimensions.[5, 6, 23], resulting in non-desired communication link failures.

www.manaraa.com

Such multipath conditions can often vary from a benign fading link, where a strong signal path is typically present constituted by a Line of Sight (LoS) between the transmitter and receiver antenna, in addition to random and weaker multipath components (i.e. Rician fading channel)[24] ; to more statistically severe channels with a large number of multipath components and no Line-of-Sight between antennas, (i.e. Rayleigh fading and Hyper-Raylegh fading links) [6, 23, 25]. Fig 2-1 shows transmission coefficient examples and channel statistics of these different fading scenarios expected in M2M and chip-to-chip communication environments.[23, 26]

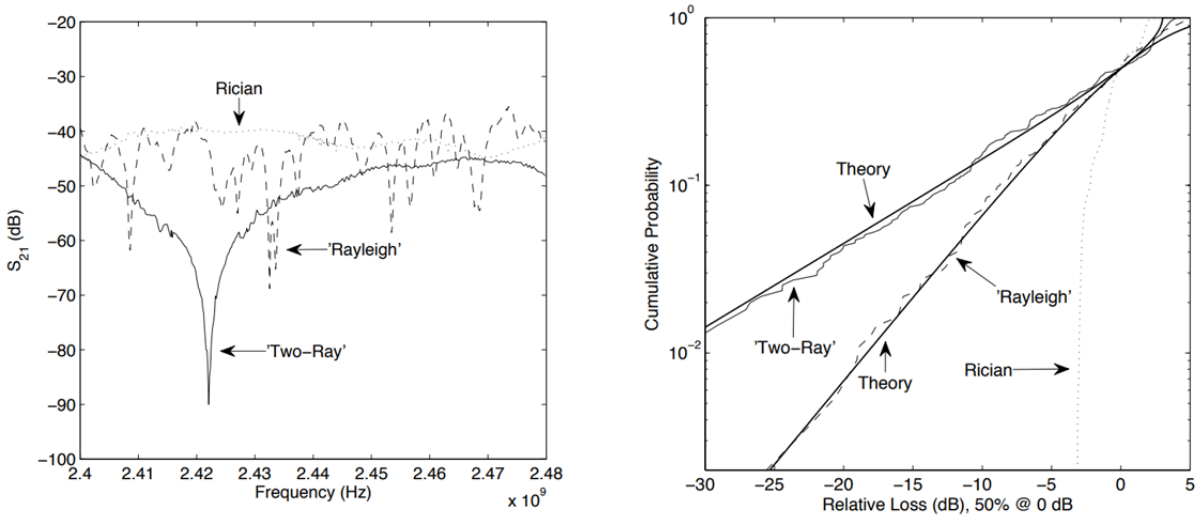

Figure 2-1: S_{21} response of different fading scenarios (left), CDF of fade-depths relative to median path loss value (right). © 2007 IEEE [25] © 2015 IEEE.[26]

Additionally it has been demonstrated how highly reflective environments are inclined to introduce depolarization effects in propagated waves across three spatial dimensions [5, 6, 26, 27]; in order to illustrate these effects Fig.2-2 shows the transmission coefficient against frequency for a Rician fading and a more severe Rayleigh fading channels for co-polarized and cross-polarized links; it is seen how the former maintains a cross polarization discrimination greater than 10 dB across the measured frequency range , while the latter shows no clear difference between co and cross polarized links [5, 26].

www.manaraa.com

A straightforward means of adaptation, and one that can be implemented by low-complexity in M2M wireless chipsets, is that of diversity techniques [24]. Time, frequency and spatial diversity are some of the common methods usually implemented to mitigate fading effects in wireless communications; but might not be effective for example on statically placed wireless sensor nodes, since the channel may be operating on a narrow band of frequencies and/or with a channel that might vary slowly over time if varying at all.

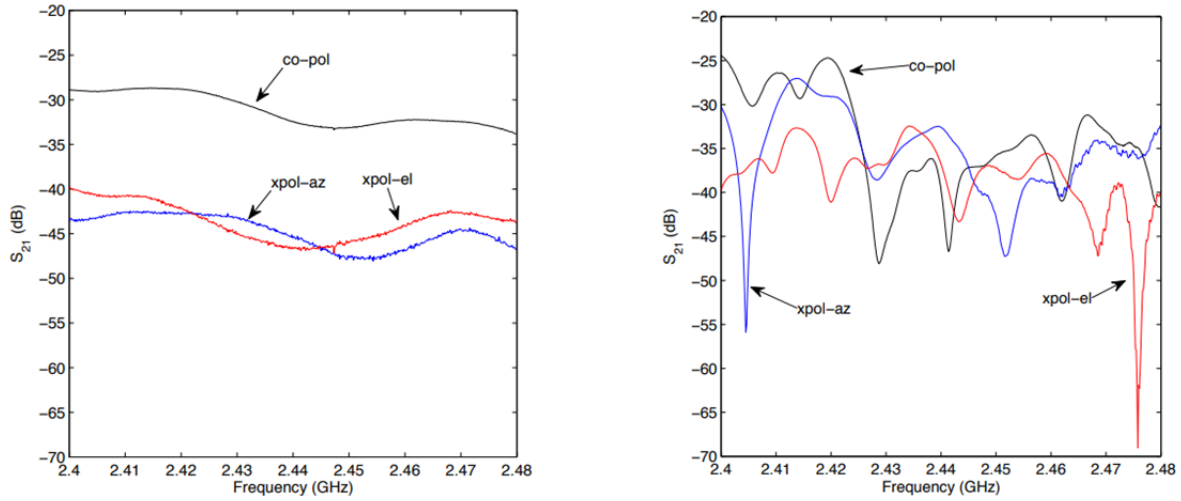

Figure 2-2: S_{21} response for a Rician channel (left), S_{21} response for a Rayleigh channel. © 2016 IEEE. [5]

In this work polarization diversity through package integrated tripolar antenna designs is proposed as a technique to "flatten" the channel and improve the overall transmission loss and channel statistics between wireless sensors and integrated circuits deployed in Machine-to-Machine or chip-to-chip communication scenarios. Some efforts [28, 29] have been made in recent years on implementing pattern diversity techniques to improve wireless communications; in [28] three non-orthogonal directional antennas are integrated in a compact 2-D system for WLAN operation, but a tripolar antenna, typically one that possesses three mutually-orthogonal polarizations [30, 31], is required to mitigate the effects presented in [5, 6, 26]. In [4] the characterization of a geometrically constrained tripolar array of

www.manaraa.com

commercial monopoles is studied. Some alternative designs have been also explored to, for example, achieve channel capacities that are comparable to single polarized 3×3 MIMO systems in rich-multipath environments [16].

2.2. Additive Manufacturing of Microwave and mm-Wave Devices

The number of additive manufacturing (AM) methods that are useful for the fabrication of microwave components has grown steadily in recent years. The size and performance of the AM-produced components are now comparable to or better than those of multi-layer, printed circuit board designs thanks to the development of advanced materials and processing techniques. Among the most important advantages of AM are the minimal infrastructure that is required, often involving only a single machine, and the use of processes that do not require toxic materials such as chemical etchants and photoresist developer. Another key advantage of AM is that it enables dense packaging of IC dies and passives up to mm-wave frequencies. AM can also be used to manufacture conformal circuits and those that are embedded into structures. Components with high inductance and capacitance per unit area, low losses, and high self-resonance frequency (SRF) are key advantages that AM provides for realizing miniaturized RF front ends.

AM technologies are typically categorized by the material deposition method, each having an associated minimum feature size and layer thickness. Aerosol jet printing (AJP) has been shown to produce passive mm-wave 3D interconnects with 0.53 dB/mm losses at 40 GHz, as shown in Fig. 2-3 [32].

By using AJP, the achievable minimum layer thickness, gap size, and line widths are 0.7 μm, 10 μm, and 10 μm, respectively [32]. Inkjet printing is another multi-material technology capable of manufacturing passive components, with a typical drop spacing of 20 μm and layer thickness of 5 μm [33, 34].

www.manaraa.com

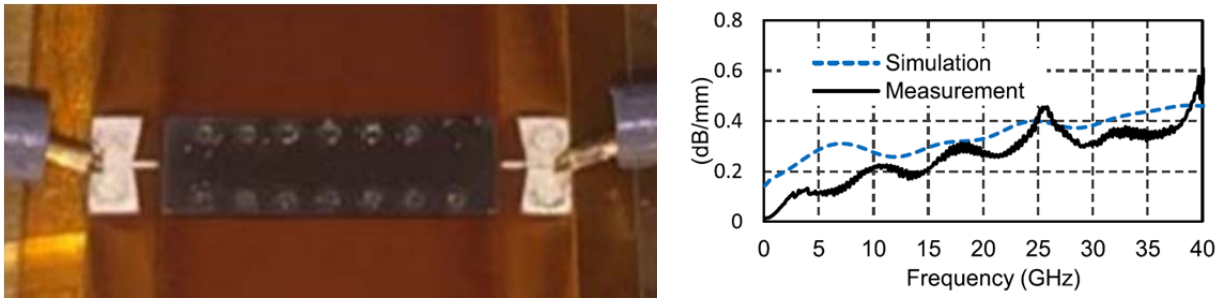

Figure 2-3: Transmission line manufactured with AJP. Setup (left), attenuation (right). [32] © 2016 IEEE.

Fig 2-4 shows inkjet printed MIM capacitors with capacitance (C), self-resonance frequency (SRF), and quality factors (Q) of 6 pF, 2.5 GHz, and 18, respectively. [33]. Fig 2-5 shows inkjet printed spiral inductors with inductance (L), self-resonance frequency (SRF), and quality factors (Q) of 7 nH, 4.25 GHz, and 11, respectively. [33]. Table 2-1 and Table 2-2 show a state-of-the-art comparison of measured performance for lumped capacitors and inductors fabricated with different technologies.

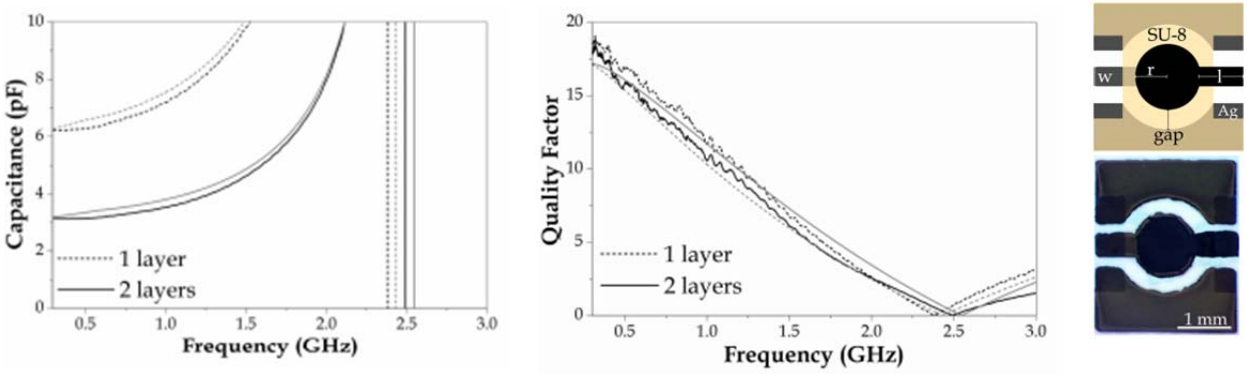

Figure 2-4: Measured and simulated capacitance (left), Q-factor (center), and MIM capacitors (right). [33] © 2017 IEEE.

Table 2-1: Comparison of state-of-the-art AM lumped capacitors

Work	Geometry	Process	Q_{max}	*C* (pF)	SRF. (GHz)
Vanukuru [35]	Interd-mom	GaAs	400	0.02	>120
Mariotti-1 et al. [33]	Circular	Inkjet	15	6	2.5
Mariotti-2 et al. [33]	Square	Copper	35	5	1
Jung et al. [36]	MIM	GaAs	1000	1.05	11.5
McKerricher [34]	MIM	Inkjet	12.9	16.6	1.3

www.manaraa.com

A third important technology is direct print additive manufacturing (DPAM), which combines fused deposition modeling (FDM) and micro dispensing to print dielectrics and deposit layers of conductive ink or paste. The typical conductor layer thickness and minimum feature sizes that can be achieved with this technology are 30 μm and 100 μm, respectively [37, 38].

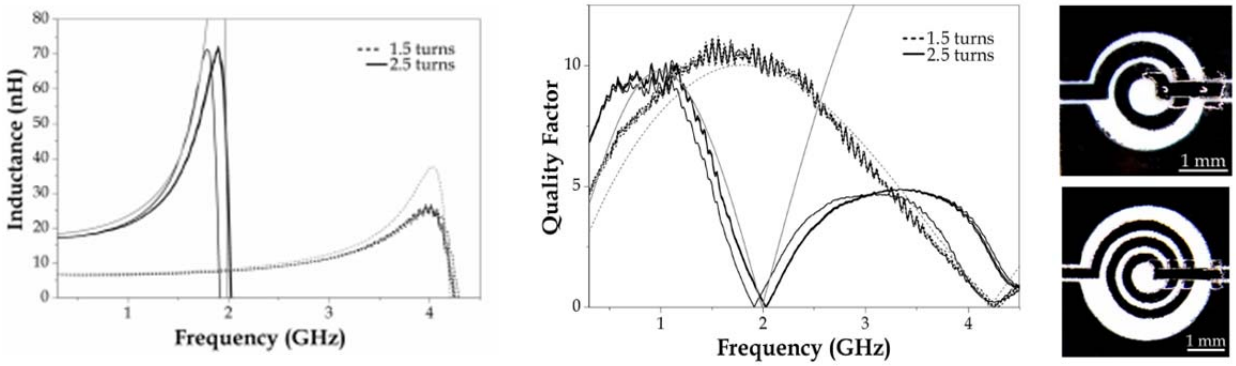

Figure 2-5: Measured and simulated inductance (left), Q-factor (center), and spiral inductors (right). [33] © 2017 IEEE.

Table 2-2: Comparison of state-of-the-art AM lumped inductors

Work	Process	Inductance (nH)	SRF (GHz)	Q_{max}	Inductance per unit Area nH/mm^2
[33]	Inkjet	7	4.25	11	0.78
[39]	Liq. Metal	92	0.71	24	0.9
[34]	Inkjet	75/9.7	0.2/0.8	3/4	1.8/0.8
[40]	LTCC	7.15	2.33	33.5	1.1
[41]	GaAs	0.7/2.8	9/24	16 /22	20/31

Fig 2-6 shows a mesh ground CPW line fabricated with DPAM including mesh sizes down to 270 μm [38]. Additionally, it has been shown that DPAM can be used to fabricate multilayer RF front ends at 2.45 GHz [42, 43].

However, along with minimum feature size limits that are characteristic of most standard AM techniques, fundamental challenges related to the electrical properties of AM materials still exist (e.g., electrical conductivity, permittivity, and dielectric losses). These are challenges that need to be over-come

www.manaraa.com

in order to enhance the performance AM components and systems intended to operate in the mm-wave range.

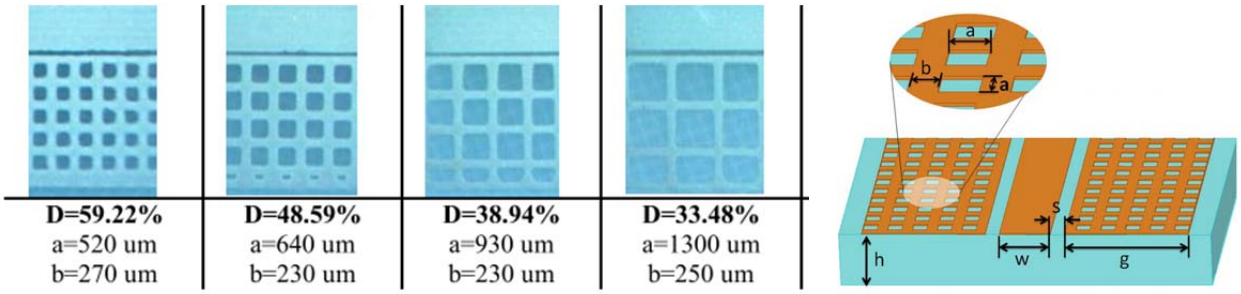

Figure 2-6: DPAM mesh ground CPW lines (left), geometry (right). [38] © 2016 IEEE.

Pulsed laser machining techniques can be combined with the DPAM process (laser enhanced (LE)-DPAM), to mitigate the effects of edge roughness, tapered line edges and limited minimum feature size that are associated with micro-dispensing [44, 45]. The laser processing of the conductive ink solidifies the metal flakes on edges of a cutting path, creating a high-conductivity region that significantly reduces the ohmic losses for coplanar waveguide interconnects [45], as shown in Fig 2-7. Among other demonstrations, LE-DPAM has been used to manufacture and mm-wave multilayer interconnects [46].

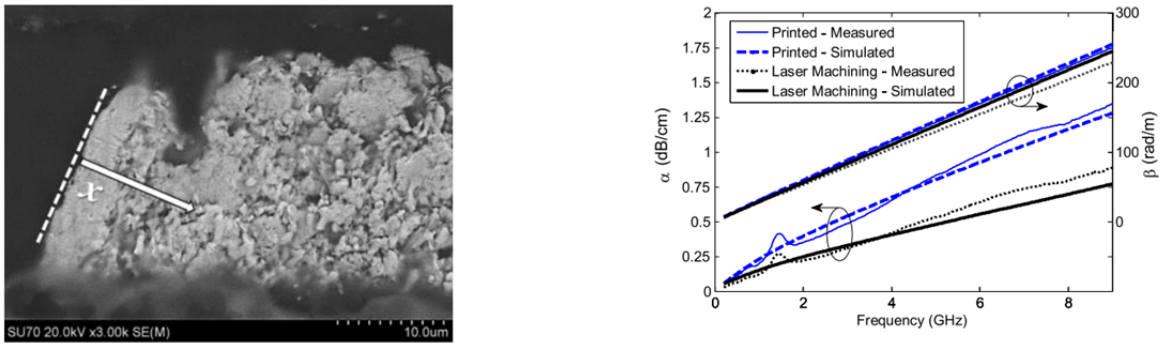

Figure 2-7: Laser machined slot with ink solidification (left), propagation constant difference between lasered and non-lasered CPW lines (right). [45] © 2017 IEEE.

www.manaraa.com

2.3. Additive Manufactured MMIC Packaging

As mentioned in the previous sections the performance of additively manufactured (AM) components continues to improve as the technology evolves; the systematic advances on the mechanical and electrical performance of 3D-printable materials, as well as the development of new fabrication techniques, are slowly taking AM from the prototyping stage to mass production. Among the most attractive promises of AM is the ability to enable complete 3D de-sign freedom in order to fabricate conformal packaged RF electronics, obtaining an expedited turnaround, minimum waste and reduced infrastructure, a notable.

MMIC packaging solutions are still of great interest especially as more applications are pushed into the mm-wave frequency range and because of the increasing use of semiconductor foundry services by fab-less design companies which often involves unpackaged chips. Although several types of non-AM packages have been developed for MMIC integration such as the wire-bonded 40GHz SMT package [47] shown in Fig. 2-8, ceramic-based packages [48], Quilt packages [49], 3D-MMIC Wafer Level Chip Size packages (WLCSP) [50], low cost 20GHz QFN [51] , and Flip-Chip packages [52, 53], popular usage is hindered by their uniqueness, operational frequency range, cost or fabrication complexity.

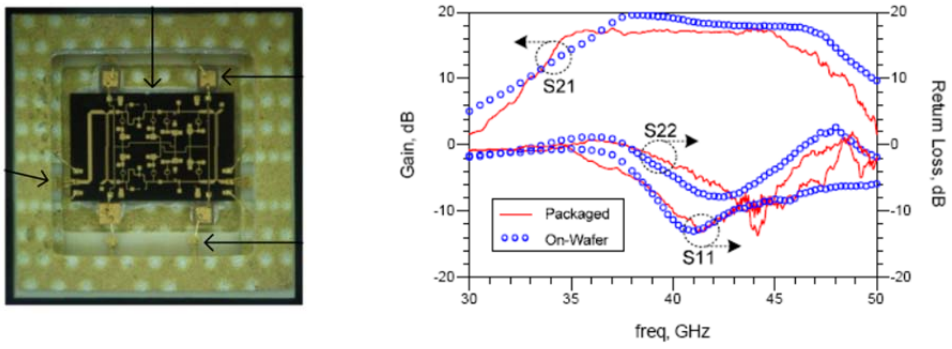

Figure 2-8: SMT MMIC package (left), response of a 40 GHz packaged LNA (right). [47] © 2013 IEEE.

www.manaraa.com

Some research efforts have been made in the recent years on the design of partially or fully additive manufactured MMIC packages and on-package interconnections systems [54-57], as shown in Fig 2-9 where a MMIC LNA is placed over a 3D printed substrate and wire-bonded to external gold plated copper foil microstrip lines, where a measured back-to-back (8.8 mm long structure) insertion loss of ~ 4dB at 15 GHz is achieved. Table 2-3 includes a comparison of measured performance of some previously published additively manufactured Hybrid board to MMIC- interconnections.

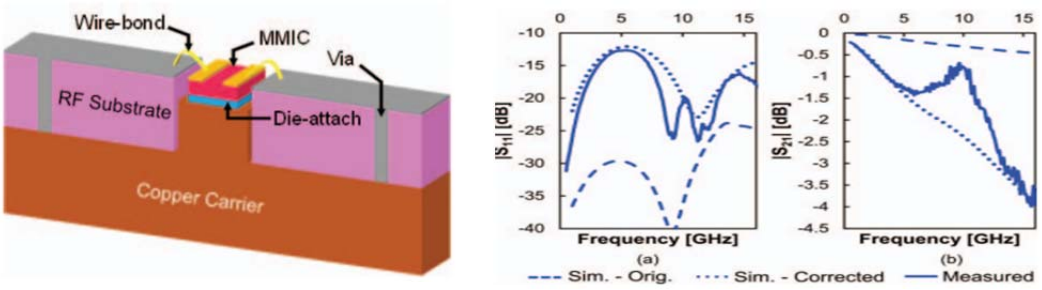

Figure 2-9: Package cross section (left), measured and simulated performance (right). [57] © 2017 IEEE

Table 2-3: Comparison of measured performance. [58] © 2017 IEEE

Reference	Substrate	IC Pad width (um)	Attenuation (dB/mm)	
			5GHz	20GHz
Tehrani [55]	Glass	200	0.25	1.45
Tehrani [56]	SU-8	230	0.40	0.60
Mehta[54]	Kapton	90	0.5	1.5
Wirebonded QFN_Package	ABS	100	0.32	NA

Additionally, improvements in chip-to-chip communication channels might require antenna integration onto the IC packaging for development of multipolar selection diversity, some of the reported package integrated antenna solutions include designs with complex foundry or post processing IC integration methods [59, 60]; or lateral interconnections [61-63] that increase the overall package footprint, as shown in Fig. 2-10.

www.manaraa.com

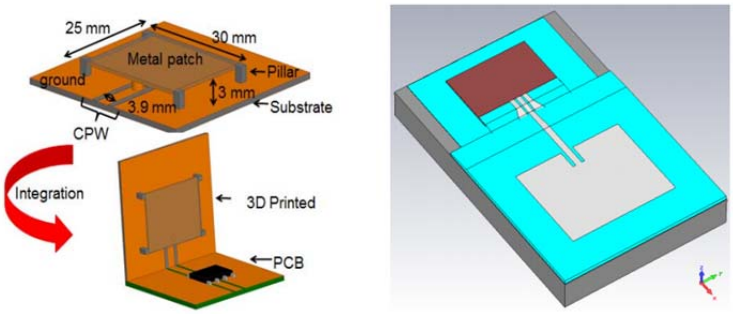

Figure 2-10: Air-lifted patch antenna and PCB integration approach (left).[63] © 2017 IEEE. Simulated model of inkjet printed System-On-Package patch antenna (right) [61] © 2016 IEEE.

www.manaraa.com

CHAPTER 3: 2.4 GHZ ON-PACKAGE ADDITIVELY MANUFACTURED TRIPOLAR ANTENNA SYSTEMS FOR HARSH COMMUNICATION CHANNELS

3.1. Introduction

This chapter presents the design of different multipolar antenna systems intended for communication channels that experience significant multipath and depolarization. A tripolar antenna is generally described as one that possesses three, typically mutually-orthogonal, polarizations [30, 31], and may be equipped with electronics to enable switching between and/or combining of polarization states. The antenna systems presented herein are integrated into the packaging of a commercial wireless sensor nodes using an additive manufacturing approach that combines fused deposition modeling (FDM) of the plastic case and micro-dispensing of conductive pastes to realize the antenna elements. The microwave performance of these antenna systems is presented using both traditional antenna characterization measures (S11, radiation patterns) and through over-the-air (OTA) testing in a harsh communications environments. The proposed tripolar antenna systems achieve a return loss greater than 15 dB at the desired frequency and, 1% channel improvement of up to 14 dB using selection diversity of system's three mutually orthogonal elements. This improvement is shown herein to correspond directly to improved bit error rate (BER) or could allow nodes to communicate either at lower transmit power (saving energy) or over greater distances.

Partial content of this chapter has been published in [66, 68], and it is included in this dissertation with permission from the IEEE. A copy of the permission is included in the Appendix A.

www.manaraa.com

3.2. Multi-piece Additively Manufactured Tripolar Antenna System

3.2.1. Antenna Characteristics

As shown in Figure 3-1, the design used in this section includes pairs of X-,Y- and Z-oriented monopoles on opposing sides of a 3D package, which are connected to microwave switches to enable selection of individual monopole pairs. The details of the 2.4 GHz antenna design are provided in Table I. An inverted-F antenna [64] is selected for the X and Y polarizations (Figure 3-1), using a parallel stub to ground for inductive loading and impedance matching. Each pair of X and Y elements is oriented in opposite directions, and separated by ~$\lambda/2$, creating a two-element broadside array. The Z-oriented polarization on the other hand, consists of two meandered $\lambda/4$ monopoles. All elements are fed through a Wilkinson power combiner and electronic switching with 180° phase difference as shown in Figure 3-2 (b).The 180° phase difference is achieved by meandering the feedline connecting to one element in each pair. The antennas and feed network are printed on 1.5 and 0.5 mm thick acrylonitrile butadiene styrene (ABS) substrates, respectively, with εr of 2.6 and tanδ of 0.0058 at 1 GHz. Figure 3-2 (a) shows the fabricated prototype where the Wilkinson combiner, switches and uniform/meandered feedlines are visible

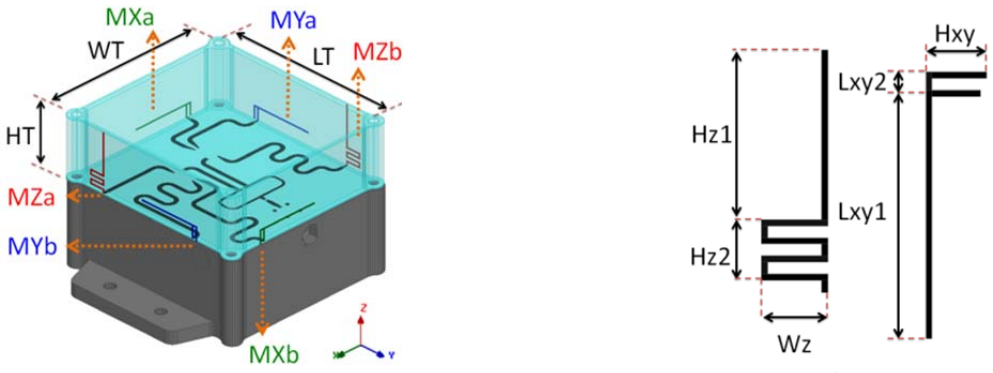

(a) (b)

Figure 3-1: Tripolar system design. The 3 monopole pairs are labeled as MXa/MXb, MYa/MYb (a), and MZa/MZb. antenna geometries (b).

www.manaraa.com

Table 3-1: Dimensions of the antenna designs (Multi-piece system).

Variable	Value(mm)	Variable	Value (mm)
HT	21.01	WT	64.94
HZ1	14.00	HZ2	05.50
LXY1	20.50	LXY2	05.00

The package with integrated antennas was fabricated using an nScrypt 3Dn tabletop printer. This tool includes an FDM head for depositing the ABS, with a minimum layer thickness of ~75 μm and typical surface roughness of 5-7 microns. The printer also includes a micro-dispensing head on the same gantry that is used to deposit the Du-Pont CB028 silver paste. The typical paste thickness is 25 μm and the conductivity is ~2 MS/m. The ABS plastic is deposited on a heated bed (90 °C) and the silver paste is dried at ~90 °C. In this preliminary design, pieces of the package were printed separately and post-assembled into the 3D form factor (64 x 60 x 21 mm^3). Future designs will use a curved upper surface and leverage the conformal capability of the printer to enable single-piece construction.

Figure 3-2: Fabricated antenna system on top of a commercial package (left), switching diagram (right).

Figure 3-3 (a,b) shows the S11 data for the three polarizations, with a return loss at 2.4 GHz that is greater than 17 dB in all three cases. Figure 3-3 (c,d) shows the co/cross-polarized radiation patterns inside an anechoic chamber at 2.4 GHz. The data show good agreement between co-pol measurements

www.manaraa.com

and simulations, and a measured broadside 10 dB difference between the cross- and co-polarized patterns.

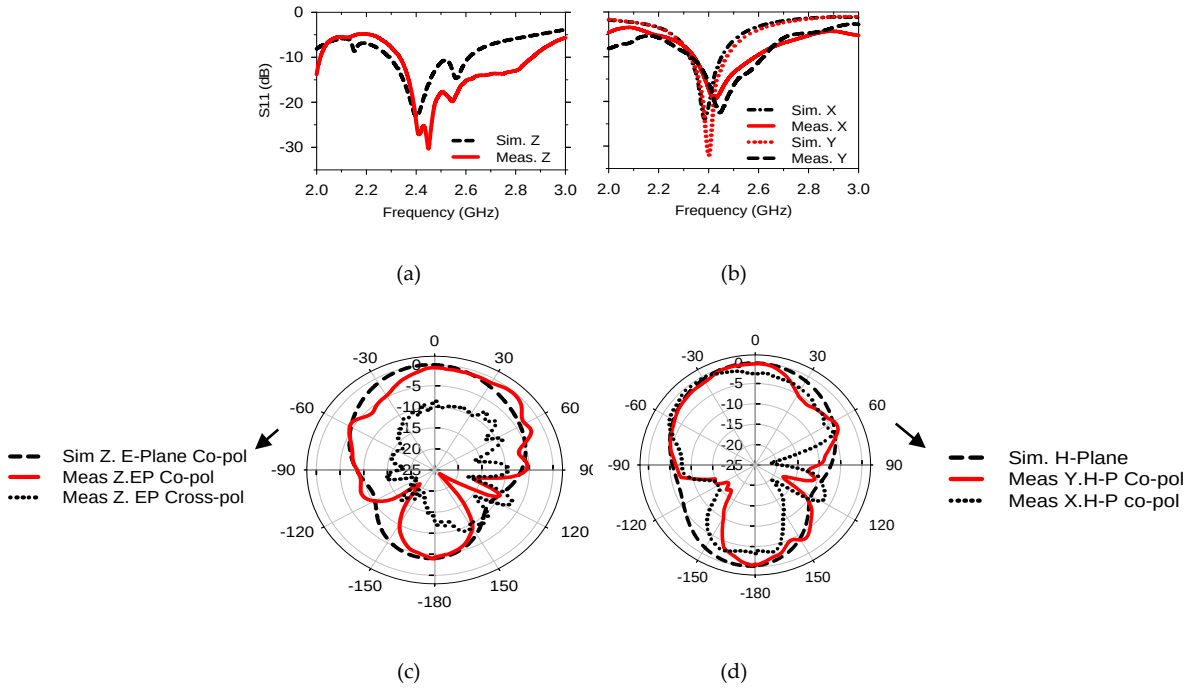

Figure 3-3: Simulated and measured S_{11} for the Z (a) and X-Y (b) oriented monopoles. Simulated and measured normalized radiation patterns for the Z (c) and X-Y (d) oriented monopoles.

3.2.2. Antenna Performance in Harsh Environments

To further demonstrate the performance of the tripolar design, channel loss was measured between each of its three mutually orthogonal elements and a vertically polarized (i.e., Z-direction) transmit antenna within a highly-reflective environment. The S21 data (Figure 3-4) illustrate the significant frequency-selectivity seen in all three paths due to the multipath caused by the environment. Note that these data correspond to a particular antenna placement; any position change could create significantly different S21 results. We note that the median S21 value, -26.9 dB, of the co-polarized link is not dissimilar from that of the two cross-polarized links: -27.3 dB and -25.8 dB, for XZ and YZ, respectively. This low cross polarization discrimination indicates the significant depolarization across all

www.manaraa.com

three spatial dimensions caused by the environment and motivates the use of an antenna that can adapt to these conditions.

A straightforward means of adaptation, and one that can be implemented by low-complexity M2M wireless chipsets, is that of selection diversity. The right panel of Figure 3-4, illustrates how this technique can "flatten" the channel and improve the overall loss to a median value of -22.6 dB, a 4.3 dB improvement over the co-pol result. A further benefit of implementing diversity methods is in improving the overall channel statistics. Figure 3-5 shows the channel cumulative distribution function for each of three links and also that for when M = 3 selection diversity is employed. The constituent links all exhibit Rayleigh-like statistics whereas leveraging the antenna's adaptability results in a more benign, K ◎ 5 dB, Rician channel. Whereas there is a 1% chance of a 15 dB or greater signal drop (relative to the median S_{21}) when using any of one of the antenna's elements, this impairment is reduced to ~3 dB using selection diversity.

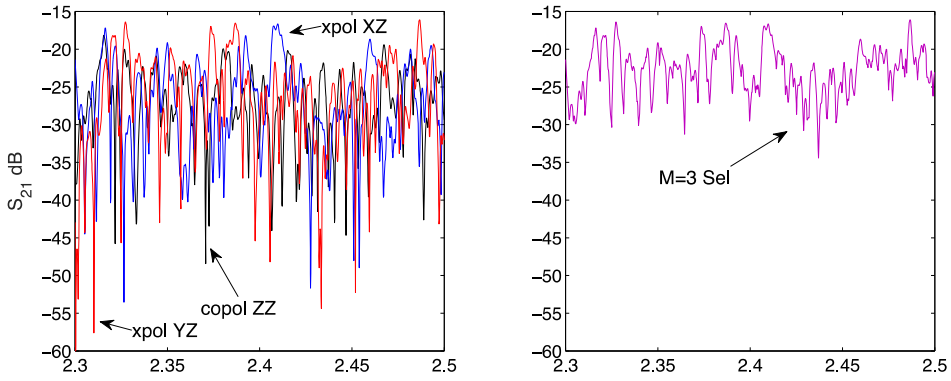

Figure 3-4: S_{21} data for the co-polarized and two cross-polarized links (left), and ability of tripolar design to "flatten" the channel using M = 3 selection diversity (right).

The mitigated system is thus one where potentially the devices could transmit at lower power to save energy without compromising link reliability. Note that these S_{21} data correspond to the particular location the tripolar antenna was placed in the environment. Slight changes in location (~λ/10) can result

www.manaraa.com

in significant changes in S21 and resulting channel statistics [65], thus further emphasizing the need for an antenna system that can adapt to device placement or dynamic environments.

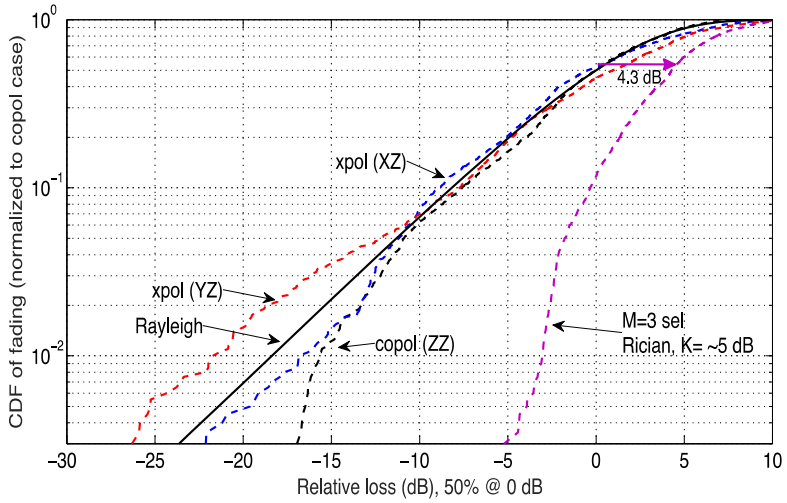

Figure 3-5: Channel statistics for each element of the received array (normalized to co-pol) and benefits of selection diversity. Median improvement seen to be 4.3 dB in addition to link significant reliability gains.

3.3. Single-piece Additively Manufactured Tripolar Antenna Systems

The multipolar antenna systems presented herein were custom designed to fit and replace covers of two commercial wireless node packages [66]; packages with different dimensions and geometries were especially selected to show the versatility of the additive manufacturing technology. These nodes are generally produced on a low to medium volume scale, making the FDM fabrication approach a valid low cost and robust alternative. Figure 3-6 (left) and Fig. 3-7 show the dimensions, geometry and angular arrangement of the first proposed, 'square' tripolar system placed on top of a 2.4 GHz sensor node, with total height of 21 mm, length of 65 mm, and width of 60 mm.. Similarly, Fig. 3-8, shows the dimensions of a second 2.4 GHz, 'circular' tripolar antenna, designed to be placed on top of a cylindrical node; with total height of 11 mm, bottom diameter of 33 mm and top diameter of 40 mm.

The antenna designs are based off three mutually orthogonal $\lambda/4$ monopoles operating at 2.4 GHz; each radiating element is directly printed over 45 ° sloped substrate walls, a value that represents

www.manaraa.com

the maximum printing angle supported by most additive manufacturing systems, including the one used for this work [67].

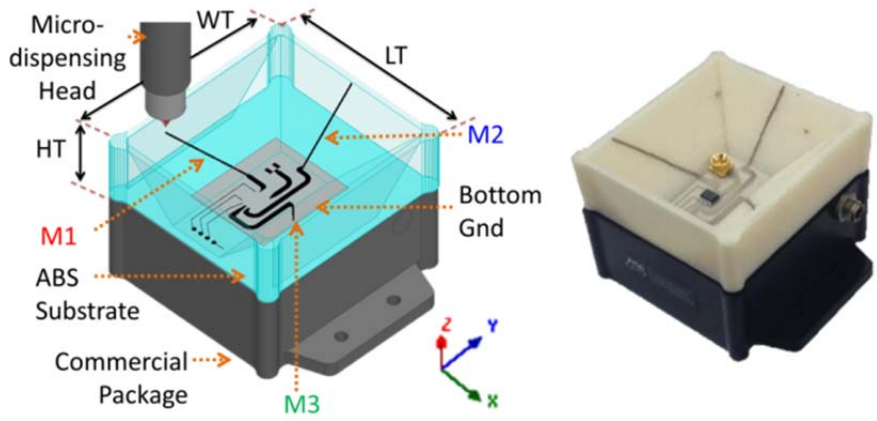

Figure 3-6: Square antenna design (left), and fabricated prototype on top of a commercial wireless node (right).

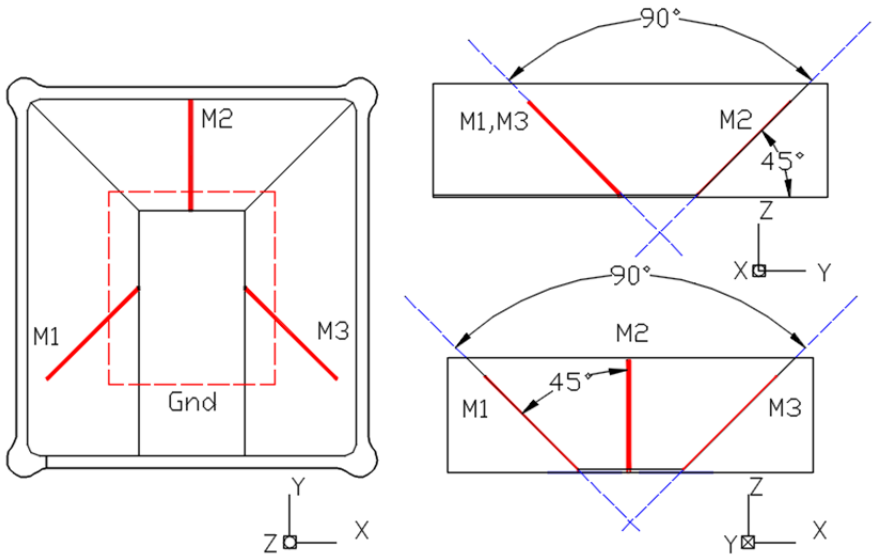

Figure 3-7: Square antenna geometry and angular arrangement between elements.

The complete process is realized in a single-piece construction and avoids the need for physical part rotations to achieve orthogonality between X, Y, and Z antenna elements. Each monopole is fed with a 50 Ω microstrip line, printed over a 500 μm thick flat substrate. The lines are subsequently connected to

www.manaraa.com

an externally controlled SP3T integrated circuit (Analog-Devices HMC245AQS1) that is used to switch between the individual polarization states without any specific phasing arrangement between them. The SP3T switch and SMP connector were manually placed and fixed onto the 500 um thick ABS substrate with a two part dielectric epoxy. Interconnection was achieved through dispensing of DuPont CB028 silver paste with a subsequent drying stage at 90° C for 60 minutes.

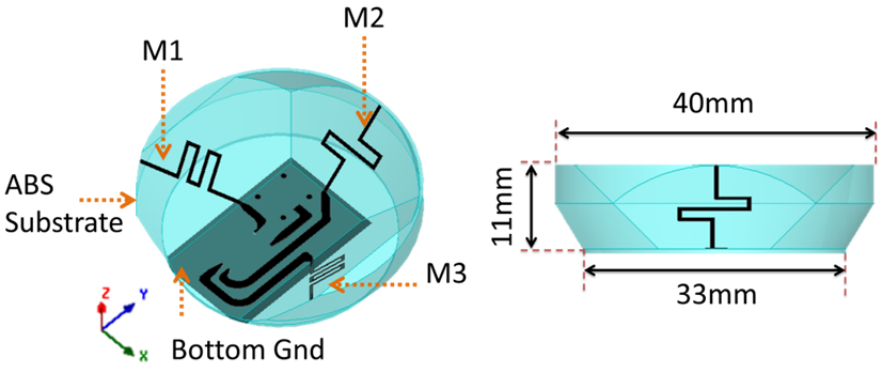

Figure 3-8: Circular tripolar antenna design

The technologies used for the fabrication of both antenna devices are known as fused deposition modeling (FDM) and micro-dispensing. FDM utilizes acrylonitrile butadiene styrene (ABS) with measured properties at 1 GHz of εr ~2.6 and tanδ~ 0.0058, to create the three-dimensional dielectric substrate. The ABS filament is extruded through a ceramic 125 μm inner diameter tip at 235 °C and patterned layer by layer onto a metallic bed pre-heated at 110°C. The 3-D surface is then laser-scanned to create a topography mesh that will guide the micro-dispensing head to conform to the surface while depositing the conductive parts, as shown in Fig. 3-6 (left) and Fig. 3-9 (top). DuPont CB028 is the material used for the conductive traces; a silver paste which possesses a conductivity of σ ~ 2 MS/m once it undergoes a 90°C drying stage for 60 minutes. All three processes are realized using an nScrypt Tabletop 3Dn printer (FDM head, laser displacement sensor and micro-dispensing head). Fig. 3-6 (right) and Fig.3-9 (bottom) show the fabricated square and circular antenna prototypes placed on top of the

www.manaraa.com

commercial sensor node packages, respectively. Coaxial SMP connectors were used on both prototypes for the RF output signal; the connector and the 3-way switch are manually placed and connected.

Figure 3-9: Micro-dispensing head on a sloped wall (top), fabricated circular antenna prototype (bottom right) on a commercial wireless node (bottom left).

3.3.1. Antenna Characteristics

In order to demonstrate radiation characteristics and advantages of implementing polarization diversity, each antenna's performance is tested in both anechoic and reflective environments. Transmission and reflection coefficients along with radiation patterns and cumulative distribution functions of fading statistics for each polarization states are shown in this section.

3.3.2. Antenna Performance in Anechoic Environments

The performance of both the square and circular tripolar antennas was measured inside an ideal anechoic environment. Fig. 3-10 (left) shows the measured and simulated reflection coefficient of the square antenna for monopoles M1 and M3, both of which are rotated 45 with respect to the Z and X axes. Similarly, Fig. 3-10 (right) shows the reflection coefficient for monopole M2, which is rotated 4 with

www.manaraa.com

respect to the Z axis. The return loss is greater than 15 dB at 2.4 GHz on all elements, with a worst case 10 dB bandwidth going from 2.1 GHz up to 2.8 GHz (i.e., 700 MHz).

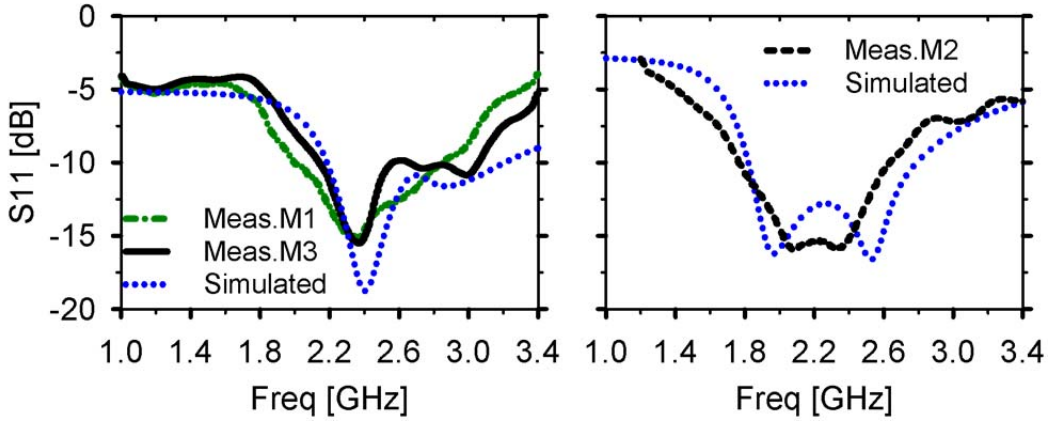

Figure 3-10: Square antenna simulated and measured reflection coefficient: for monopoles M1,M3 (left) and M2 (right).

Fig. 3-11 (a) and (b) show the measured and simulated radiation gain patterns at 2.4 GHz for monopoles M1, M3 and M2, respectively. The data correspond to the antenna azimuth plane against a vertically oriented transmitter horn antenna. That is, the X-Y plane follows the reference axes shown in Fig. 3-6 and Fig. 3-8. Similarly, Fig. 3-11 (c,d) and (e,f) show simulated radiation patterns on the X-Z plane and Y- Z plane respectively; some angles are noted to indicate the locations of radiation nulls. Fig. 3-11 (g-i) show the simulated 3D gain pattern when each individual monopole is selected. From each pattern, one will note a null is aligned along the monopole axis, ensuring pattern orthogonality and reasonable decoupling/independence between the three elements.

Fig. 3-11 (b) and Fig. 3-14(b) show the simulated cross-polarization pattern for monopoles M2 on the square and circular system with a maximum cross polarization discrimination of 35 dB and 25.8 dB, respectively, with similar values seen on the other elements. Common cross polarization discrimination levels in multi polarized systems often vary from 10 dB to 30 dB [13, 68, 69].

www.manaraa.com

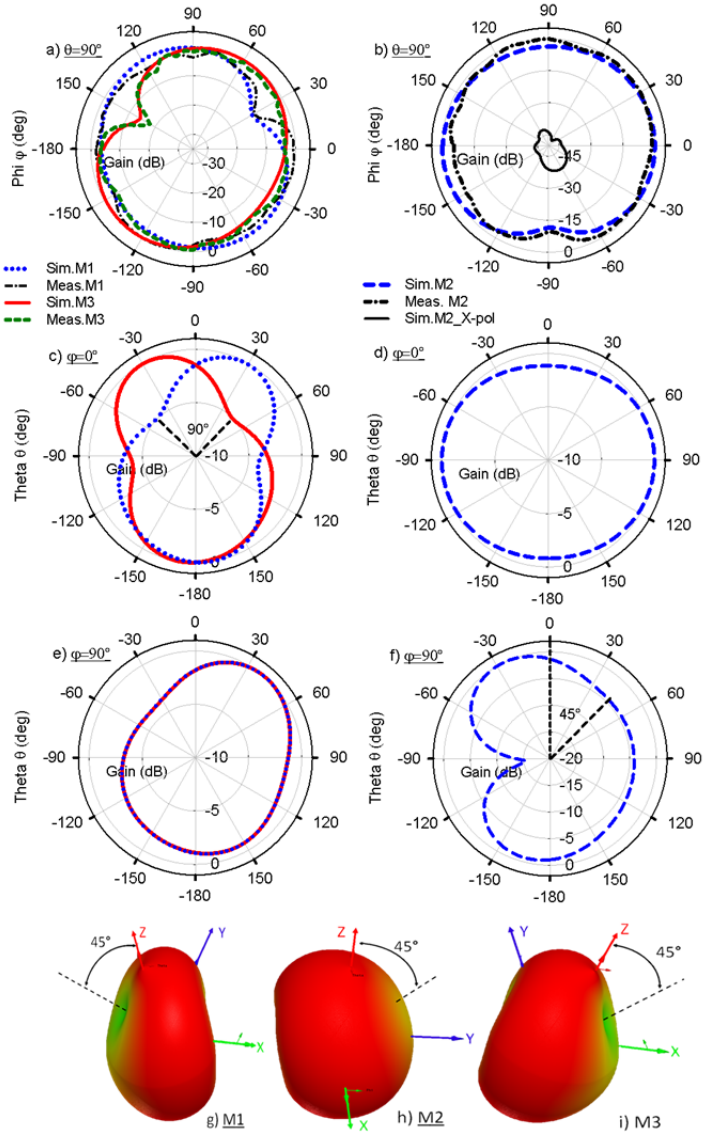

Figure 3-11: Square antenna simulated and measured normalized gain pattern (X-Y cut) / (X-Z cut) / (Y-Z cut) : M1-M3 (a)/(c)/(e), M2 (b)/(d)/(f),and simulated 3D gain pattern for each polarization M1(g)- M2(h)-M3(i).

Fig. 3-12 (left) presents the simulated coupling between each monopole for the square antenna system, where a maximum mutual coupling level of -15.7 dB is seen at 2.4 GHz. To further evaluate the antenna diversity performance envelope correlation coefficients (ECCs) are computed between each element from simulated far field radiation patterns [70]. ECC values up to a threshold limit of 0.5 are often considered as acceptable [69, 71], while values of zero and one would suggest complete uncorrelation or overlapping radiation patterns, respectively. The proposed square antenna demonstrates

www.manaraa.com

low correlation between all polarizations within the ISM band 2.4- 2.5 GHz with a maximum ECC value of 0.05 as shown in Fig. 3-12 (right).

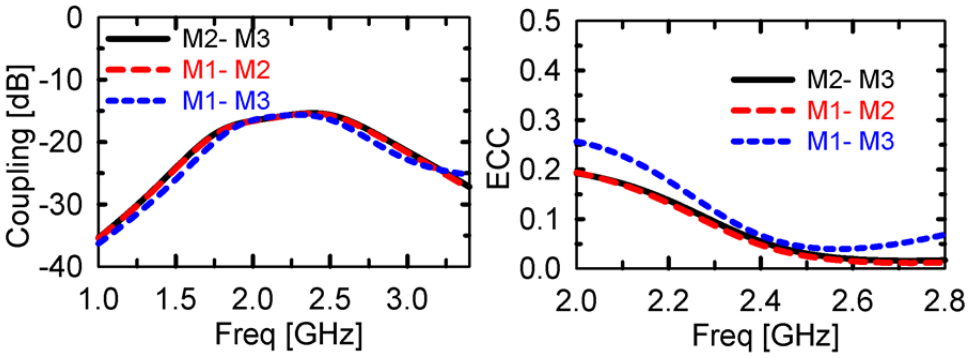

Figure 3-12: Square antenna simulated coupling between elements (left), envelope correlation coefficients (right).

Similarly, Fig. 3-13 (left) and (right) show the measured and simulated reflection coefficient of the circular antenna for the monopoles M1, M3 and M2, respectively. A return loss greater than 20 dB at 2.4 GHz is achieved for all three monopoles, with a worst case 10 dB bandwidth from 2.19 GHz up to 2.56 GHz (i.e., 370 MHz).

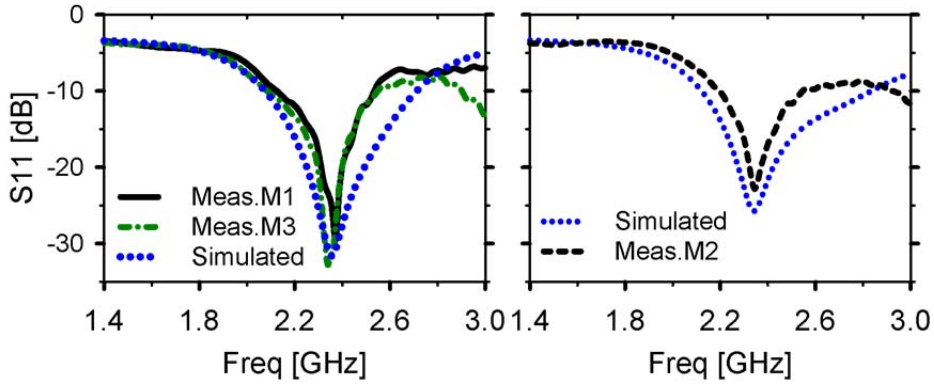

Figure 3-13: Circular antenna simulated and measured reflection coefficient for monopoles M1, M3 (left) and M2 (right).

www.manaraa.com

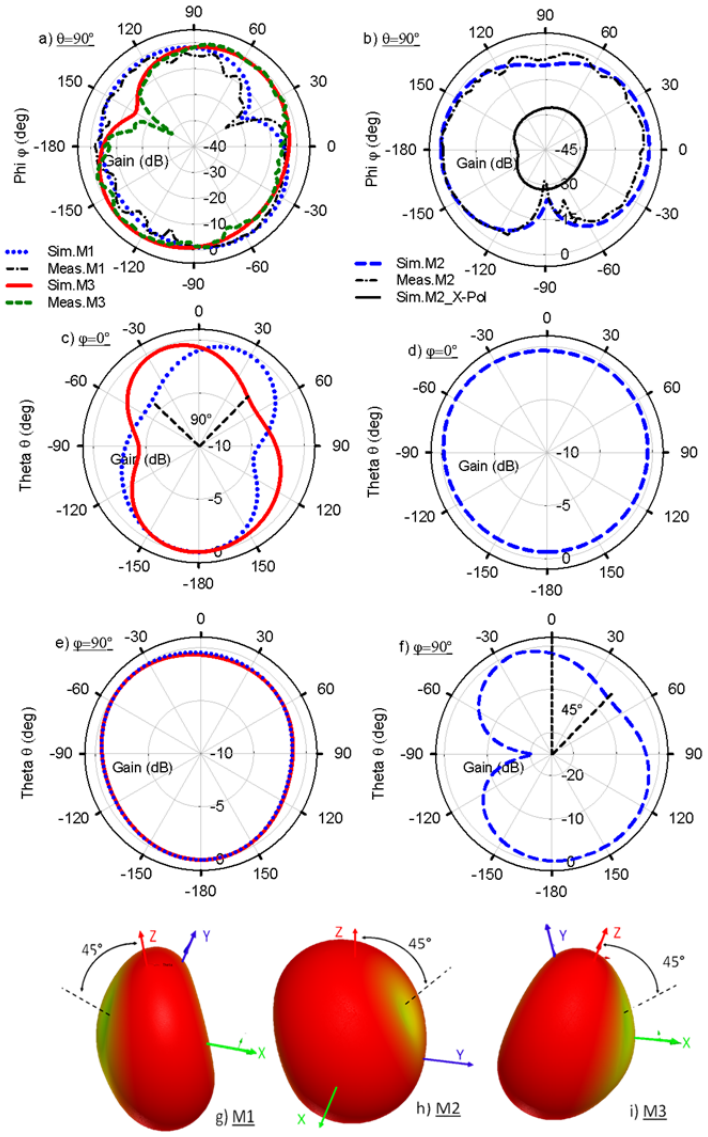

Figure 3-14: Circular antenna simulated and measured normalized gain pattern (X-Y cut) / (X-Z cut) / (Y-Z cut): M1-M3 (a)/(c)/(e), M2 (b)/(d)/(f),and simulated 3D gain pattern for each polarization M1(g)- M2(h)-M3(i).

Fig. 3-14 (a) and (b) illustrate the measured and simulated radiation gain patterns at 2.4 GHz for monopoles M1, M3 and M2, respectively. The data correspond to the antenna azimuth plane against a vertically oriented transmitter horn antenna, showing good agreement between measured and simulated traces. Similarly, Fig. 3-14 (c,d) and (e,f) show simulated radiation patterns on the X-Z plane and Y- Z plane respectively; some angles are also noted to indicate location of radiation nulls. Fig. 3-14 (g-i) show the simulated 3D gain pattern when each individual monopole is selected; as in the previous design it is

www.manaraa.com

seen how each radiation null is aligned in the direction of the corresponding monopole, ensuring pattern orthogonality and reducing the mutual coupling between arms. Some ripples observed on the X-Y plane measured radiation patterns can be attributed to the presence of the SMP connector on the top surface; its placement may be switched to the bottom surface in order to reduce scattering.

Fig. 3-15 (left) presents the simulated coupling between elements on the circular antenna system with a maximum level of -13.5 dB at 2.4 GHz. Slightly higher correlation coefficients are observed in this case while compared to the square system as shown in Fig. 3-15 (right), with values below the accepted 0.5 threshold within the ISM band 2.4-2.5 GHz and a maximum ECC value of 0.159. The increase can be attributed to non -orthogonal field components created by meandered traces on each monopole.

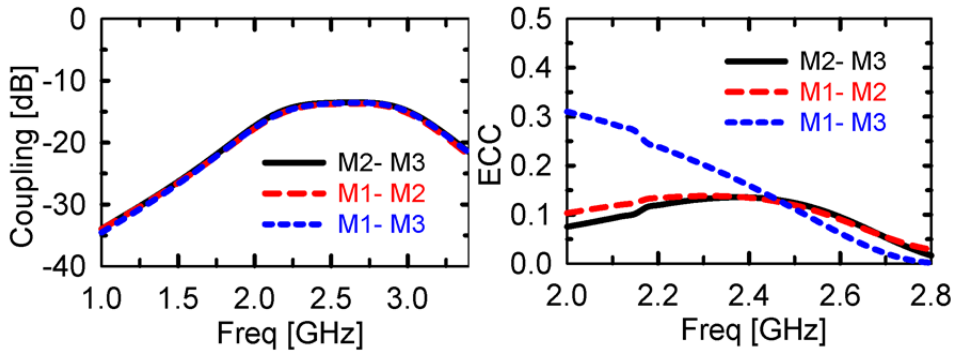

Figure 3-15: Circular antenna simulated coupling between elements (left), envelope correlation coefficients (right).

3.3.3. Antenna Performance in Multipath Environments

The anechoic chamber results presented in Section 3.4.1 represent those expected in terms of functionality for an array of monopoles (albeit that our design has these oriented mutually orthogonal in three dimensions). However, in terms of performance of the antenna system for its intended application (i.e., IoT devices in cluttered environments), a more representative test environment is required. For this, we employed a compact (0.9 m x 0.9 m x 0.3 m) reverberation chamber (Fig.3-16), capable of emulating channel conditions ranging from benign (i.e., Rician, high K) to very severe (i.e., two-ray, hyper-Rayleigh)

www.manaraa.com

[72]. As reverberation chambers have been shown to emulate channel characteristics similar to industrial sites [73], we contend our test environment will similarly emulate conditions that may be seen by M2M systems.

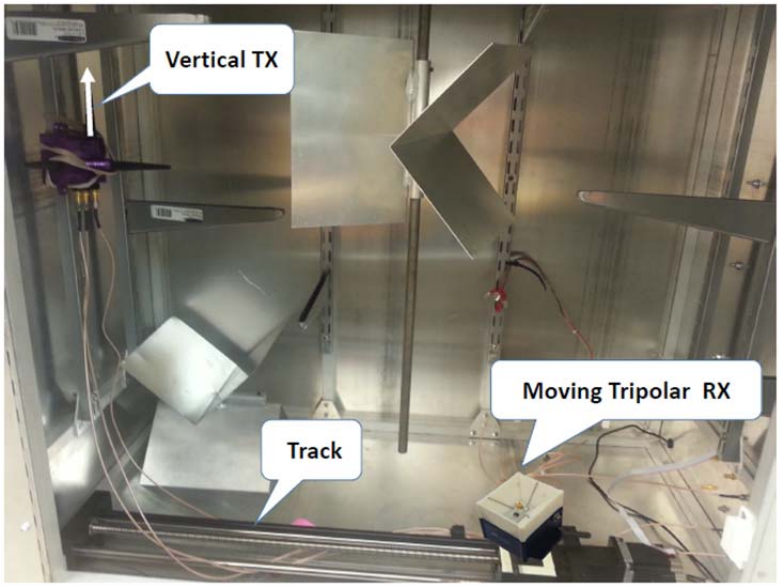

Figure 3-16: Test setup inside highly reflective, compact reverberation chamber.

Figs. 3-17 (left) and (right) show the reflection (S11) coefficient for the monopoles M3 'square' and M2 'circular', respectively, inside an aluminum reverberation chamber (solid line) for a fixed stirrer position. Although the measured return loss is strongly affected by the antenna placement and conditions inside the chamber, the impedance match is still preserved at 2.4 GHz; moreover the overall frequency response follows the trend of the anechoic coefficient shown with the dashed line [74].

www.manaraa.com

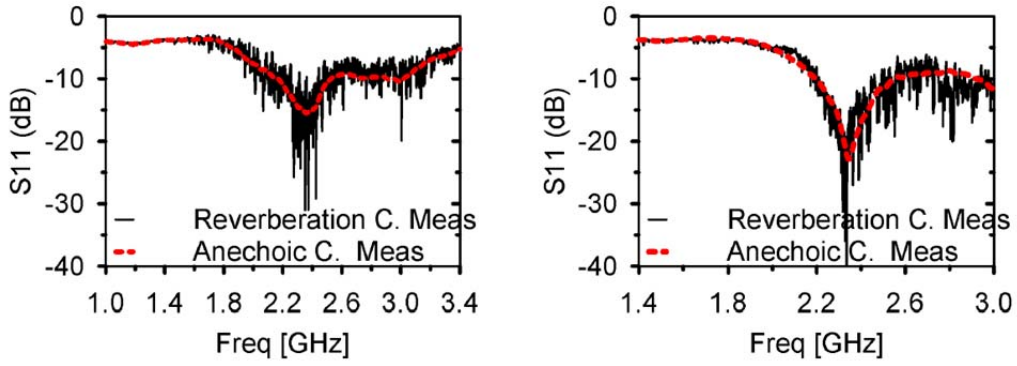

Figure 3-17: S_{11} data in reverberation chamber for the square antenna (left) and circular antenna (right).

Chamber testing was conducted by placing each individual tripolar array mounted on a LabView controlled linear track that allowed positioning to one of 50 repeatable locations in 1 cm (i.e., $\lambda/10$) increments. An Anritsu MS2036A vector network analyzer was then used to measure S_{21} (i.e., path loss) between a vertically polarized (i.e., Z-oriented) transmit antenna and one element of the receive tripolar array. Measurements (Fig. 3-18 (left)) and (Fig. 3-19 (left)) were made at 551 frequencies in the range of 2.40 GHz to 2.48 GHz and at 50 positions inside the chamber. For the 'square' antenna, the individual links have comparable characteristics with median losses ranging from approximately 39.7 to 40.3 dB. Thus, over 25,000 test conditions, we found that no single element (M1, M2, or M3) exhibit any superior performance over the other two.

Also implemented was M = 3 selection diversity where the best (i.e., lowest link loss) path was selected for each frequency. The resulting cumulative distribution function (CDF) is seen in Fig. 3-18 (right). This diversity technique yields 1% link improvement of 11 dB. The value is significant in that it could be traded for reducing transmit power by an order of magnitude, thereby saving node energy and extending battery life or be leveraged to reduce the link outage probability and/or BER (as we demonstrate later).

www.manaraa.com

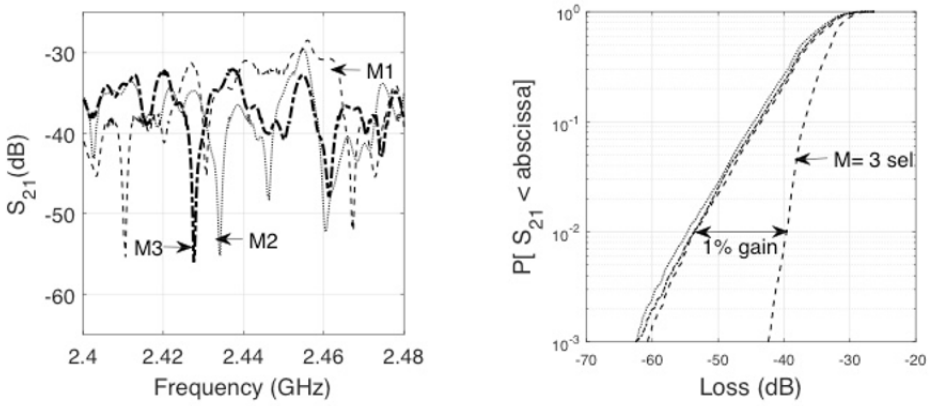

Figure 3-18: Square antenna results. Link loss, i.e., S21, for three mutually orthogonal receive elements when transmit element is vertically polarized (left). CDF plots of S21 data for individual elements and when M = 3 selection diversity is leveraged. 1% link improvement is found to be ~11 dB (right).

The results obtained from the circular antenna shows that the individual links have comparable characteristics with median S21 ranging from approximately -36 to -37.5 dB. Employing selection diversity among the three elements improves the 1% link margin by 14 dB (Fig. 3-19 (right)), a significant improvement in overall link characteristics.

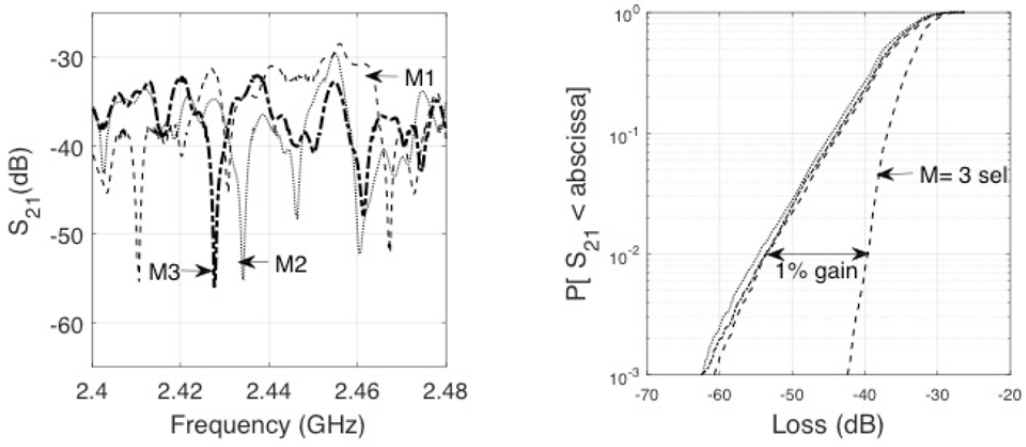

Figure 3-19: Circular antenna results. Link loss, i.e., S21, for three mutually orthogonal receive elements when transmit element is vertically polarized (left). CDF plots of S21 data for individual elements and when M = 3 selection diversity is leveraged. 1% link improvement is found to be ~14 dB (right).

www.manaraa.com

3.3.4. BER Measurements

Transmission over a link in a wireless network is prone to error due to noise and multipath effects. Bit error rate (BER) is often used to evaluate the link quality. BER has also been employed as a performance metric for routing protocols in wireless sensor networks [75, 76].

To understand how the tripolar antenna system might improve BER in very harsh environments, over-the-air BER measurements were performed in the reverberation chamber. The measurement setup for obtaining the BER is shown in Fig. 3-20. Unlike the previous S_{21} over-the-air measurements that were taken at 50 locations and 551 distinct frequencies, the BER measurements were conducted for one configuration of transmit and receive antenna array and at 16 channels with bandwidths of 375 kHz in the range of 2.4 GHz to 2.48 GHz. A vector signal generator (Agilent E4438C) was used to generate BPSK modulated signals with symbol rate of 250 kb/s.

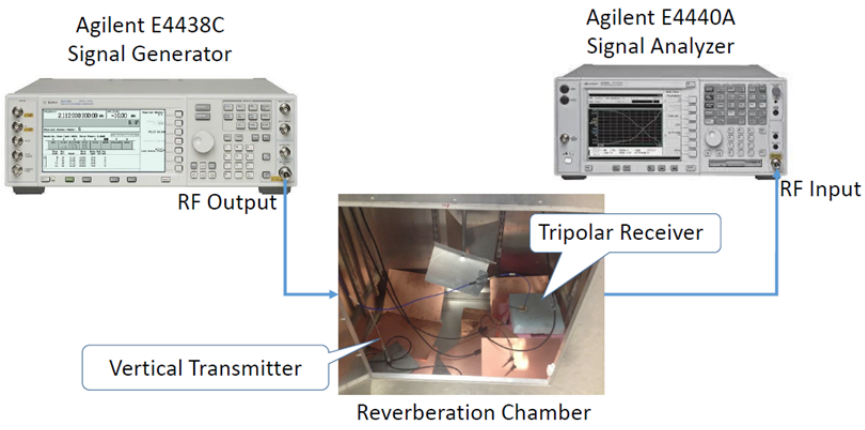

Figure 3-20: Test setup for BER measurements.

To receive and demodulate the signals, a vector signal analyzer (Agilent E4440A) was employed. In order to measure the BER, the received bits were compared with transmitted bits. These measurements were made 1000 times. The BER graphs at E_b/N_0 = 20 dB for three antenna links over channel frequency, which are presented in Fig. 3-21, indicate frequency selectivity of the channel. Theoretical BER values for

www.manaraa.com

Rayleigh channel and Rician channels with two different K values are plotted in order to see qualitative effects. The lowest BER among three links is selected at each frequency and shown in Fig. 3-21.

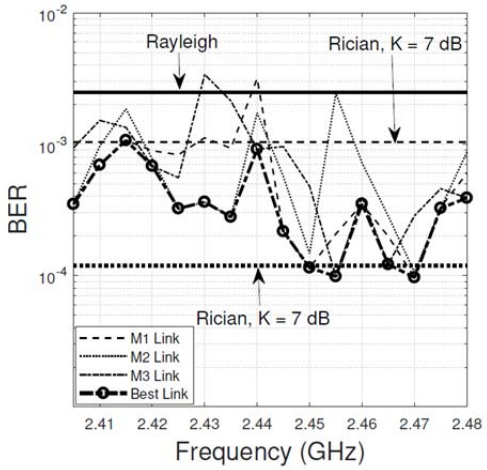

Figure 3-21: BER of three links and the best link of the square tripolar antenna.

The data are summarized in Table 3-2. We find that employing diversity methods for this particular measurement scenario decreased the average BER by 42% compared to leveraging just any single element. The same BER measurements were repeated for the circular antenna. Based on the data presented in Fig. 3-22 and Table 3-3, the average BER decreased by 44% when employing the tripolar antenna. It should be noted that the nominal $E_b/N_0 = 20$ is a relatively robust channel and that greater improvement can be expected at lower E_b/N_0 values.

Table 3-2: Statistics of BER of square tripolar antenna

Link	Min	Mean	Max
M1	9.6×10^{-5}	7.0×10^{-4}	3.20×10^{-3}
M2	1.1×10^{-4}	7.6×10^{-4}	2.40×10^{-3}
M3	9.8×10^{-5}	9.2×10^{-4}	3.40×10^{-3}
Best	9.6×10^{-5}	4.0×10^{-4}	1.10×10^{-3}

www.manaraa.com

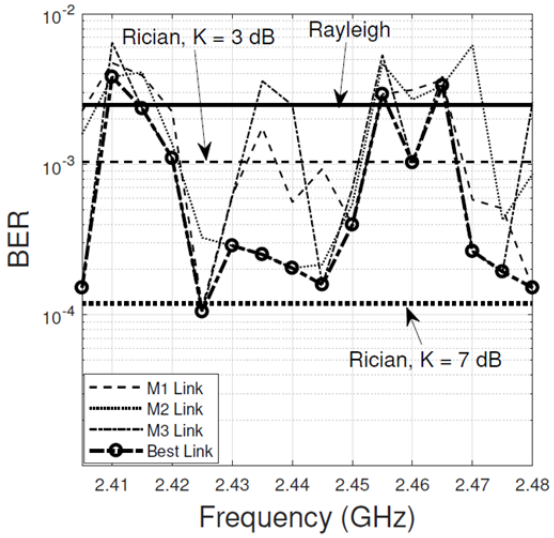

Figure 3-22: BER of three links and the best link using the circular tripolar antenna.

Table 3-3: Statistics of BER of circular antenna links

Link	Min	Mean	Max
M1	1.1×10^{-4}	1.8×10^{-3}	4.7×10^{-3}
M2	2.0×10^{-4}	1.9×10^{-3}	6.2×10^{-3}
M3	1.0×10^{-4}	1.9×10^{-3}	6.5×10^{-3}
Best	1.0×10^{-4}	1.0×10^{-3}	3.8×10^{-3}

3.3.5. Sensor Node Integration

The S_{21} measurements (Section 3.3.3) and BER data (Section 3.3.4) have shown experimentally that the prototype tripolar antennas provide an effective means of mitigating frequency and space dependent multipath effects in highly reflective communication environments. In this section, we demonstrate results of integrating our prototype antenna system with a commercially available wireless sensor node (Fig.3-6 (right)). To implement true selection diversity as analyzed in the prior sections, the antenna system would need to be able to monitor concurrently the power on each of the three branches. In contrast, we leverage the ability of the wireless chipset to monitor the received signal strength indicator (RSSI) but only of the branch presently being used. When the RSSI drops below a certain

www.manaraa.com

threshold relative to the mean of the received signal, the node will switch to the other elements searching for a larger RSSI. This approach is referred to as switch diversity in the literature [24]. The gain that can be obtained utilizing switch diversity is smaller than selection diversity and is also dependent on the threshold value as it can be seen in Fig. 3-23. For our demonstration, the 'best' channel is determined after post-processing the data and thus would be representative of what would be achieved using true selection diversity.

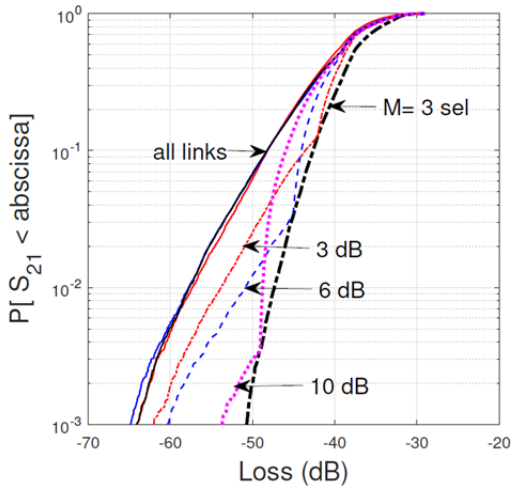

Figure 3-23: Cumulative distribution function (CDF) plots of S21 data for the three individual elements ('all links') with statistically similar fading behavior. M = 3 selection diversity and switching diversity with different threshold values is then applied. Threshold values for implementing switching diversity are set to 3 dB, 6dB, and 10 dB below the mean.

The RSSI, a normalized power value in dB, can infer path loss as it provides a relative dB value of the signal strength over a link. As noted at the onset of this work, the prototype antenna systems were physically designed to be integrated with commercial wireless sensor nodes. The nodes in mind during the development were the LORD Sensing G-Link2 for the square antenna and the LORD Sensing G-Link-200-8G for the circular design.

www.manaraa.com

In our demonstration, RSSI data is captured using the square antenna, integrated with firmware from a LORD Sensing WSDA-Base-104 gateway/basestation. The firmware was developed and the experiment was run using a Silicon Labs Mighty Gecko EFR32MG development board. This board is designed to operate at 2.4 GHz with a maximum power of 13 dBm. A test script was then written using LORD Sensing's open source MSCL library. The script successively pings the node 50 times, saves the average RSSI value, repeats the process for each antenna element, and then repeats the process for each channel frequency (LORD Sensing wireless networks use 16 channels between 2.40 and 2.48 GHz).

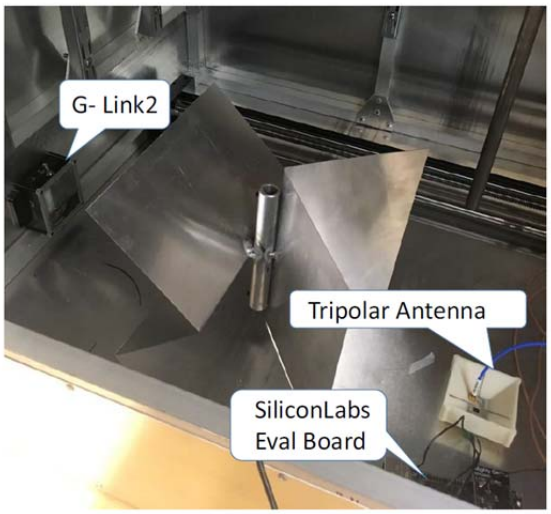

Figure 3-24: The set-up for the RSSI experiments. The LORD G-Link2 is present on the left of the chamber, while the tripolar is on the right, with the LOS component blocked.

The tripolar antenna is placed in the reverberation chamber, connected to the SL board with the basestation firmware, and a link is established with a LORD Sensing G-Link2 with the line-of-sight blocked (Fig. 3-24). Applying selection diversity using this tripolar antenna improves the RSSI measurements substantially (Fig. 3-25), with the supporting statistics displayed in Table 3-4. From Table 3-4 it can be seen that selection diversity between the three antenna elements improves the median RSSI 10 dB from the "worse" performing antenna element (M2). Selection diversity also provides "flatter" (i.e.,

www.manaraa.com

more consistent) performance across the channels (Fig. 3-25) as there is between 3 to 6 dB decrease in standard deviation when compared to the individual elements.

Table 3-4: RSSI data (Square antenna system)

Link	Median	Standard Deviation
M1	-13 dB	5.93 dB
M2	-17 dB	6.94 dB
M3	-8.0 dB	9.66 dB
Best	-7.5 dB	2.59 dB

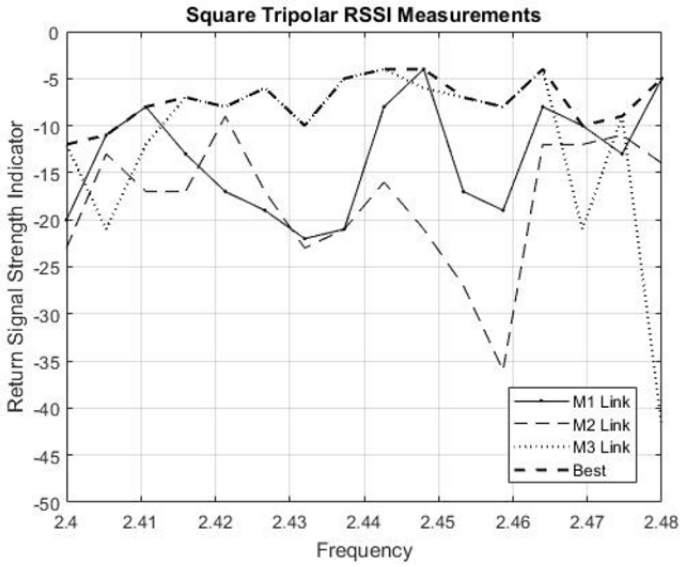

Figure 3-25: SSI data captured within the reverberation chamber. The measurements taken at each antenna element are displayed, along with the 'best' scenario that could be attained with selection diversity.

3.4. Conclusions

Three distinct 3D printed tripolar antennas have been developed and characterized for operation at 2.4 GHz. Each antenna system is fabricated through additive manufacturing techniques and is designed to mitigate harsh channel conditions by implementing polarization diversity between three mutually orthogonal ($\lambda/4$) monopoles. Performance was demonstrated under ideal and high multipath conditions, showing return loss values greater than 15 dB at the frequency of interest. Over the air testing

www.manaraa.com

demonstrated a 1% channel improvement of up to 14 dB across over 500 locations in a multipath environment and 44% reduction in BER at a representative location. Additionally, full integration with commercial hardware was performed resulting in the antenna array's capability for providing more consistent conditions over all selectable communication frequencies/channels. Future work includes developing on-chip mm-Wave multipolar antenna systems fabricated with additive manufacturing and laser machining to diminish depolarization effects present in wireless chip-to-chip communication channels.

www.manaraa.com

CHAPTER 4: MMIC PACKAGING, PACKAGE INTEGRATED ANTENNAS AND ON-CHIP LOW-LOSS LATERAL INTERCONNECTION USING ADDITIVE MANUFACTURING AND LASER MACHINING

4.1. Introduction

Additive manufacturing (AM) has grown rapidly in recent years and numerous 3-D printed RF circuits and antennas have been fabricated with excellent quality and RF performance that is on par with printed circuit board technology [77]. Inkjet 3D printed interconnects using coplanar waveguide transmission lines were recently demonstrated [55], however the performance of this design is impaired by the relatively lossy dielectric that was used. This section presents the development of a flexible, low loss integration methodology using both 3-D printing technology and laser machining. The 3-D fabrication process is outlined including characterization of the laser machining. A complete package with encapsulation for a distributed amplifier chip is fabricated and measured for demonstrating the performance of the package, along with analysis and comparison of S-parameters.

4.2. DPAM and Laser Machined Integration Process

4.2.1. Design and Fabrication

An overview of the proposed direct print additive manufac-tured (DPAM) packaged and interconnected device is illustrated in Fig. 4-1. The low-cost and low-loss packaging and interconnection technique enables integration of a wide range of MMICs with hybrid, digitally manufactured boards, specif-ically designed for microwave and mm-wave applications

---

The content of this chapter has been published in [44, 58] and it is included in this dissertation with permission from the IEEE. A copy of the permission is included in the Appendix A.

www.manaraa.com

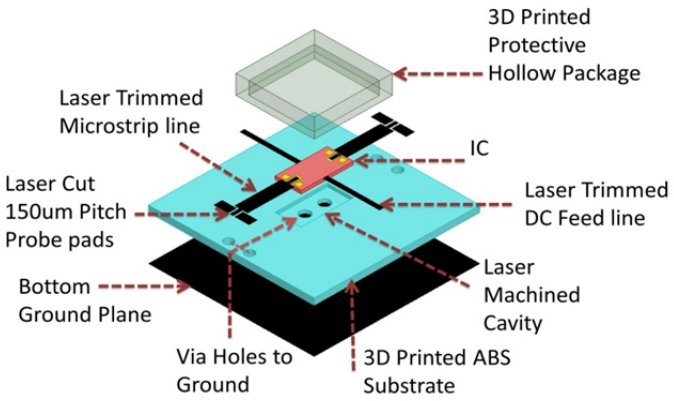

Figure 4-1: The overview schematic illustration of the DPAM fabricated MMIC packaging.

The three main technologies utilized to fabricate the package are fused deposition modeling (FDM), micro dispensing and laser machining. Combined, these tools allow integration of ICs with diverse footprints and thicknesses for single or cascaded systems.

Acrylonitrile butadiene styrene (ABS) is the dielectric selected to form the package substrate and protective cover. The conductive traces are realized by micro-dispensing DuPont CB028 conductive paste. Fig 4-2 (b) shows a 75 μm inner diameter ceramic tip on top of a 100 μm IC pad. With this tip, feature sizes down to 60 μm are achievable when pressure, speed and valve aperture are properly adjusted. In the first step of the process the picosecond laser (Lumera Laser's SUPER RAPID-HE) is programmed to cut a cavity with the exact area and depth of the device to be packaged with an x-y resolution of 20 μm. The IC is then placed inside this machined cavity to keep a minimum height difference between the surface level of the chip and the printed substrate since any variance of the cavity depth can have a considerable effect on the quality of final printed interconnects. The laser etch rate is characterized at a repetition rate of 100 kHz and several average power settings. The cavity depth is measured with a Dektak 150 profilometer and plotted in Fig. 4-2(a).

www.manaraa.com

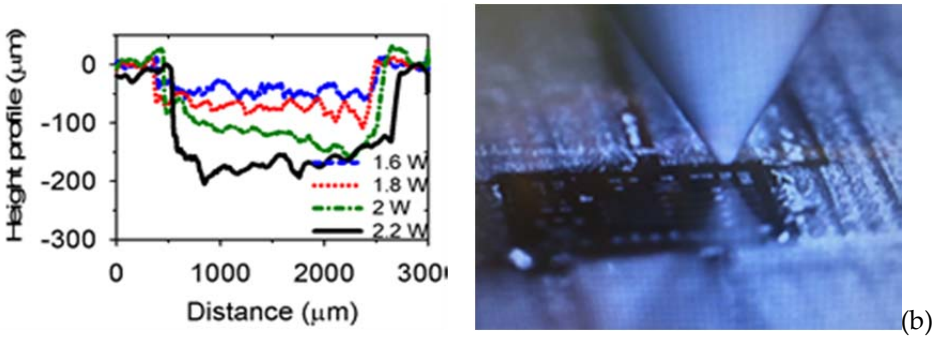

(a) (b)

Figure 4-2: Cavity cross-section profile with different power settings of laser machining (a), and precise alignment on the MMIC chip for interconnect (b).

4.3. Integration of a MMIC Low-Noise Amplifier

In order to demonstrate the effectiveness of the proposed packaging and interconnection process, a MMIC LNA is successfully integrated to an additive manufactured substrate. The specifications of the low-noise distributed amplifier, package fabrication and measurement are described in the following section. Additionally, the measured results are con-firmed using Keysight ADS EM simulations, along with the performance comparison with a generic Quad Flat No-leads (QFN) package mounted over an identically prepared ABS board.

4.3.1. LNA Specifications and Package Fabrication

Fig. 4-3(a) shows a top-view photo of the broadband low-noise distributed amplifier (DA) of dimensions 1.8 x 1.5 x 0.1 mm3. It is implemented using a 0.5 μm GaAs substrate E/D-mode (Enhancement and Depletion mode) pHEMT (pseudo-morphic high-electron mobility transistor) fabricated by the Qorvo's foundry service, offering up to 30 GHz ft and 100 GHz fmax. This four-stage DA is designed to provide a flat gain of 11 dB with ±0.5 dB ripple from 2 to 22 GHz, along with 1.8 VSWR for both input and output. Fig. 4-3(b) shows the DA embedded on a 3D printed ABS substrate with 50 ohm microstrip interconnects and DC feed lines.

www.manaraa.com

A 400 μm thick ABS substrate with a measured εr ~ 2.1 and tanδ ~ 0.0058 at 17 GHz is printed using FDM. The ABS filament is extruded through a ceramic tip at 235°C and patterned onto a 110°C heated metal bed. Four consecutive thin layers of ~100 ◎m are deposited in order to minimize surface roughness mainly created by the filament diameter.

a) 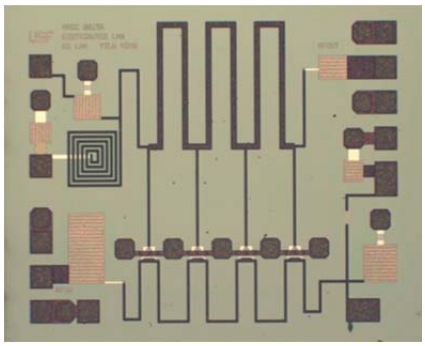 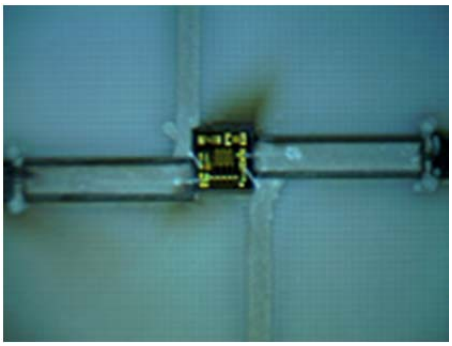 b)

Figure 4-3: Top view photos of LNA die (a), and hybrid integrated LNA (b)

The picosecond laser is utilized with an average power of 2.2 W to machine a slot of 2.15 mm² in area and ~100 μm in depth, representing the occupied area of the IC to be pack-aged. Fig 4-4(a) shows an SEM image of the generated cavity. The connection to ground is achieved by filling drilled holes of 0.5mm in diameter with conductive paste, as shown in the block scheme of Fig. 4-4(b). Conductive layers are then micro dispensed on top of the plastic substrate and directly on the chip using a 75 μm inner diameter tip as shown in Fig. 4-2(b) to form two 6 mm long microstrip lines with characteristic impedance of 50 Ω for both RF input and output paths, as well as two traces for gate/drain DC bias.

Even though the conductive ink is deposited on a specific location with high precision (~ ± 5 μm), overspreading occurs due to the natural viscosity and roughness of the CB028 paste and substrate, respectively. It is at this point as shown in Fig. 4-4(c-e) that laser machining provides the necessary accuracy for post processing of the conductive traces, ensuring smooth edges and an accurate 50 Ω line width along the whole microstrip transmission line, including the narrow transition to the IC's 100 μm

www.manaraa.com

wide pad. Fig. 4-4(e) displays a laser generated 150 μm pitch probe pads, where ground and center signal pad are separated by a ~20 μm wide slot; a close-up SEM photo of this slot is shown in Fig. 4-4(f). Final packaging is completed using FDM to deposit a 500 ◎m-thick ABS layer above the chip, with a 300 ◎m-high air gap between the chip and ABS (Fig 4-5(a)).

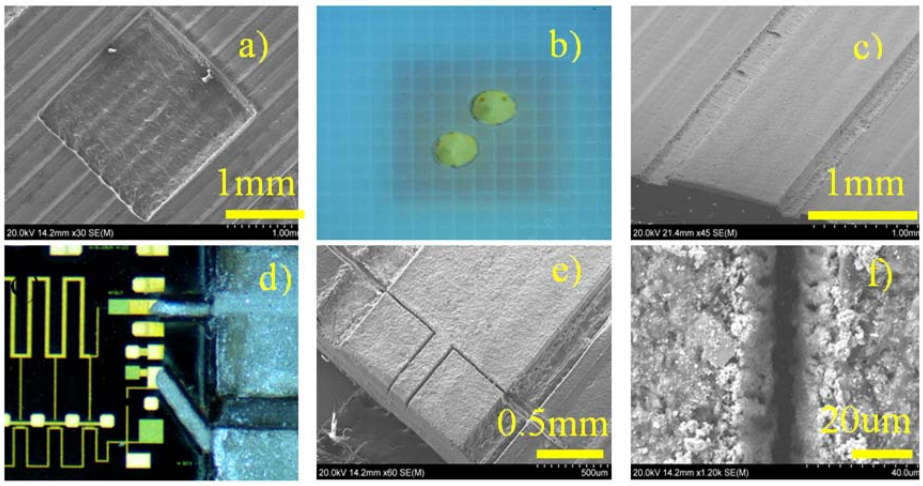

Figure 4-4: Pictures of packaged device and interconnects. SEM image of laser machined cavity (a), drilled vias for ground connection (b), SEM image of laser trimmed microstrip line (c), interconnects to the MMIC (d), SEM image of laser machined 150 μm pitch probe pads (e) and close-up SEM image of a typical laser cut on printed CB028 ink (f).

4.3.2. Measured Results

The S-parameters of the stand-alone LNA as well as the amplifier with the 3D printed package are characterized from 1 to 30 GHz using a Keysight PNA N5227A. Standard 150μm pitch ground-signal-ground (GSG) probes from GGB Industries Inc. and two DC needle probes for gate / drain biasing are used for the measurement setup as shown in Fig. 4-5(a). From the measured S-parameters plotted in Fig. 4-5(e), it is seen that the stand-alone device has a flat gain of 10.5dB and an input/output reflection coefficient less than -10 dB within its operating frequency range when it is biased with 80mA of total drain current and a 3V supply voltage.

www.manaraa.com

An EM simulation is performed with Keysight Advanced Design System (ADS), and its response is shown in Fig. 4-5. The model which includes via effects, transmission line losses, field coupling, silver ink conductivity, etc. predicts the behavior of the measured characteristics, showing an insertion loss difference against the stand alone device of 1.5 dB at 5 GHz and 2.4 dB at 20 GHz. From these results it is seen that the loss per unit length of the microstrip line is 0.125 dB/mm and 0.2 dB/mm, at 5 GHz and 20 GHz, respectively. Additionally, the S_{11} and S_{22} values lie below -10 dB within the frequency band of interest. It is important to mention that the DA in the 3D printed package is measured with and without the ABS encapsulation, having a similar response on both cases. An identical DA chip is also integrated into a QFN package using wirebonds as interconnects as illustrated in Fig. 4-5(b). The measured S-parameters of the QFN-packaged DA are plotted in comparison with the 3D printed packaged DA in Fig. 4-5. Due to strong parasitic effects of the wirebonds and the frequency limitation of the QFN package, the bandwidth of the DA is limited to 12 GHz showing a gain reduction of 2 dB when compared to the DA in the 3D printed package.

Table 4-1 summarizes the obtained attenuation results of the interconnection in dB/mm and compares them with those of similar prior works. It is seen that the DPAM package outperforms previous printed interconnects in terms of insertion loss by at least 0.125 dB at 5 GHz and 1.2 dB at 20 GHz.

Table 4-1: Comparison of measured performance

Reference	Substrate	IC Pad width (um)	Attenuation (dB/mm)	
			5GHz	20GHz
This Work	ABS	100	0.125	0.20
Tehrani [55]	Glass	200	0.25	1.45
Tehrani [56]	SU-8	230	0.40	0.60
Pavlidis [57]	VeroWhite	NA	0.15	>0.45
Mehta[54]	Kapton	90	0.5	1.5
QFN_P	ABS	100	0.32	NA

www.manaraa.com

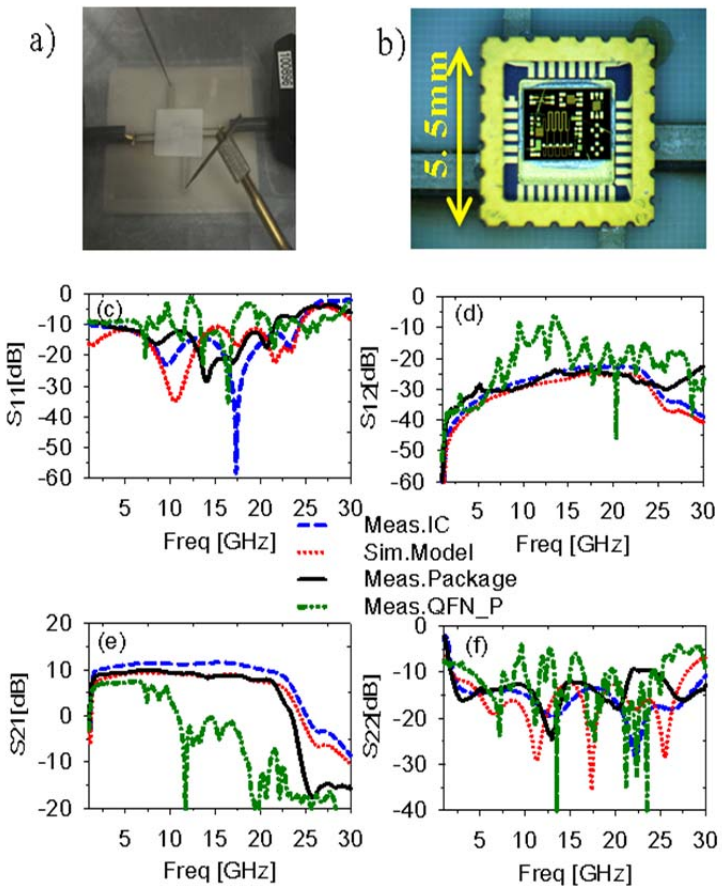

Figure 4-5: Measured results. Packaged DA and measurement setup (a), DA wire-bonded inside a QFN package (b), measured and simulated S-parameters of the unpackaged and packaged die and DA assembled inside a commercial QFN package, respectively (c-f).

4.4. Cascaded Interconnections

As noted in the previous sub-section (4.3), DPAM is a low temperature process that enables the fabrication and packaging with lateral interconnection of MMIC (monolithic microwave integrated circuit) dies. Fig. 4-6 shows a distributed low noise amplifier (LNA) cascaded with a transistor-based tunable band pass filter. Both dies are embedded within a 100 um deep laser machined cavity over a 3D-printed ABS substrate and interconnected using micro-dispensed, laser-defined microstrip transmission lines. Fig 4-7. Shows the measured S-parameters of the stand-alone GaAs pHEMT LNA (solid), stand-alone GaAs Filter (dashed) and the cascaded response (dotted). This measurement is performed by RF probing directly into the package. The LNA exhibits a gain of 11dB +/- 0.5 dB ripple from 2 to 10 GHz

www.manaraa.com

along with 1.8 VSWR for both input and output terminals. The transistor based bandpass filter shows a resonant frequency centered at 5 GHz with a return loss greater than 30 dB and 0.52 dB insertion loss as shown in Fig. 4-7(a) and Fig. 4-7(b), respectively. The measured insertion loss due to the 3D printed overall package interconnections is 0.2 dB at 7 GHz.

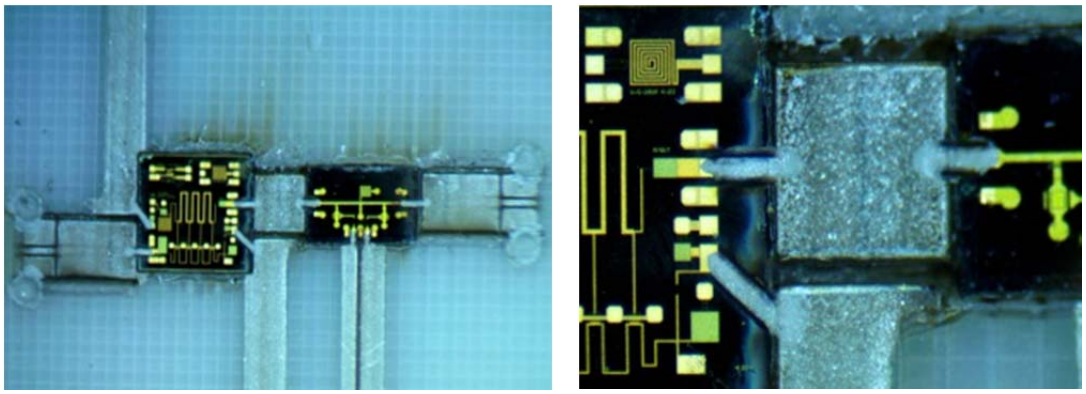

Figure 4-6: Cascaded MMIC LNA and filter (left), RF lateral interconnection close-up (right)

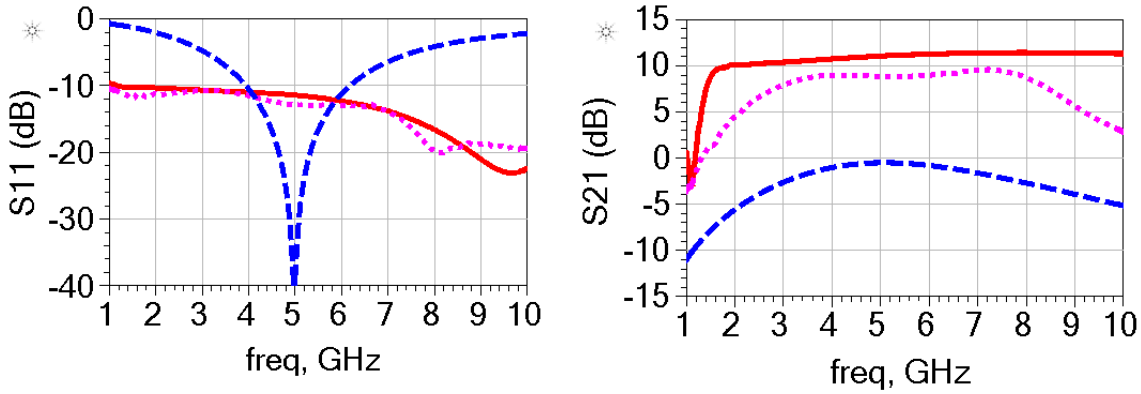

Figure 4-7: Measured input reflection coefficient (a) and transmission coefficient of packaged DA (b).

4.5. AM Vertically Interconnected On-Package Microstrip Patch Antenna

In this sub-section a versatile and fully additively manufactured (AM) on-package antenna design, intended to be vertically interconnected to an integrated circuit is presented and characterized for operation at 17 GHz.

www.manaraa.com

4.5.1. Antenna Design and Fabrication

Following the MMIC packaging process introduced in the previous sub-sections (4.3 and 4.4), where a Low Noise Amplifier GaAs die operating up to 22 GHz was successfully encapsulated, interconnected and cascaded with external dies and hybrid systems. The on-package antenna proposed herein will be incorporated to this package on a multilayer and multi-material 3-D printing process. Fig. 4-8 shows the stack-up geometry of the proposed package integrated broadside antenna; it is important to note that in this section the antenna will be characterized independently without the interconnection to the IC.

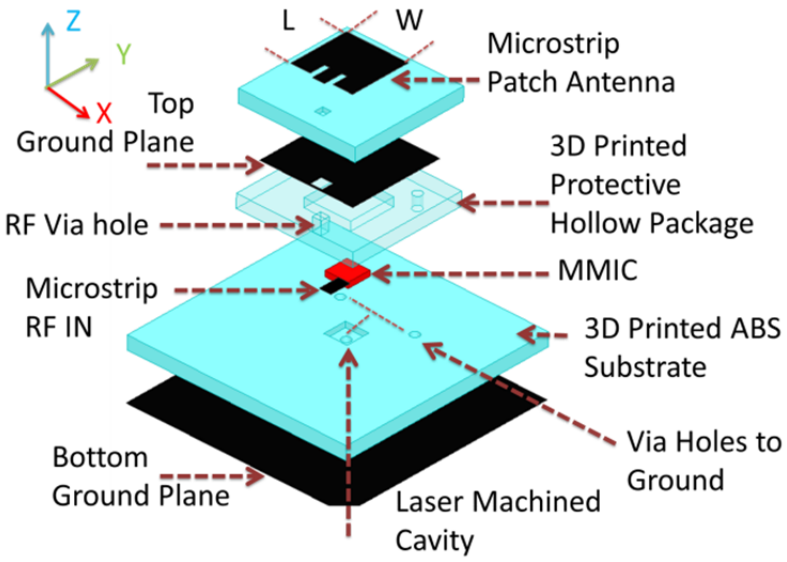

Figure 4-8: On-Package microstrip patch antenna stack-up. (RF line to IC)

The patch antenna's length is set to a value of approximately half guided wavelength ($\lambda g/2$) at an operating frequency of 17 GHz, general optimized dimensions are L= 5.35 mm and W=5.6 mm. Impedance matching is consequently achieved by controlling the microstrip inset feed location. Fig. 4-9 shows a cross section view with general dimensions of the fabricated prototype

www.manaraa.com

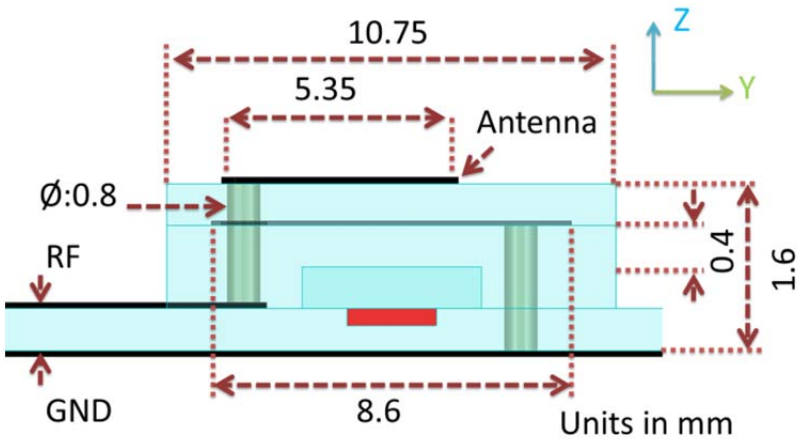

Figure 4-9: Cross-section view with general dimensions. (RF line to coaxial connector)

The fabrication is carried out with the nScrypt 3Dn tabletop system, a tool that combines different technologies such as fused deposition modeling (FDM), micro-dispensing, and pico-second laser machining. Acrylonitrile butadiene styrene (ABS) is implemented on the dielectric parts, with measured properties of $\varepsilon r \sim 2.35$ and $\tan\delta \sim 0.0065$ at 30GHz; the ABS filament is extruded through a ceramic tip at 235 °C and deposited layer by layer onto a metallic bed at 90°C . On the other hand DuPont CB028 is micro-dispensed over the printed substrate and oven dried at 90°C for an hour.

As shown in [44, 58] once the 400 μm thick main ABS substrate is deposited, laser processing is performed to machine a cavity so that the integrated circuit can be precisely placed inside of it; over this substrate layer, conductive traces will be micro-dispensed to form the RF interconnection and necessary DC supply lines. Subsequently, a protective 800 μm thick hollow cover (with clearance of 400 μm) is printed, with additional specific vias to account for the antenna's ground plane and RF signal output. The top ground plane is then micro-dispensed, in order to avoid unwanted coupling with the IC and RF output lines. The process is followed by a third 400 μm thick ABS layer, to finally micro-dispense the planar patch antenna and vertically interconnect it to the main RF line. Fig. 4-10 shows the fabricated

www.manaraa.com

prototype, where the RF microstrip line is directly connected to an end-launch coaxial connector for characterization.

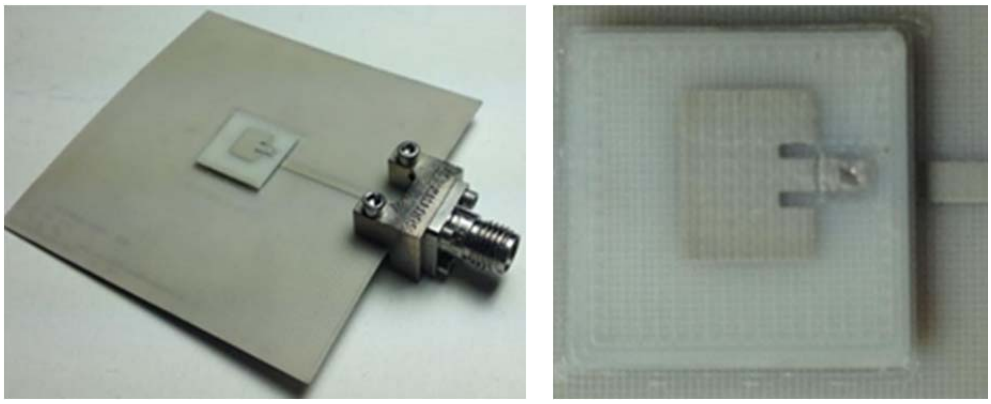

Figure 4-10: Fabricated package integrated microstrip patch antenna (left), package close-up (right)

4.5.2. Simulated and Measured Results

Fig. 4-11 (left) shows the simulated and measured reflection coefficient, results were obtained with Ansys HFSS EM 18.1 and a Keysight N5227A network analyzer, respectively. A return loss greater than 19 dB is obtained at the desired frequency of 17 GHz, and a 10 dB bandwidth from 16.8 GHz up to 17.4 GHz is achieved. Fig. 4-11 (right) shows the simulated and measured H-plane normalized radiation pattern, showing agreement between both traces, and a peak gain of 4.2 dBi.

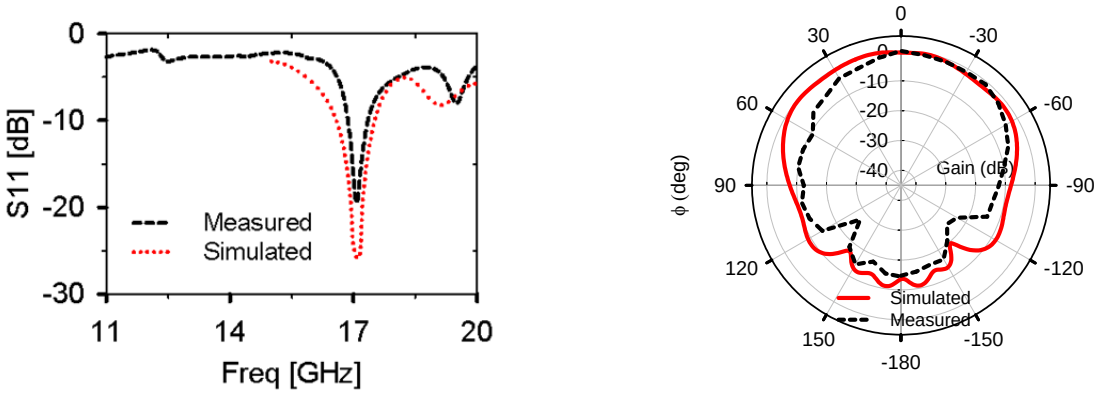

Figure 4-11: Measured and simulated reflection coefficient (left), H-plane normalized radiation pattern (right)

www.manaraa.com

4.6. Conclusions

A novel MMIC packaging and interconnection solution that combines additive manufacturing and laser machining has been developed for microwave and mm-wave applications. An MMIC chip is successfully integrated into the proposed package with lateral interconnects and sealed with ABS encapsulation with no significant effects on the overall performance. On-wafer probe measurements of the broadband amplifier reveal only 0.2 dB/mm insertion loss at 20 GHz for a transmission line on ABS substrate and exhibits satisfactory return loss at both input and output terminals with the 3-D printed package. DPAM integration technology has the potential to become a next generation solution for systems in package

A novel 17 GHz additively manufactured package integrated antenna is presented for vertical integration with MMIC dies for chip-to-chip communication applications. A half wavelength ($\lambda g/2$) on-package microstrip patch antenna is implemented for radiation on a multi-layer and multi-material process. Antenna performance was demonstrated under anechoic conditions achieving a return loss greater than 19 dB at the desired frequency of 17 GHz, with a 10 dB bandwidth from 16.8 GHz up to 17.4 GHz; additionally broadside radiation is observed with a peak gain of 4.2 dBi.

www.manaraa.com

CHAPTER 5: LASER ASSISTED ADDITIVE MANUFACTURING OF MM-WAVE LUMPED PASSIVE ELEMENTS

5.1. Introduction

Microwave lumped passive components are critical elements of wireless systems, which are typically used for matching or filtering purposes. In mobile RF front ends, lumped components are embedded into laminates or dies, or surface mounted. These often prevail over transmission line stubs due to their compact form factor. AM technologies such as aerosol jet printing (AJP) [32], inkjet printing [33], and micro-dispensing [43, 78] have been shown as a viable technology for the fabrication of microwave interconnects, capacitors, inductors, and resistors.

It has been proven that pulsed laser processing of AM layers can considerably improve the performance of additive manufactured microwave components, specifically coplanar wave-guide (CPW) circuits, to levels comparable to that obtained by using traditional fabrication techniques at frequencies well into the mm-wave range [45]

In this chapter the fabrication process, measurements, and modeling of coplanar waveguide (CPW) capacitors, and multilayer inductors are described. The LE-DPAM process is used to fabricate multilayer spiral inductors and interdigital capacitors, where micro-dispensed silver ink (DuPont CB028) is used as the conductor, acrylonitrile butadiene styrene (ABS) is used for the dielectric layers [79],and picosecond laser processing is employed to machine the features on the conductive ink layers.. Results show that capacitances in the range of 0.05 – 0.5 pF are achieved at 30 GHz, with Q factors up to 750 and self-resonant frequencies above 120 GHz. On the other hand, inductance values in the range of 0.4 – 3 nH, with quality factors up to 21-8.6, and self-resonance frequencies up to 88 GHz are achieved. Design

www.manaraa.com

curves for the passive components are also included. Results show that LE-DPAM can be effectively used to fabricate mm-wave passives that can be used in conjunction with MMICs for RF front ends

5.2. General Fabrication Process

The components in this paper are fabricated using a multi-layer LE-DPAM process that involves interleaving FDM steps for dielectric deposition with micro-dispensing steps for conductor deposition. The substrate dielectric is ABS, which has an electric permittivity of 2.35, and a loss tangent of 0.0065 (at 30 GHz) [80].The vertical interconnects between layers are achieved by laser machining the ABS and filling the cavities using micro-dispensing of DuPont CB028, a silver paste with a reported DC bulk conductivity of 0.76 x 10^6 S/m when dried at 90°C [81]; the complete via fabrication process is described in [46]

The fabrication process starts with a printing bed that is heated to 90 °C. ABS is printed using FDM, as shown in Fig. 5-1 (a), by extruding with a ceramic tip at a temperature 235 °C. The tip inner diameter is 75 μm, which allows ABS to be printed in layers that are 50 μm thick. The first conductive layer is printed on the ABS using micro-dispensing (Fig. 5-1 (b)), with printing height, air pressure and printing speed of 70 μm, 12 psi and 25 mm/s, respectively. The thickness of the resulting CB028 conductive ink layer is approximately 30 μm. This first conductive layer is then machined using a Lumera SUPER RAPID-HE picosecond laser, with a wavelength, scanning speed, average power, and repetition rate of 1064 nm, 25 mm/s, 2.4 W, and 100 KHz, to achieve the geometry needed for an interconnect (Fig. 5-1 (c)). ABS is printed again, covering the conductive traces, and laser machining is used to machine the via cavities as shown in Fig. 5-1 (d). For this step, the laser average power is changed to 0.8 W, for an accurate and controlled etch rate. The cavities are then filled using micro-dispensing as depicted in Fig. 5-1 (e). A final conductive layer is deposited using micro-dispensing, and the laser is used to machine the slots required to realize the inductor (Fig. 5-1 (f)). This process is also used to fabricate the interdigital capacitors. Note that the capacitors in this paper do not require the steps to fabricate the via.

www.manaraa.com

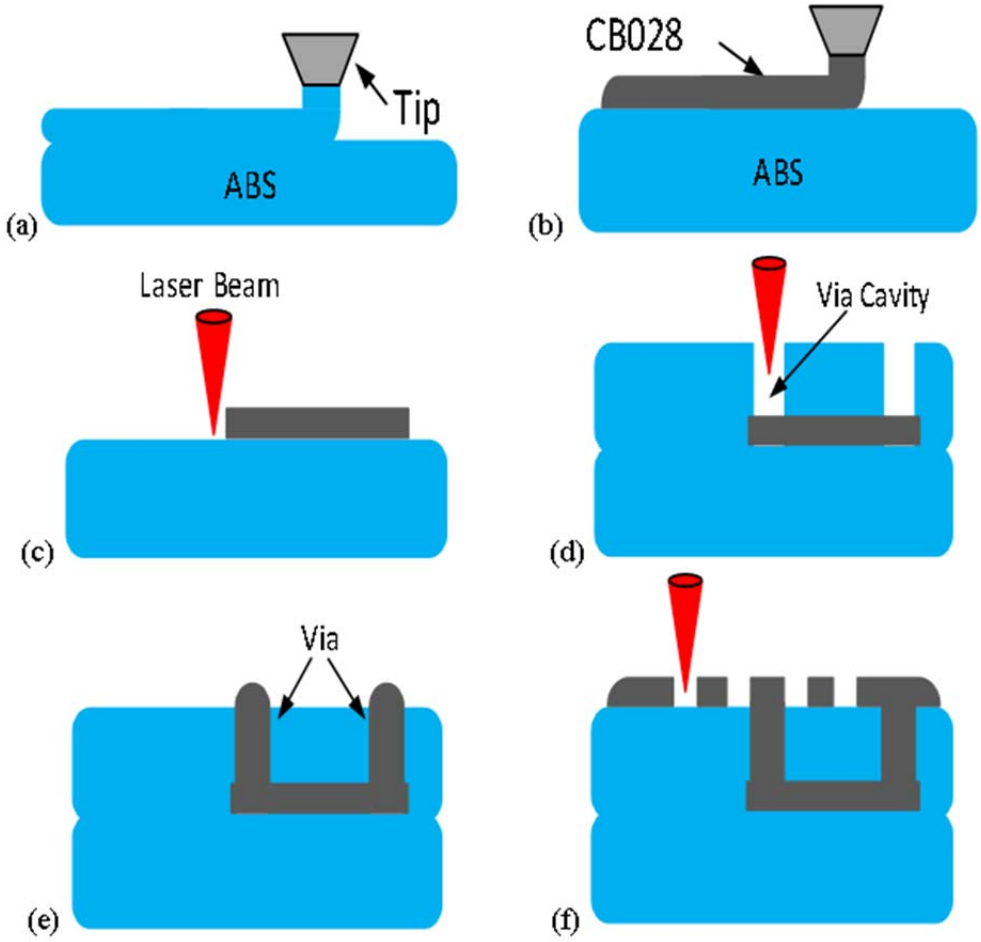

Figure 5-1: Laser enhanced DPAM process used to fabricate the inductors.

Fig. 5-2 (a) depicts the typical profile of a via with dimensions of around 200 μm x 200 μm x 150 μm, measured with a Dektak D150 profilometer. To accurately predict the depth of the cavities, the etch rate for CB028 and ABS as a function of the number of laser passes is calculated as shown in Fig. 5-2 (b), using an average laser power of 0.8 W. The etch rates are around 5 μm/pass and 8 μm/pass for CB028 and ABS, respectively.

www.manaraa.com

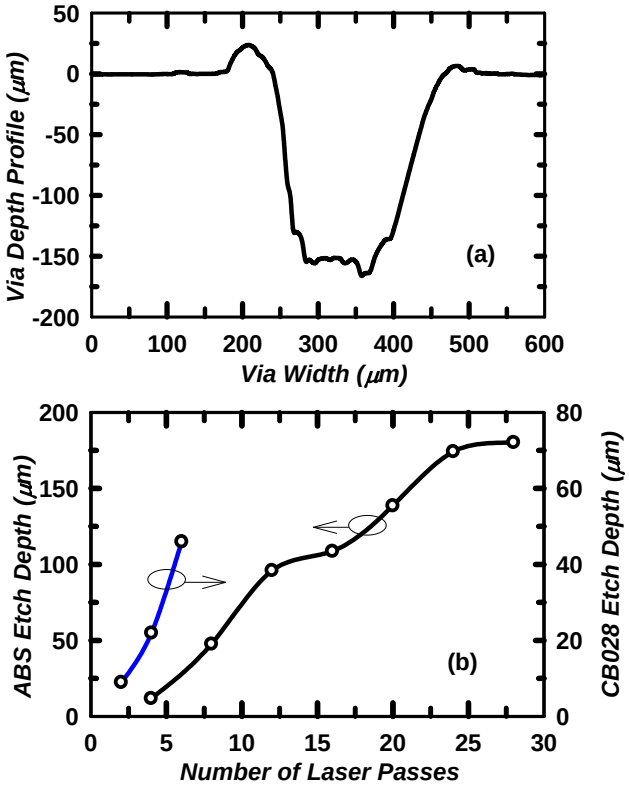

Figure 5-2: Profile of a via cavity (a), and etch depth for ABS and CB028 as a function of the number of passes (b).

5.3. Spiral Inductors

Following the fabrication procedure introduced in the previous section, different spiral inductors are presented with characterization data up to 30 GHz. Simulated, modeled and measured data are shown to demonstrate feasibility and control of the proposed process.

5.3.1. Design and Fabricated Prototypes

The geometry of the inductor is a spiral that is patterned inside the center conductor of a coplanar waveguide (CPW), as illustrated in Fig. 5-3. The center of the spiral is connected to the output port by using a buried bridge or underpass and two vertical vias. A set of four inductors with 0.5, 1, 2.5, and 3 turns are designed and fabricated to demonstrate the described fabrication technique. The linear size of these elements is designed to be much smaller than the guided wavelength (i.e. < $\lambda g/8$) at the desired

www.manaraa.com

frequency range, taking into account design drivers such as self-resonant frequency, quality factor and effective series inductance. The dimensions of the fabricated samples are listed in Table 5-1

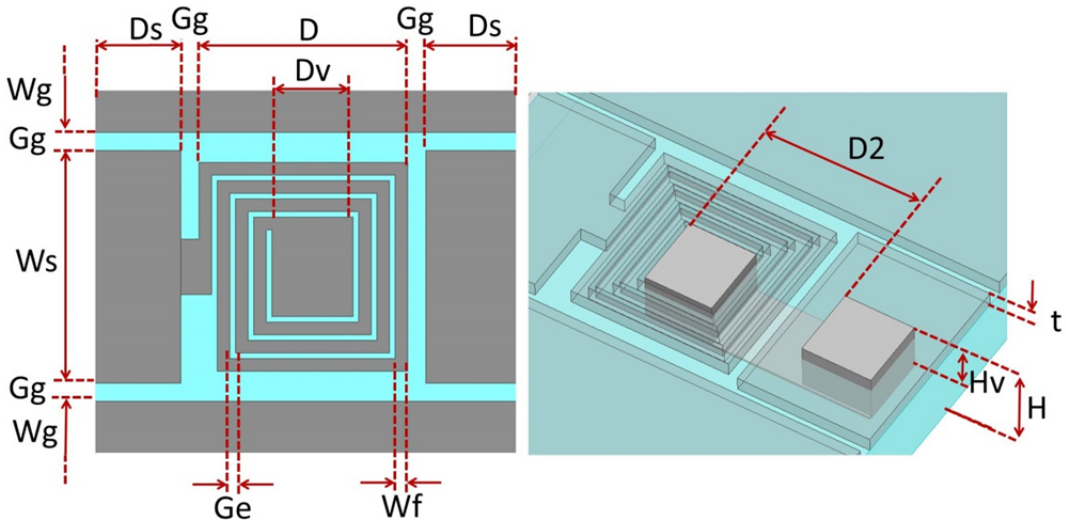

Figure 5-3: Geometry of proposed CPW spiral inductor.

Table 5-1: Spiral inductor general dimensions

N° of Turns(N)	**0.5**	**1**	**2.5**	**3**
D(μm)	340	470	600	750
D2(μm)	450	498	602	657

The following variables remain unchanged for all designs. Ws = 834.6 μm; Gg= 65 μm; Wg = 2 mm, Wf= 46 μm; Ds=520 μm; Ge ~ 12 μm; t= 30 μm; H= 300 μm; Hv= 150 μm; Dv ~ 200μm.

Fig. 5-4 shows top views of the fabricated spiral inductors. The SEM micrographs of two inductors with non-filled vias are included in Fig. 5-4 (a-b) to indicate their location in the geometry. Fig. 5-4 (c-f), show fabricated inductors with different number of turns (N=0.5, 1, 2.5, 3). The details of the machined windings and slots are depicted in close-up images in Fig. 5-4 (g-i), where gaps with dimensions ~12-15 μm are observed, creating ~ 2:1 aspect ratio cuts.

www.manaraa.com

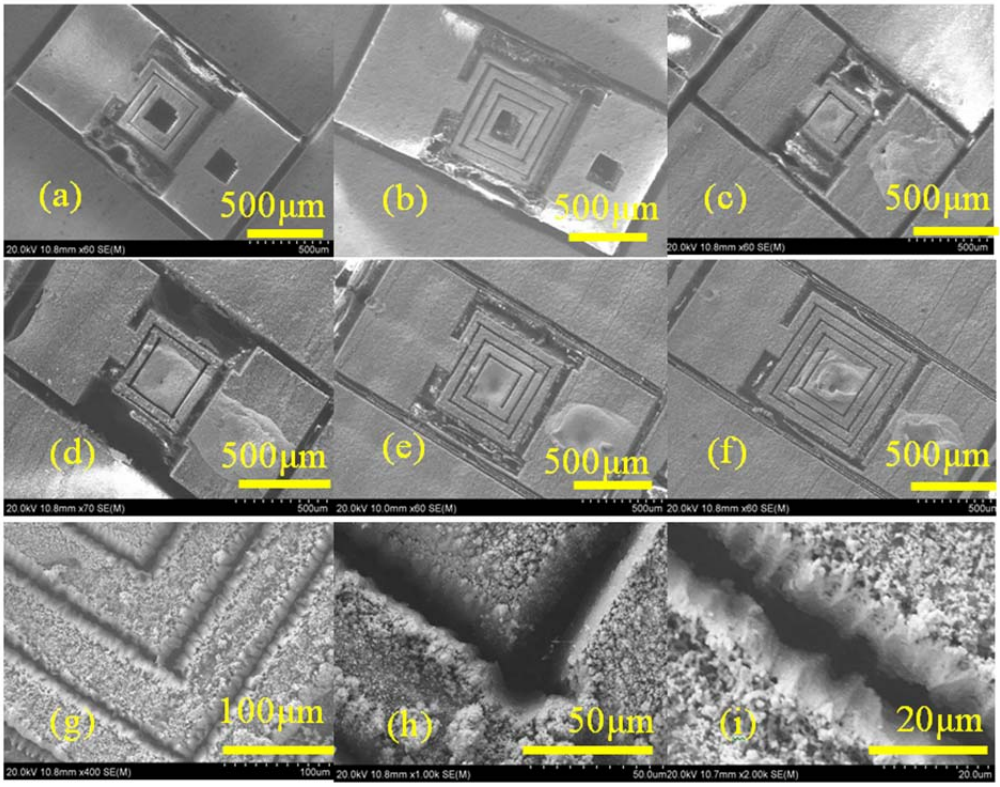

Figure 5-4: Fabricated prototypes. Picture of 0.5 and 1 turn inductors with via hole (a)-(b), top view of the fabricated inductors with different number of turns (N=0.5, 1, 2.5, 3 (c-f), and close-up images of the machined slots and windings (g-i).

5.3.2. Measured and Simulated Results

The results in this work were obtained using HFSS 17.1 for 3D EM simulations and Keysight Advanced Design System 2016.01 for circuit modeling. Measured data were obtained with an Agilent PNA-N5227A, a JMicro-Tech Jr-2727 probe station and 650 µm GGB picoprobes. Fig. 5-5 shows the measurement setup.

www.manaraa.com

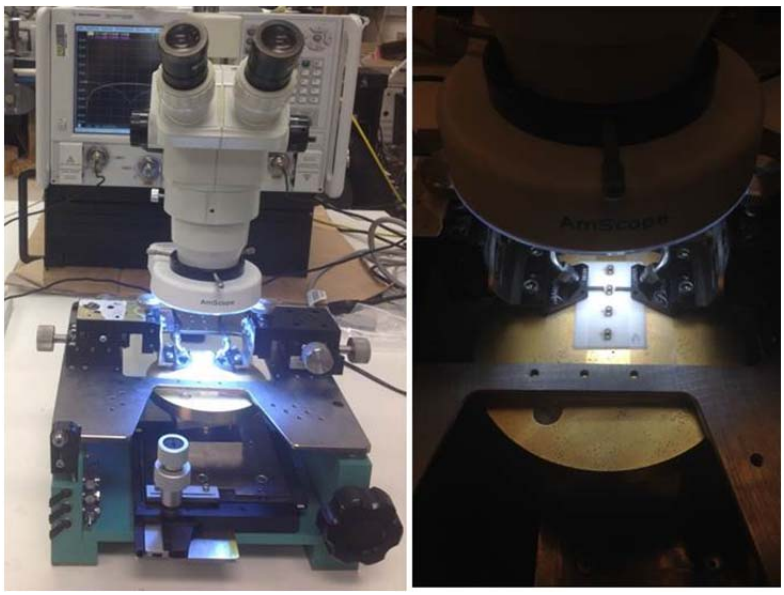

Figure 5-5: Measurement setup.

Fig.5-6 shows the measured and EM-simulation S-parameter data up to 30 GHz for the fabricated spiral inductors with different numbers of turns. There is good agreement between measured and simulated data, indicating a high degree of process control and simulation accuracy.

The properties and performance of the fabricated spiral inductors can be modeled using the RLC equivalent circuit model shown in Fig. 5-7. The parameter *LS* describes the main self-inductance of the device, directly proportional to the total length of the strip line that creates the spiral and the number of turns *N*. The parameter *CSh* depicts the parasitic capacitance of the spiral winding to ground, while *Cg* accounts for the parasitic capacitive coupling within the spiral winding, a value heavily affected by the CB028 thickness t and the gap *Ge* between different turns. Finally, *RS* describes the ohmic losses across the inductor. Complete values are listed in Table 5-2.

www.manaraa.com

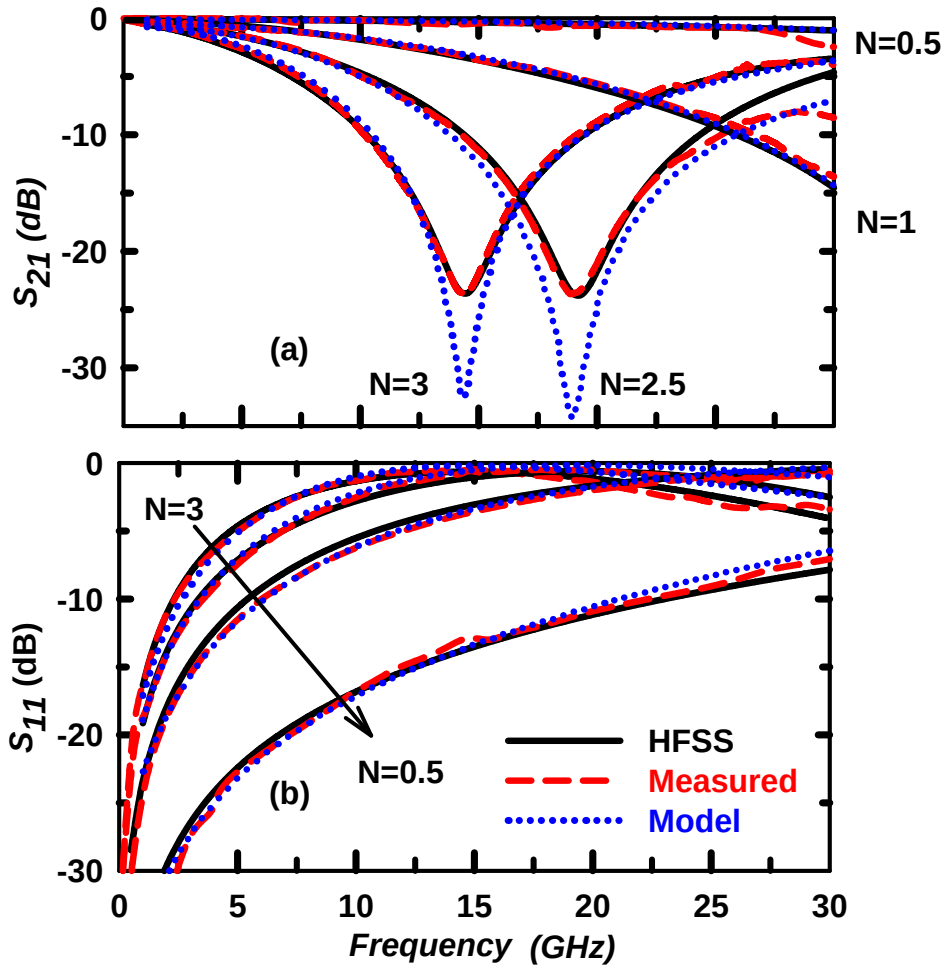

Figure 5-6: Measured, simulated and modeled magnitude of the transmission coefficient (a) and reflection coefficient (b) of four spiral inductors fabricated with LE-DPAM

For the same fabricated devices, Fig. 5-8 (a) shows the simulated, modeled and measured inductance over frequency, computed from (Eq.5.1), where values of 0.4 nH (for N=0.5) and 2.87 nH (for N=3) are achieved at 5GHz; similarly, values of 0.46 nH (for N=0.5) and 2.70 nH (for N=1) are achieved at 30 GHz. Close agreement between the measured and simulated data is also observed here.

$$Inductance\ "L" = \frac{1x10^9}{Im[-Y_{21}] * (2 * \pi * freq)}\ [nH] \tag{5.1}$$

www.manaraa.com

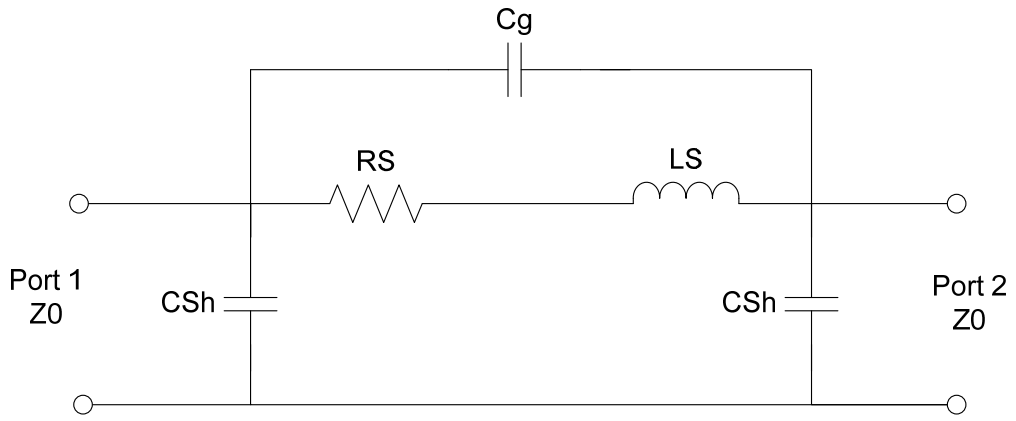

Figure 5-7: Spiral inductor equivalent circuit model.

Table 5-2: Spiral inductor equivalent circuit model values

Parameter	N=0.5	N=1	N=2.5	N=3
RS (Ω)	1.373	5.473	6.966	8.012
Cg (*ρ*F)	0.003	0.0215	0.044	0.060
LS (nH)	0.399	0.879	1.582	2.24
CSh (*f*F)	35.06	35.12	38.02	39.13

K = mutual inductor coupling coefficient

Fig. 5-8 (b) shows the measured and simulated quality factor (Q) computed from (Eq. 5.2); the measured Q values are extracted from the measured 2-port S-parameters.

$$Q = \left|\frac{Im\{-1/Y_{21}\}}{Re\{-1/Y_{21}\}}\right| \tag{5.2}$$

Maximum Q values vary from ~8.42, 10.04 and 15.6 for spiral inductors with N= 1, 2.5, 3, respectively. It is seen from Fig. 5-8 (b) how this maximum value occurs at different frequencies, depending on the ratio of parasitic reactance and the series self-inductance LS. The Q value decreases at higher frequencies when the equivalent parasitic reactance is dominant in the circuit [41]

www.manaraa.com

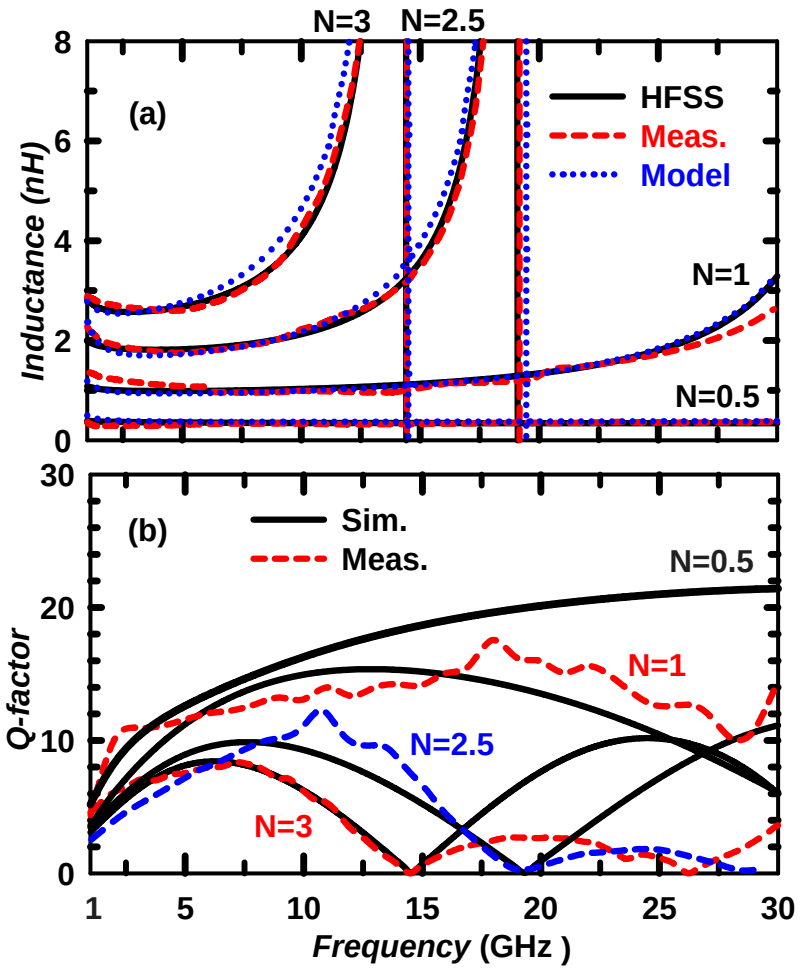

Figure 5-8: Measured, simulated and modeled inductance (a) and quality factor (b) for spiral inductors with different number of turns.

To understand the main sources of loss in the inductor, as well as the limitations of the geometry, the quality factor (Q) versus conductivity of the metal layer and loss tangent (tanδ) of the substrate are extracted from simulations. Results show that variation in tanδ from 0.02 (FR4) to 0.0009 (Zeonex) [82] causes only a 5% change in Q. On the other hand, the conductivity has a greater effect on the quality factor, as shown in Fig. 5-9

www.manaraa.com

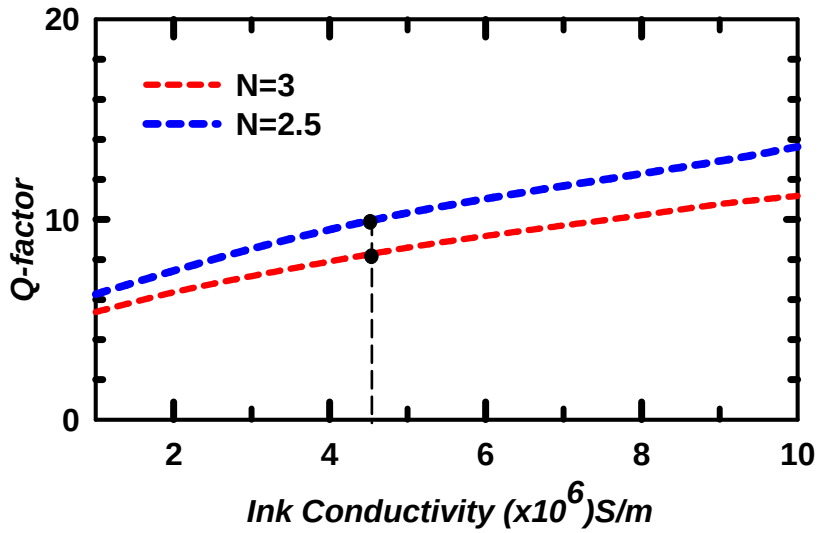

Figure 5-9: Spiral inductor quality factor plotted against ink conductivity.

Based on the measured Q values, the effective conductivity of the laser machined CB028 is in the range of 4.6 MS/m, which is better than the typical 0.76 MS/m DC conductivity of CB028 when dried at 90°C. This suggests that the laser processing improves the performance of the inductor. Note that for a 10 MS/m conductivity, simulations show that the Q values would be in the range of 13.8 and 11.4 for this particular geometry with N=2.5 and N=3, respectively.

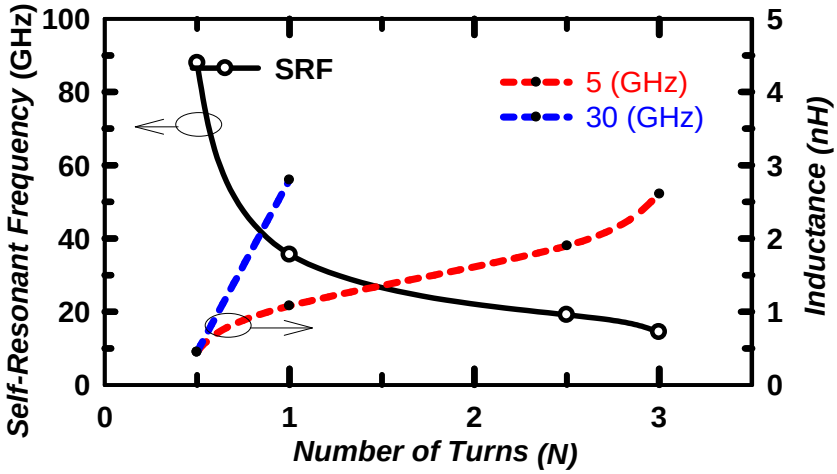

Figure 5-10: Spiral inductor simulated self-resonant frequency and inductance plotted against the number of turns.

www.manaraa.com

Fig 5-10. shows the predicted changes in effective inductance at 5 GHz and 30 GHz for variations in the number of turns N, obtaining inductance values ranging from 0.4 nH up to 2.87 pF at 5 GHz, and from 0.4 nH up to 3 nH at 30 GHz. Moreover, the first self-resonant frequency (SRF) was studied via HFSS simulation, to determine effective operational frequency range of the device. Fig. 5-10 shows the value of the SRF for variations in the number of spiral turns, obtaining values of 88 GHz and 15 GHz for N=0.5 and N=3, respectively.

Table 5-3: Comparison with state-of-the-art AM lumped inductors

Work	Process	Inductance (nH)	SRF (GHz)	Q_{max}	Inductance per unit Area nH/mm^2
[33]	Inkjet	7	4.25	11	0.78
[39]	Liq. Metal	92	0.71	24	0.9
[34]	Inkjet	75/9.7	0.2/0.8	3/4	1.8/0.8
[40]	LTCC	7.15	2.33	33.5	1.1
[41]	GaAs	0.7/2.8	9/24	16 /22	20/31
*This Work**	LEDPAM	0.4/3	88/15	8.6/21	4.3/5.3

**LEDPAM = laser enhanced direct print additive manufacturing*

Table 5-3 shows a comparison of measured performance with previously published related work, including different geometries and fabrication technologies. Note that AM inductors tend to have lower Q, when compared to the ones obtained from GaAs dies. The main reasons for this are the lower conductivity of the inks, and the high tanδ of the printed dielectrics. In this work, higher Q values are achieved when compared to other AM devices due to the use of laser machining, which increases the effective conductivity of the silver pastes [45].

5.4. Interdigital Capacitors

The LE-DPAM process is also utilized for the realization of high performance lumped CPW interdigital capacitors (IDC), elements that can be integrated with matching, filtering or biasing networks and fabricated in a single layer process as depicted in Fig. 5-1 (a-c). In this section, several IDCs are

www.manaraa.com

presented, characterized and compared with previous related work up to 30 GHz. The content in this section includes results shown in [83] that are used to propose and validate a circuit model.

5.4.1. Design and Fabricated Prototypes

As in the previous section where spiral inductors were introduced, some of the critical parameters that are often considered as drivers in lumped passive element design include the overall size, self-resonant frequency, quality factor and effective series capacitance. Fig. 5-11 shows the proposed IDC geometry and Table 5-4 includes all the general dimensions for the different capacitors fabricated. Effective capacitances in the range of ~0.05 pF up to 0.5 pF at 30 GHz are achieved by changing the IDC length (D). Fig. 5-12 shows the fabricated interdigital capacitor prototypes with different finger lengths (a-d) and typical laser cuts in a 2:1 aspect ratio (e-f).

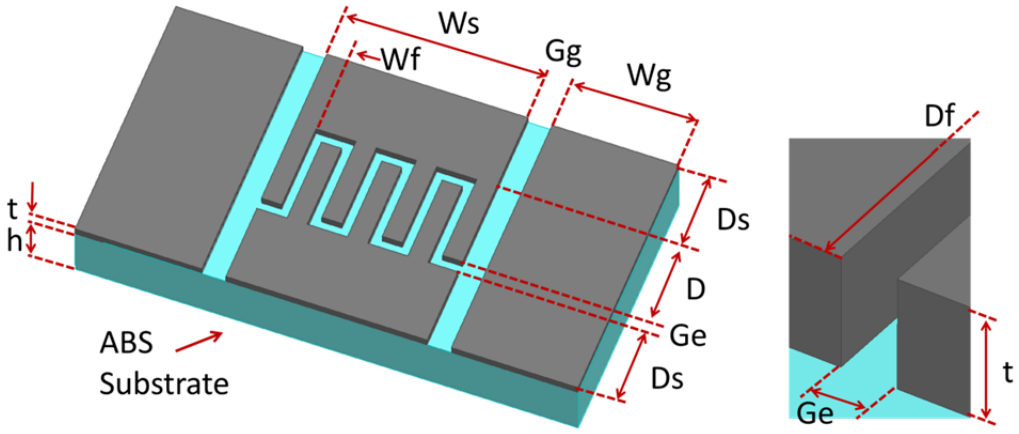

Figure 5-11: Proposed CPW interdigital capacitor geometry.

Table 5-4: Proposed CPW interdigital capacitor geometry.

N° of Fingers	**3**	**7**	**9**	**11**	**13**
Wf (μm)	264.8	102	74.9	57.6	45.7

The following variables remain unchanged for all designs. Ws = 834.6 μm; Gg= 65 μm; Wg = 2 mm; Ds=520 μm; Ge ~ 15 μm; t= 30 μm; h= 300 μm.

www.manaraa.com

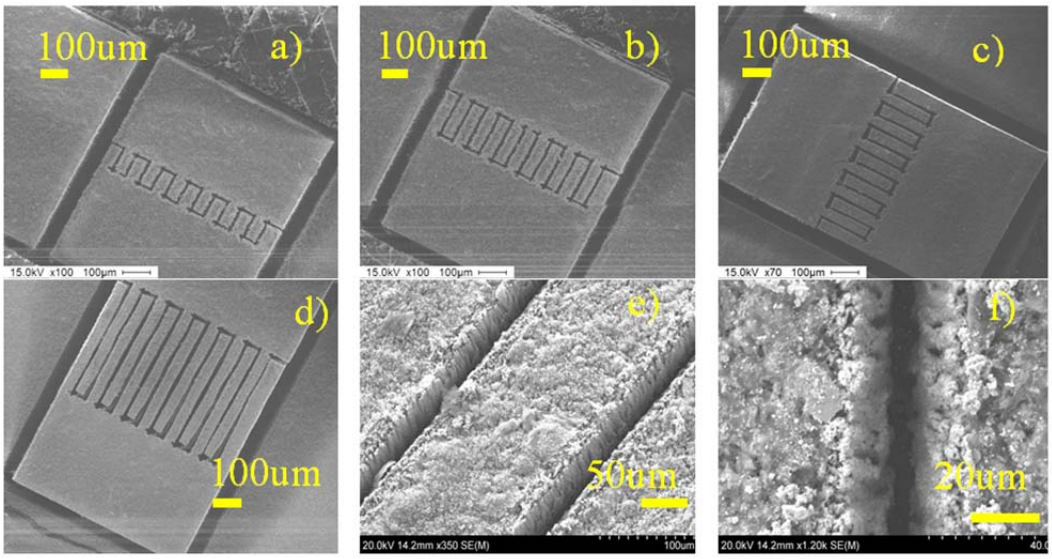

Figure 5-12: Fabricated prototypes. SEM images of interdigital capacitor for different finger lengths (L= 100 µm , 200 µm, 300 µm and 500 µm) (a-d), SEM image of a laser cut with a ~ 2:1 AR (e); and close-up SEM image of a typical laser cut on CB028 slot width ~15 µm and ink thickness ~30 µm (f).

5.4.2. Measured and Simulated Results

The simulated and measured reflection and transmission coefficient results of IDC capacitors with 13 fingers and different finger lengths (*D*) are shown in Fig. 5-13 [83]. The effective capacitance of the component is computed using (Eq. 5.3), and shown in Fig. 5-15 (a), achieving 0.05 pF and 0.25 pF for d= 100 µm and d=600 µm, respectively [83].

$$Capacitance\ "C" = \frac{1x10^{12}}{Im\left[\frac{1}{-Y_{21}}\right] * (2 * \pi * freq)}\ [\rho F] \tag{5.3}$$

The properties and performance of the fabricated devices is emulated using the lumped element model in Fig. 5-14. The parameter *CS* describes the main electric coupling between fingers representing the series capacitance of the device, a value directly proportional to the total length of the fingers, number of fingers *N* and thickness of CB028 t. The parameter *CSh* represents the parasitic capacitance of the input

www.manaraa.com

and output interdigital structure to ground, whereas the two inductors *LS* and mutual inductive coupling factor *K* account for the parasitic magnetic coupling between fingers. Finally, the *RS* resistors describe the ohmic losses across the device.

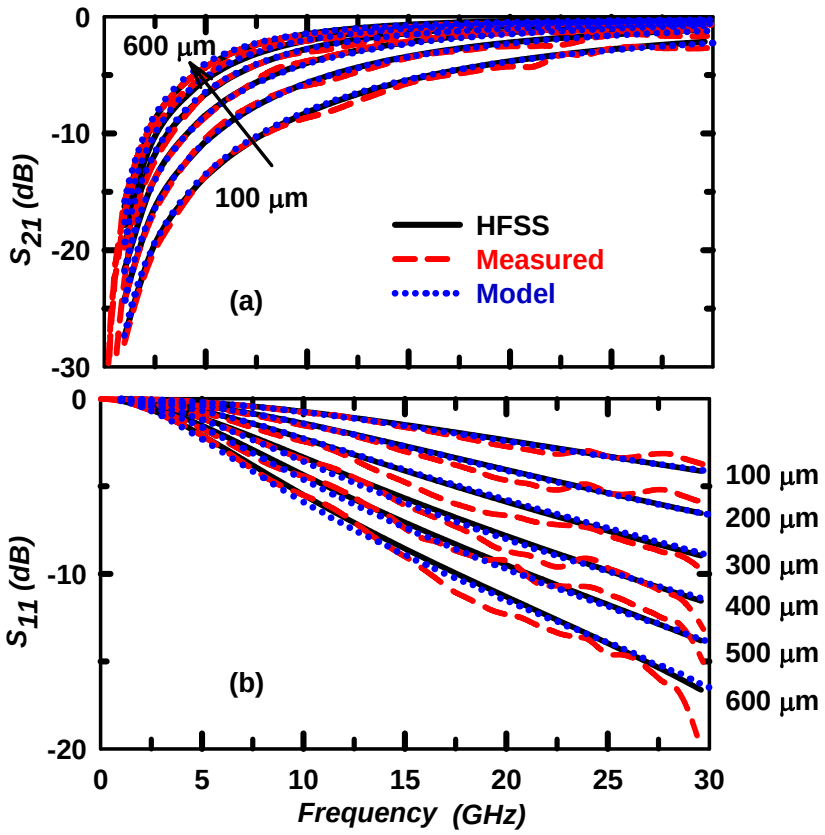

Figure 5-13: Measured, simulated and modeled magnitude of the transmission coefficient (a), and reflection coefficient (b) of several interdigital capacitors with different finger length (identified on the right axis) fabricated with LE-DPAM.

Fig. 15 (b) shows the simulated and measured Q factor, computed using (2); the measured Q values are as in the previous case extracted from the measured 2-port S-parameters, while simulated values are obtained from an equivalent RLC circuit model.

www.manaraa.com

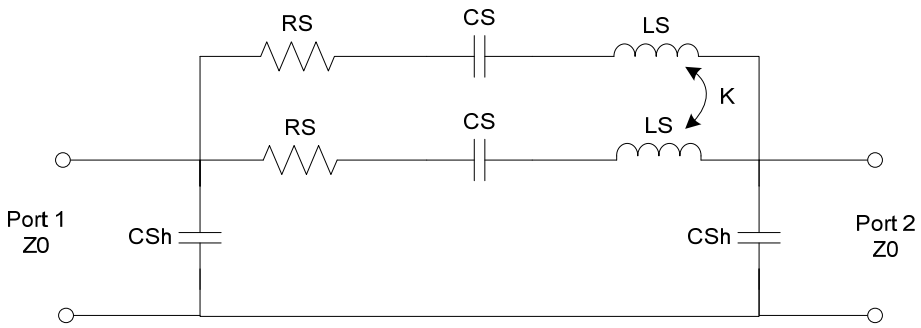

Figure 5-14: Interdigital capacitor equivalent circuit model.

Table 5-5: Interdigital capacitor equivalent circuit model values

Parameter	L=100μm	200μm	300μm	400μm	500μm	600μm
RS (Ω)	5.466	5.57	5.88	6.337	6.486	6.60
CS (ρF)	0.034	0.048	0.065	0.084	0.104	0.125
LS (nH)	0.01	0.04	0.201	0.130	0.151	0.183
CSh (ρF)	0.005	0.005	0.030	0.042	0.045	0.048
K	0.52	0.55	0.68	0.68	0.69	0.7

K = mutual inductor coupling coefficient, N Fingers= 13.

A set of simulation-based design curves that show the behavior of the capacitance at 5 GHz and 30 GHz vs. finger length, as well as self-resonance frequency vs. finger length are depicted in Fig. 5-16. These design curves cover capacitances in the range of 0.05-0.35 pF and self-resonance frequencies of 20-120 GHz.

The performance of the capacitors in this work are compared to some obtained with other AM techniques, as well as with traditional GaAs MMIC processing in Table 5-6. Compared to other AM approaches, the high Q values obtained with LE-DPAM are associated mainly with the effect of the laser processing on the walls of the silver ink slots that increases the effective conductivity, as noted above. Note that the quality factor of the capacitor and its capacitance are inversely related, and both parameters are dependent on the materials and fabrication process.

www.manaraa.com

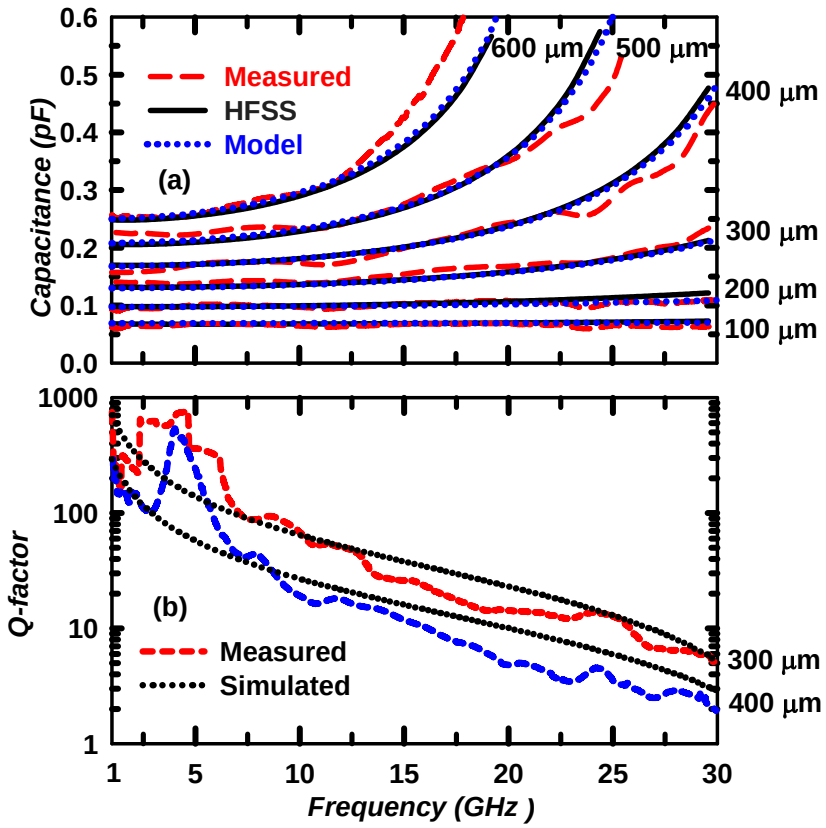

Figure 5-15: Measured, simulated and modeled capacitance (a), and quality factor (b) for interdigital capacitors with different finger lengths.

Table 5-6: Comparison with state-of-the-art AM lumped capacitors

Work	Geometry	Process	Q_{max}	C (pF)	SRF. (GHz)
This work *	Interdigital	LEDPAM	750	0.14	47
Vanukuru [35]	Interd-mom	GaAs	400	0.02	>120
Mariotti-1 et al. [33]	Circular	Inkjet	15	6	2.5
Mariotti-2 et al. [33]	Square	Copper	35	5	1
Jung et al. [36]	MIM	GaAs	1000	1.05	11.5
McKerricher [34]	MIM	Inkjet	12.9	16.6	1.3

LE DPAM: laser enhanced direct print additive manufacturing. * D=300 µm

www.manaraa.com

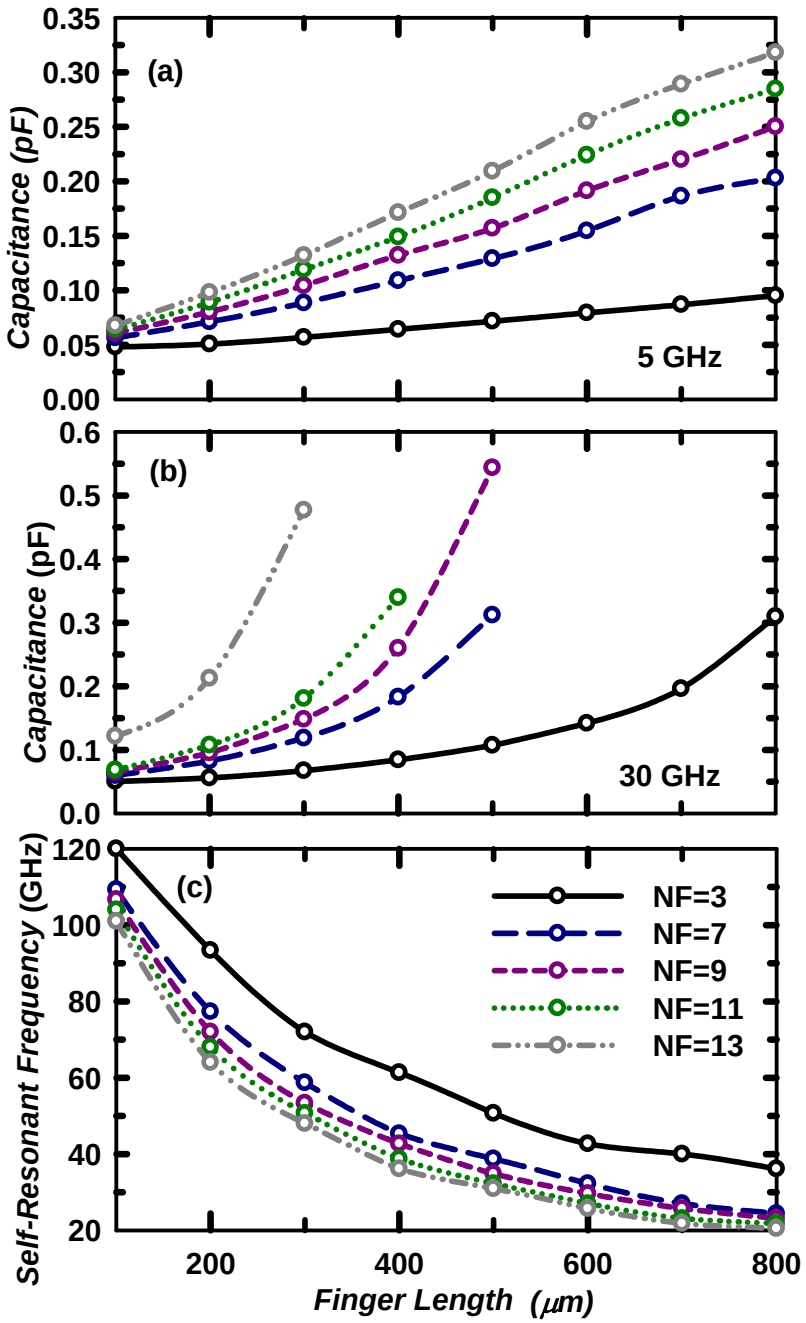

Figure 5-16: Simulated capacitance at (a) 5 GHz and (b) 30 GHz, simulated self-resonant frequency (c), for different finger length and different N° fingers.

5.5. Conclusions

A novel manufacturing process for lumped CPW interdigital capacitors and spiral inductors is presented in this section. Pico-second laser post-processing is combined with standard fused deposition

www.manaraa.com

modeling and micro-dispensing in order to develop passive elements with good performance up to mm-wave frequencies. S-parameter measurements of different prototypes were made up to 30 GHz demonstrating good agreement with simulated results. Capacitances up to 0.3 pF at 5 GHz and 0.5 at 30 GHz, with self-resonances up to 120 GHz were achieved. A maximum measured Q-factor of 750 was obtained at 1 GHz showing an improvement of 715 when compared to the next highest device in the selected published works. The same laser is used to fabricate vertical interconnects that allow for the fabrication of multilayer inductors. Inductances in the range of 0.4-3 nH are achieved, with a maximum quality factor of 21, self-resonance frequencies up to 88 GHz, and an inductance per unit of area of 5.3 nH/mm2. Interdigital capacitors in the range of 0.05-0.5 pF are fabricated, having a maximum quality factor of 750

www.manaraa.com

CHAPTER 6: ANTENNA SYSTEMS FOR RFID APPLICATIONS

6.1. Introduction

RFID applications continue to increase in number and new uses of the technology have prompted innovative tag design. Achieving smaller tag footprints is of particular importance, motivating the development of 3D designs which make more efficient use of the antenna volume [84, 85]. However, most commercial tag designs that are currently available are optimized for either on-metal or off-metal conditions, and the performance is greatly diminished when the surrounding environment differs from the intended one. As demonstrated in [84-86] dipole antennas are commonly used for off-metal systems, but fail to operate properly when mounted horizontally over or near metallic objects. On the other hand patch antennas and folded dipoles have been implemented for on-metal systems [87, 88], generally with a low off-metal read range.

In the case of a dipole antenna located close to a ground plane (e.g. separation < $\lambda g/8$), the currents of the original sources and their images are in opposite directions, therefore resulting in diminished radiated fields. Electromagnetic Band Gap (EBG) structures [89], used to create high impedance surfaces, or the introduction of folded arms to increase the radiation efficiency [88] are some of the ways that are used to address this drawback. In this chapter, different RFID antennas are presented for operation in the ISM UHF band.

The content of this chapter has been published [93] and it is included in this dissertation with permission from the IEEE. A copy of the permission is included in the Appendix A.

www.manaraa.com

6.2. UHF RFID Tags for On/Off Metal Applications Fabricated using AM

In this section, four RFID tag designs are presented that are optimized to operate in both on-metal and off-metal conditions. These designs are particularly useful for medium size to heavy equipment tracking, where the thickness of the tag is not a critical factor. The impedance matching to the passive RFID integrated circuit (IC) is achieved by two parallel stubs to ground, allowing the tags to cover both ISM RFID UHF bands (864-868 MHz and 902-928 MHz). The best achieved on-metal read range is greater than 12 m, improving upon the tag presented in [116] by ~4 m and a comparable performance with the tag presented in [117] while also having a significantly smaller footprint due to its 3D geometry. The antennas were fabricated using additive manufacturing processes: fused deposition modeling (FDM) of thermoplastic and micro-dispensing of silver paste. Meshed ground planes are used to reduce the conductive ink usage (by ~50%) and printing time, while having minimal effect on the performance. Two different planar or 2D tags with areas of 13126.5 mm2 (2DL) and 5898.7 mm2 (2DS) are presented first, followed by two 3D designs with footprints of 4639.2 mm2 (3DL) and 2524.2 mm2 (3DS)

6.2.1. Baseline 2D Tag Antenna Design and Fabrication

The geometry of the planar 2DL antenna is shown in Fig. 6-1 and is similar in size to the design in [89]. This antenna includes a thick (6 mm), low permittivity substrate for the purpose of having constructive, in-phase reflections from the ground plane. A conventional monopole antenna is used as the radiating element, aiming to achieve broadside radiation particularly while mounted on metallic objects. The dipole is also chosen due to its ease of manufacturing and integration with printed circuit boards or surface mount components, in this case the NXP UCODE G2il SL3S1203_1213 RFID passive IC, which has a sensitivity of -18 dBm. The measured electrical properties of the ABS substrate at 1 GHz are $\varepsilon r = 2.6$ and $\tan\circledcirc = 0.0058$. The monopole radiating arm measures 67.5 mm and is optimized from a $\lambda g/4$ length at the center frequency of the European (862-868MHz) and American (902-928MHz) ISM RFID bands.

www.manaraa.com

The antenna is designed to be conjugate matched to the passive IC which has normal mode impedances at 866 MHz and 915 MHz of Zin = (25-j237) Ω and Zin = (23-j224) Ω, respectively; the stable impedance over frequency makes the chip useful for dual band operation. The impedance matching from the antenna to the IC is achieved using a matching loop [85]consisting of two parallel tuning stubs connected from ground to the antenna, where the length L12 coming from ground to the monopole connection point and the width W11 are adjustable parameters to provide the necessary susceptance to achieve a matched condition. A simulated broadside gain of 3.16 dBi is achieved both on- and off-metal

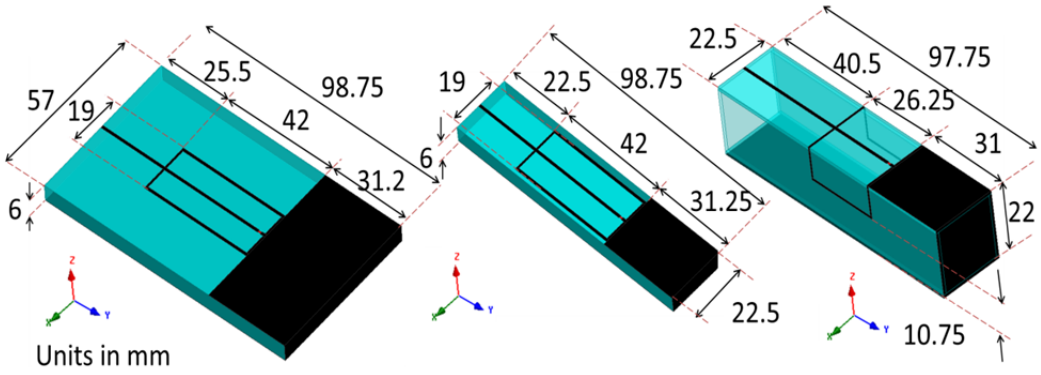

Figure 6-1: Proposed 2DL (left), 2DS (center), 3DL (right) tag geometries

6.2.2. 2D and 3D Reduced Footprint Tag Designs

Miniaturization techniques were applied to the baseline 2DL tag design, in order to reduce its footprint while aiming to maintain similar performance for both on- and off-metal applications. Fig. 6-1 (center) shows the 2DS geometry which is based on the 2DL design but has a reduced width from 57 mm to 22.5 mm, and footprint reduction of 222%.

The 2DS design keeps the substrate thickness, the geometry of the radiating element, and the matching loop from the 2DL tag constant, however the reduction of the ground plane width compromises the antenna radiation efficiency and therefore the peak broadside gain due to an increase in

www.manaraa.com

edge radiation; the simulated off-metal broadside gain for the 2DS design is 1.8 dBi compared to 3.16 dBi for the 2DL tag. The reduction in peak gain can be addressed by increasing the height of the antenna with respect to the ground plane, since often this is a dominant factor in determining the radiation properties [90].

Another approach to account for the gain reduction of the smaller ground plane is to introduce a 3D geometry. Fig. 6-1 (right) shows the proposed 3DL tag antenna which has a height of 22 mm and is printed on a 1 mm-thick substrate; its simulated off-metal peak broadside gain is 3.06 dBi. Further size reduction is achieved in the 3DS design (Fig. 6-2) by including a meandered structure, as a technique to compress the antenna into a reduced area. The 3DS tag, with a similar height of 22 mm is also fabricated on a 1 mm-thick substrate. In this design, however, a longer radiating arm is needed to overcome the reduction in effective length which is produced by greater electric field coupling between the traces [64]

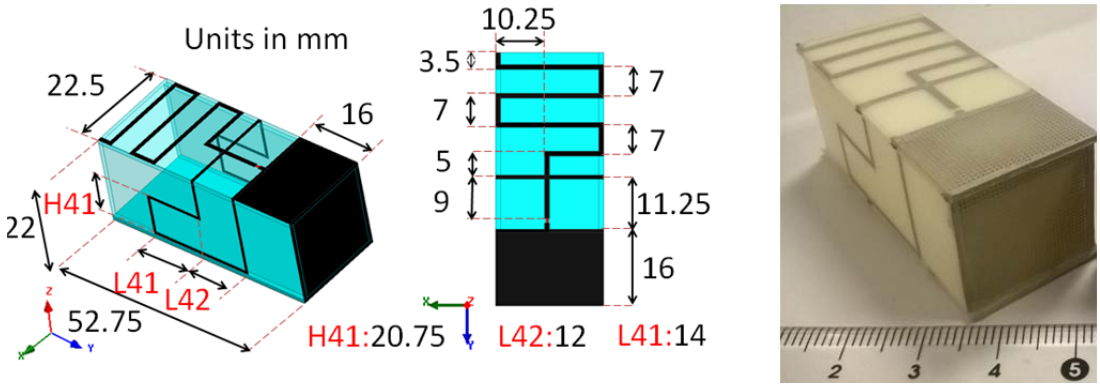

Figure 6-2: Proposed 3DS tag antenna geometry (left, center) and fabricated prototype (right).

The *3DS* geometry takes advantage of the available radiation sphere in a more efficient way when compared with the other designs [64], with an electrical size at 915 MHz of ka=0.588 compared to 1.093 (*2DL*), 0.972 (*2DS*) and 0.983 (*3DL*). The *3DS* geometry allows an area reduction compared to the *2DL* design of 520%, keeping a similar on-metal performance, with a broadside simulated gain of 5.02 dBi

www.manaraa.com

while mounted over a 0.9 m diameter copper disc, and 3 dBi gain while mounted over a 300x300 mm² rectangular ground plane. The four tag antennas show a simulated -10 dB reflection coefficient bandwidth that allows them to operate in both the European and American RFID ISM frequency bands. Simulations were performed with ANSYS HFSS 15

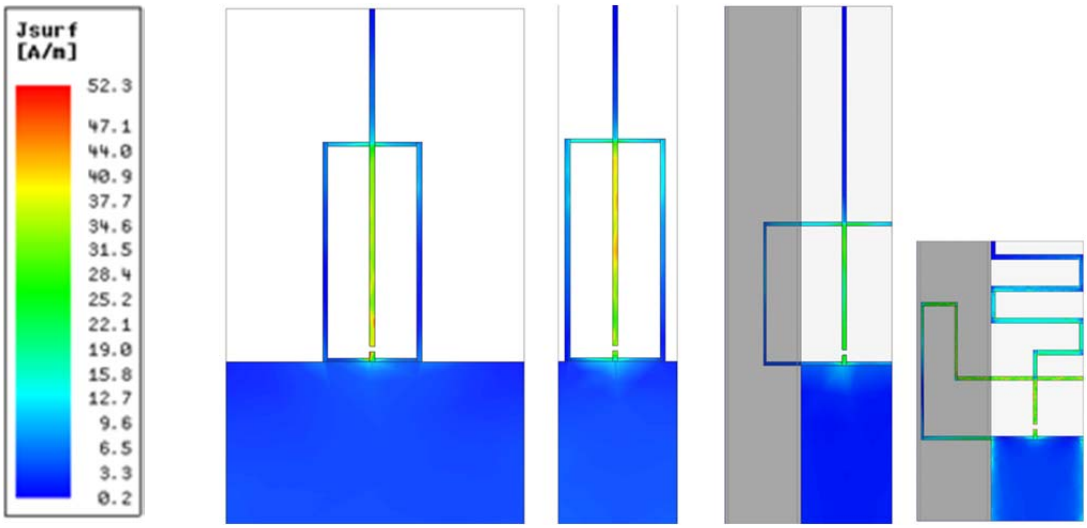

Figure 6-3: 915 MHz Current distribution. From left to right: 2DL, 2DS, 3DL, 3DS.

Fig.6- 3 shows the simulated current density at 915 MHz for the proposed tags. It is seen that the current is mainly distributed along the center arm, with a high value at the IC connection and a minimum at the end of the arm. For all the designs presented in this work the simulated polarization is linear and aligned with the main arm of the tag, Similar current distributions are observed at 864 MHz.

The 3DS meshed ground tag shown in Fig. 6-4 has an advantage of requiring less ink usage and printing time. As described in [38], the ground density (D) defines the ratio of the conductor used with the meshed ground to the conductor needed for a solid ground. If the mesh dimensions are selected as a=0.45 mm and b=0.45 mm (as illustrated in Fig. 6-4 left) the ground density is 51.5%, which means that approximately half as much ink is needed to fabricate the ground plane; a close-up of the fabricated mesh

www.manaraa.com

is shown in Fig. 6-4 (right). The simulated return loss referenced to the chip impedance for all designs is given in Fig. 6-4 (bottom).

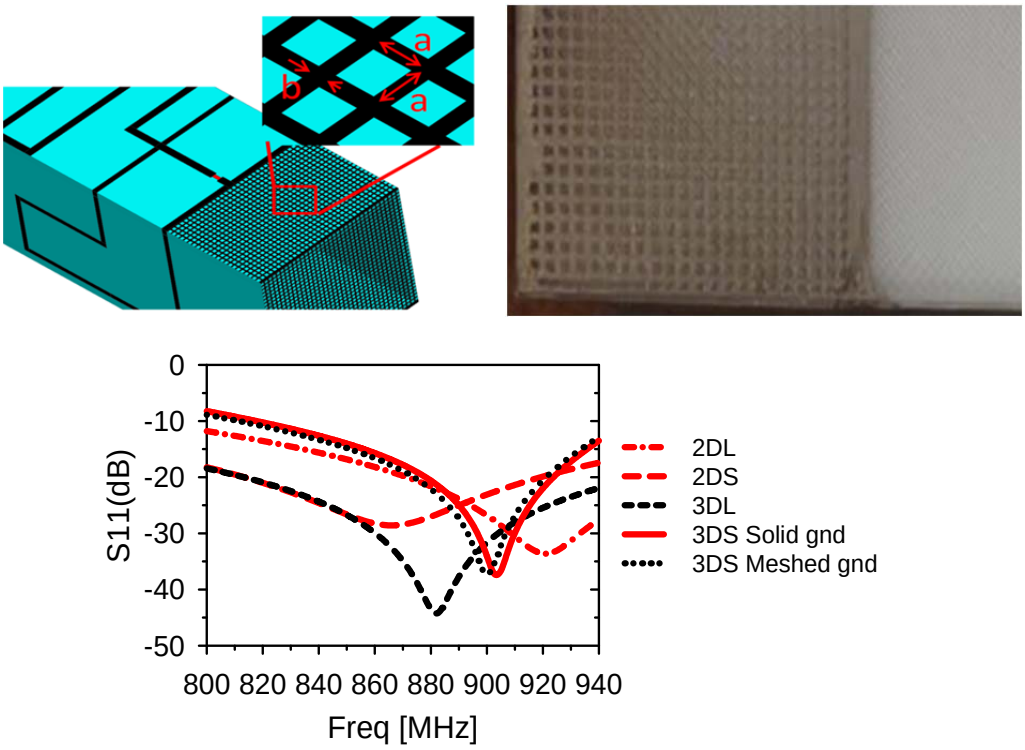

Figure 6-4: Proposed mesh ground geometry (top left), fabricated meshed ground close-up (top right) and simulated return loss (bottom)

Impedance tuning of the 3DS design to accommodate different ICs or operating frequencies can be accomplished by manipulating the length of the tuning stubs during the initial design stage. These stubs are connected to ground and wrapped around the cuboid outer walls before making contact with the radiating monopole arm, as shown on Fig. 6-2. The length L41 can be adjusted on both stub arms to fine tune the antenna's reactance, and consequently the resonant frequency. Fig. 6-5 shows changes in the antenna Zin for different L41.

The sensitivity of the 3DS antenna to the coupling between the line (L41+L42) and the ground plane is comparable to the sensitivity observed for changes in the tuning stub geometry. This observation

www.manaraa.com

is supported by simulated and measured data for designs where the line to ground plane separation varies from 1.25 mm to 3.25 mm. From these results it can be concluded that changes in the parasitic stub height H41 can be compensated by adjustments in the overall stub length, to maintain a desired resonant frequency without perturbing the antenna's performance.

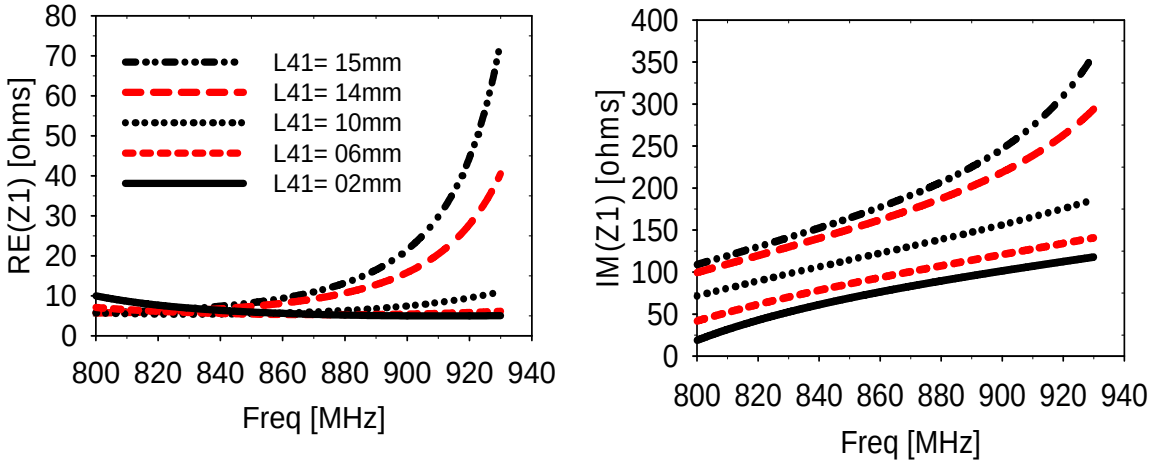

Figure 6-5: Real (left) and imaginary part (right) of the simulated 3DS input impedance

6.2.3. General Fabrication Process

Fused deposition modeling (FDM) and micro-dispensing are the technologies used to fabricate the dielectric and conductive layers, respectively. Both processes are realized using an nScrypt Tabletop 3Dn printer. The dielectric sections for both 3D designs are fabricated by printing each of the 1 mm-thick ABS slabs individually with FDM using 0.25 mm-thick layers. The printer temperature settings are 110° C for the bed, and 235°C for the nozzle, printing speed is 20 mm/s and the tip used has a 250 ◎m inner diameter. The micro-dispensing head is then used to deposit the silver paste (Dupont CB028) to pattern the antenna elements; the paste is dried at 90°C for 1 h. The printer settings are pressure of 12 psi and printing height of 100 ◎m. Finally, the parts are manually bound into a hollow package using a two part epoxy resin.

www.manaraa.com

6.2.4. Measured Results

The on/off-metal performance of the four fabricated tags was measured and compared against those of each other, different commercially available tags and previously published tags. Radiation pattern measurements were made inside an anechoic chamber. Read range measurements were performed using a movable fixture to manually adjust the distance following an approach similar to [91]. A CS101 Handheld RFID and Motorola MC9090-G readers were used to determine read range for each tag, due to their power adjustment capability; the distance was measured with a BOSCH GLM15 laser measure tool. The reader power setting (threshold power) was increased from 10 dBm up to 31 dBm and plotted against maximum read distance. Data was fitted with a model consistent with the Friis equation: $log10\ (1/d2)$, where d is the distance between the reader and the tag.

Fig. 6-6 (a) and 6-6 (b) show the measured off-metal and on-metal threshold power, respectively, against maximum read distance. For a 31 dBm threshold power the 3DL and 3DS tags reach an off-metal read distance of approximately 11 m, almost 2 meters better than what is obtained with the larger 2DL design. The on-metal measurements were performed with the tags placed on a 300x300 mm2 copper plane. For a 31 dBm threshold power the 3DL and 3DS tags reach an on-metal read distance of approximately 12.5 meters, almost 4 meters better than what is obtained with the larger 2DL design. Fig. 6-6 (c) shows a comparison of the on-metal 3DS tag performance against commercially available tags from Xerafy ® (NanoX II and Platinum Metal Skin label) and Confidex ® (Steelwavemicro and Ironside Micro) for three scenarios: off-metal, on-metal, and separated one inch from ground with a plastic stand-off (Fig. 6-6 (d)). The stand-off is intended to emulate the height of the 3DS geometry. Although the on-metal measured read distance improves with the additional height, the largest distance obtained is below the one achieved with the 3DS tag. Fig. 6-7 shows the simulated and measured off- and on-metal E- and H-plane normalized gain patterns.

www.manaraa.com

Table 6-1 shows a comparison of measured read range of the four proposed tags and several previously published tags. With an on-metal read range of 12.5 meters, the 3DS geometry has an improvement of 3.8 meters with respect to [89]. Although the tag reported in [92] shows better read range, it occupies 12.8 times the volume of the 3DS tag.

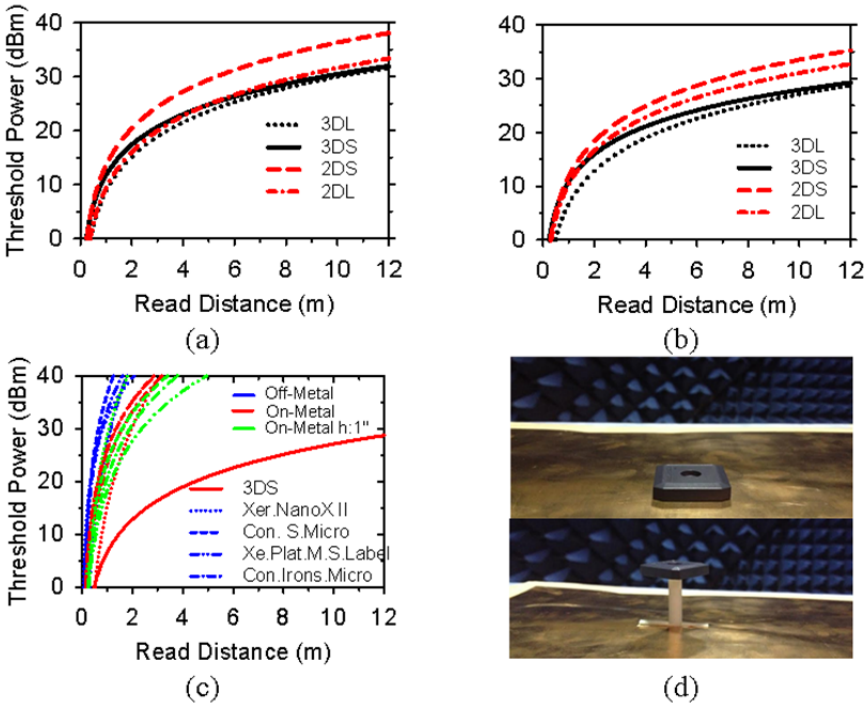

Figure 6-6: Read distance comparisons. Off-metal (a), on-metal (b), and against commercially available tags (c). Tags on-metal and 1" away from metal (d).

Table 6-1: Measured read range comparison

Element	Size (mm^3)	Off Metal (m)	On Metal (m)	Reader Power (W)
2DL [93]	98.7x57x6	10.0	10.2	1.25
2DS [93]	98.7x22x6	6.5	7.9	1.25
3DL [93]	97.7x22.5x22	11.5	12.5	1.25
3DS [93]	52.7x22.5x22	11.3	12.1	1.25
AMC M [89]	83.6x83.6x2.5	10.0	8.3	4
3-Arm[88]	125.5x140x1.5	2.0	5.0	2
Patch[87]	140x40x2	-	2.5	4
PIFA Array [94]	127x52x0.8	2.5	2.4	1.25
Dual PIFA [95]	64x64x2	-	10.2	4
Compact PIFA [96]	39x40x4	-	6.33	4
Cavity Structure[92]	176x61x31	11.0	15.0	4

www.manaraa.com

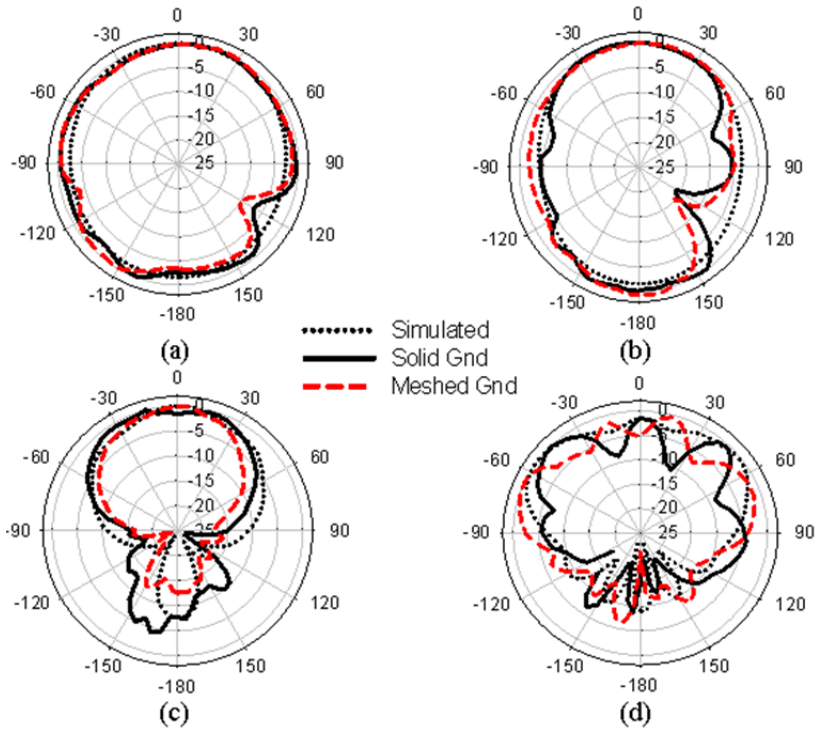

Figure 6-7: Normalized radiation patterns. Off-metal E-plane (a) and H-plane (b); on-metal E-plane (c) and H-plane (d)

6.3. Conclusions

In this chapter, four different RFID tag antennas built on ABS substrates have been developed for dual band operation (ISM UHF 864-868 MHz and 902-928 MHz). A baseline 2DL tag design was presented initially with a similar on- and off-metal performance; this design was then compressed into 3 different versions with smaller footprint and volume. For a threshold power of 31 dBm the maximum measured on- and off –metal read distance is 12.5 m and 11.5 m respectively from the 3DL design with dimensions of 97.75x 22.5x 22mm3, a similar performance was then obtained with a more compact design 3DS with dimensions of 52.75x 22.5x 22mm3 and read range on/off-metal of 12.1m and 11.3m respectively. Impedance matching and tunability was obtained by two stubs to ground, allowing functionality with multiple RFID passive ICs. It is also shown that for the 3D printed versions, the ink needed to print the tags can be reduced by ~50% by using a meshed ground approach with minimal effect

www.manaraa.com

on the read range. The performance is compared with that of tags commercially available and reported in the literature, under on- and off-metal conditions. Designs described in this work are useful in applications were the thickness of the tag is not critical, presenting an improvement in read range, gain, and area.

www.manaraa.com

CHAPTER 7: SUMMARY AND RECOMMENDATIONS

7.1. Summary

This work is focused mainly on the development and characterization of additively manufactured on-package multipolar antenna systems intended for machine-to-machine and chip-to-chip communications in high multipath environments. Three different 2.4 GHz additively manufactured 3D tripolar antenna system are presented for integration with commercial wireless sensor nodes. Each individual system switches electronically between three mutually-orthogonal $\lambda/4$ monopoles or array of elements to achieve distinct polarization states, improving link reliability significantly through selection diversity. Antenna performance was demonstrated under ideal anechoic conditions but more importantly in a harsh multipath and depolarization environment where it was shown to effectively mitigate these effects with little added complexity to the system design.

In order to incorporate the proposed multipolar system into integrated circuit dies for inter chip data transmission at microwave and mm-wave frequencies, a novel MMIC packaging and interconnection solution is presented, the process is realized with Laser Enhanced Direct Print Additive Manufacturing (LE-DPAM) a technology that combines fused deposition modeling (FDM) of plastics, micro-dispensing of silver paste and pico-second laser machining. A low noise amplifier is packaged, integrated and cascaded with an external hybrid board and MMIC die with no significant effects on the overall performance. On-wafer probe measurements of the broadband amplifier reveal only 0.2 dB/mm insertion loss at 20 GHz for a transmission line on ABS substrate and exhibits satisfactory return loss at both input and output terminals. A 17 GHz microstrip patch antenna is then fabricated and characterized

www.manaraa.com

on top of the proposed package as a demonstration of a package integrated single polarity planar antenna.

Additionally the results in this work show that LE-DPAM enables the fabrication of lumped mm-wave components with high capacitance or inductance per unit area. The quality factors are in general better than those obtained with other AM techniques, and are reaching the performance obtained with GaAs MMIC processing. Such passive components are important for the realization of RF front ends using AM. The LE-DPAM approach offers broad design freedom, where MMIC dies can be packaged and interconnected with multilayer passive elements, all using a single tool. These packages can be integrated into larger systems, to achieve structural electronics with reduced size and weight.

Finally, different RFID tag antennas built on ABS substrates were developed for dual band operation (ISM UHF 864-868 MHz and 902-928 MHz) , specially designed for on- and off-metal scenarios achieving read ranges up to 12.1 m The performance is compared with that of tags commercially available and reported in the literature, under on- and off-metal conditions presenting improvements in read range, gain, and area.

7.2. Recommendations for Future Work

Based on the systems, devices and fabrication processes presented in this work some additional topics are presented as motivation for future work.

a) It has been shown that Laser Enhanced Direct Print Additive Manufacturing (LE-DPAM) is a very useful technology for the fabrication of microwave and mm-Wave devices, especially for the manufacturing of low-cost, high performance MMIC packaging and interconnections. Future work might include a thorough study and characterization of the package mechanical properties including thermal performance and humidity absorption, as well as a better characterization of the electrical interconnection between the IC's gold plated pad and the micro-dispensed silver paste transmission line.

www.manaraa.com

b) It has been shown that the integration of tripolar antenna systems into wireless sensor nodes at microwave frequencies successfully mitigate harsh channel conditions presented in many M2M deployments; conditions such as multipath and depolarization. It is proposed as future work to develop a tripolar antenna system integrated onto the package presented in Chapter 4 for chip-to chip communications at mm-Wave frequencies. The tripolar antenna might be integrated to an MMIC SP3T switch following a similar procedure to the one presented in Section 4.5 where a single polarity planar antenna was fabricated and characterized.

c) Further improvements can be made into the fabrication and performance of lumped passive elements, smaller sizes with higher self-resonance frequencies can be obtained with different laser settings (i.e. wavelength, optics) to achieve cuts down to ~ 3 μm wide. Additionally, further enhancement in 3D printable material properties (i.e. Ink conductivity and substrate loss tangent) will yield better overall performance with higher quality factor values.

d) Implementation of the presented lumped passive elements, (i.e. interdigital capacitors and spiral inductors) in mm-Wave filters, resonators and matching circuits is proposed as a mean to evaluate combined performance.

e) The LE-DPAM technology utilized in this work allows the fabrication of conformal 3D systems for microwave and mm-Wave applications, future work might include successful integration of multi-layer and multi-material devices onto 3D structures.

.

www.manaraa.com

REFERENCES

[1] Y. Mehmood, N. Haider, M. Imran, A. Timm-Giel, and M. Guizani, "M2M Communications in 5G: State-of-the-Art Architecture, Recent Advances, and Research Challenges," *IEEE Communications Magazine,* vol. 55, pp. 194-201, 2017.

[2] (Jul. 2017). *Global machine to machine (M2M) market*. Available: http://www.marketsandmarkets.com/Market-Reports/machine-tomachine-market-732.html.

[3] (Nov. 2016). *Projected machine-to-machine industry size*. Available: https://www.statista.com/topics/1843/m2m-machine-to-machine.

[4] M. Golmohamadi, R. Ramirez, B. Hewgill, J. Jamison, J. Frolik, and T. Weller, "Characterization of a geometrically constrained tripolar antenna under M2M channel conditions," in *2017 11th European Conference on Antennas and Propagation (EUCAP)*, 2017, pp. 2998-3002.

[5] M. Golmohamadi and J. Frolik, "Depolarization in three dimensions: Theoretical formulations and empirical results," in *2016 IEEE 17th Annual Wireless and Microwave Technology Conference (WAMICON)*, 2016, pp. 1-6.

[6] J. Frolik and M. Golmohamadi, "On Random and Multidimensional Channel Effects in Cluttered Environments," *IEEE Antennas and Wireless Propagation Letters,* vol. 16, pp. 1863-1866, 2017.

[7] A. Goldsmith, *Wireless Communications*: Cambridge University Press, 2005.

[8] C. J. William and C. C. Donald, *Microwave Mobile Communications*: Wiley-IEEE Press, 1994.

[9] L. Simic, S. M. Berber, and K. W. Sowerby, "Energy-Efficiency of Cooperative Diversity Techniques in Wireless Sensor Networks," in *2007 IEEE 18th International Symposium on Personal, Indoor and Mobile Radio Communications*, 2007, pp. 1-5.

[10] B. Kusy, D. Abbott, C. Richter, C. Huynh, M. Afanasyev, W. Hu, *et al.*, "Radio diversity for reliable communication in sensor networks," *ACM Trans. Sen. Netw.,* vol. 10, pp. 1-29, 2014.

[11] L. Vallozzi, H. Rogier, and C. Hertleer, "Dual Polarized Textile Patch Antenna for Integration Into Protective Garments," *IEEE Antennas and Wireless Propagation Letters,* vol. 7, pp. 440-443, 2008.

[12] P. Vanveerdeghem, P. V. Torre, C. Stevens, J. Knockaert, and H. Rogier, "Flexible dual-diversity wearable wireless node integrated on a dual-polarised textile patch antenna," *IET Science, Measurement & Technology,* vol. 8, pp. 452-458, 2014.

[13] M. R. Andrews, P. P. Mitra, and R. deCarvalho, "Tripling the capacity of wireless communications using electromagnetic polarization," *Nature,* vol. 409, p. 316, 01/18/online 2001.

www.manaraa.com

[14] D. J. Edwards, T. Hao, W. Q. Malik, and C. J. Stevens, "Planar tripolar antenna," ed: Google Patents, 2011.

[15] A. S. Konanur, K. Gosalia, S. H. Krishnamurthy, B. Hughes, and G. Lazzi, "Increasing wireless channel capacity through MIMO systems employing co-located antennas," *IEEE Transactions on Microwave Theory and Techniques,* vol. 53, pp. 1837-1844, 2005.

[16] N. Das, T. Inoue, T. Taniguchi, and a. Y. Karasawa, "An experiment on MIMO system having three orthogonal polarization diversity branches in multipath-rich environment," presented at the Vehicular Technology Conference, Los Angeles CA, Sept. 2004.

[17] O. A. Peverini, M. Lumia, F. Calignano, G. Addamo, M. Lorusso, E. P. Ambrosio, *et al.*, "Selective Laser Melting Manufacturing of Microwave Waveguide Devices," *Proc. IEEE,* vol. 105, pp. 620-631, Apr. 2017.

[18] C. Guo, X. Shang, J. Li, F. Zhang, M. J. Lancaster, and J. Xu, "A Lightweight 3-D Printed X-Band Bandpass Filter Based on Spherical Dual-Mode Resonators," *IEEE Microw. Compon. Lett.,* vol. 26, pp. 568-570, 2016.

[19] W. Su, B. S. Cook, and M. M. Tentzeris, "Additively Manufactured Microfluidics-Based "Peel-and-Replace" RF Sensors for Wearable Applications," *IEEE Transactions on Microwave Theory and Techniques,* vol. 64, pp. 1928-1936, 2016.

[20] K. Shi and X. Qin, "Stigmergy based autonomous shop floor control with wireless sensor networks," in *2011 9th IEEE International Conference on Industrial Informatics*, 2011, pp. 375-380.

[21] J. Åkerberg, M. Gidlund, and M. Björkman, "Future research challenges in wireless sensor and actuator networks targeting industrial automation," in *2011 9th IEEE International Conference on Industrial Informatics*, 2011, pp. 410-415.

[22] R.Ketcham and J.Herbst, "Integration of a wireless sensor data aggregation system and HUMS," in *American Helicopter Society (AHS)International 69th Annual Forum & Technology Display*, Phoenix AZ, 2013.

[23] J. Frolik, V. Sipal, and D. J. Edwards, "Leveraging Depolarization to Increase the Link Reliability for Wireless Sensors Operating in Hyper-Rayleigh Environments," *IEEE Sensors Journal,* vol. 14, pp. 2442-2446, 2014.

[24] A. Molisch, *Wireless Communications*: Wiley-IEEE Press, 2005.

[25] J. Frolik, "A case for considering hyper-Rayleigh fading channels," *IEEE Transactions on Wireless Communications,* vol. 6, pp. 1235-1239, 2007.

[26] J. Frolik, "Mitigating severe channel effects using tripolar antenna diversity," in *2015 9th European Conference on Antennas and Propagation (EuCAP)*, 2015, pp. 1-4.

[27] S. C. Kwon and G. L. Stuber, "Geometrical Theory of Channel Depolarization," *IEEE Transactions on Vehicular Technology,* vol. 60, pp. 3542-3556, 2011.

www.manaraa.com

[28] H. Wang, L. Liu, Z. Zhang, Y. Li, and Z. Feng, "Ultra-Compact Three-Port MIMO Antenna With High Isolation and Directional Radiation Patterns," *IEEE Antennas and Wireless Propagation Letters,* vol. 13, pp. 1545-1548, 2014.

[29] W. Tzuenn-Yih, F. Shyh-Tirng, and W. Kin-Lu, "Printed diversity monopole antenna for WLAN operation," *Electronics Letters,* vol. 38, pp. 1625-1626, 2002.

[30] B. N. Getu and J. B. Andersen, "The MIMO cube - a compact MIMO antenna," *IEEE Transactions on Wireless Communications,* vol. 4, pp. 1136-1141, 2005.

[31] D. Edwards, T. Hao, W. Malik , and a. C. Stevens, "Planar Tripolar Antenna," US Patent US20110006960, January 13, 2011.

[32] F. Cai, Y. H. Chang, K. Wang, C. Zhang, B. Wang, and J. Papapolymerou, "Low-Loss 3-D Multilayer Transmission Lines and Interconnects Fabricated by Additive Manufacturing Technologies," *IEEE Trans. Microw. Theory Techn.,* vol. 64, No. 10, pp. 3208-3216, 2016.

[33] C. Mariotti, F. Alimenti, L. Roselli, and M. M. Tentzeris, "High-Performance RF Devices and Components on Flexible Cellulose Substrate by Vertically Integrated Additive Manufacturing Technologies," *IEEE Trans. Microw. Theory Techn.,* vol. 65 No. 1, pp. 1-10, 2017.

[34] G. McKerricher, J. G. Perez, and A. Shamim, "Fully Inkjet Printed RF Inductors and Capacitors Using Polymer Dielectric and Silver Conductive Ink With Through Vias," *IEEE Transactions on Electron Devices,* vol. 62, pp. 1002-1009, 2015.

[35] V. N. R. Vanukuru, "Millimeter-wave bandpass filter using high-Q conical inductors and MOM capacitors," in *2016 IEEE Radio Frequency Integrated Circuits Symposium (RFIC)*, 2016, pp. 39-42.

[36] Y. H. Jung, T.-H. Chang, H. Zhang, C. Yao, Q. Zheng, V. W. Yang, *et al.*, "High-performance green flexible electronics based on biodegradable cellulose nanofibril paper," *Nature Communications,* vol. 6, p. 7170, 05/26/online 2015.

[37] E. A. Rojas-Nastrucci, T. Weller, V. Lopez Aida, C. Fan, and J. Papapolymerou, "A study on 3D-printed coplanar waveguide with meshed and finite ground planes," in *Wireless and Microwave Technology Conference (WAMICON), 2014 IEEE 15th Annual*, 2014, pp. 1-3.

[38] E. A. Rojas-Nastrucci, A. D. Snider, and T. M. Weller, "Propagation Characteristics and Modeling of Meshed Ground Coplanar Waveguide," *IEEE Transactions on Microwave Theory and Techniques,* vol. 64, pp. 3460-3468, 2016.

[39] S.-Y. Wu, C. Yang, W. Hsu, and L. Lin, "3D-printed microelectronics for integrated circuitry and passive wireless sensors," *Microsystems &Amp; Nanoengineering,* vol. 1, p. 15013, 07/20/online 2015.

[40] I. A. Ukaegbu, K. s. Choi, O. Hidayov, J. Sangirov, T. w. Lee, and H. h. Park, "Small-area and high-inductance semi-stacked spiral inductor with high Q factor," *IET Microwaves, Antennas & Propagation,* vol. 6, pp. 880-883, 2012.

[41] I. Wolff, *Coplanar Microwave Integrated Circuits*: Wiley, 2006.

www.manaraa.com

[42] T. P. Ketterl, Y. Vega, N. C. Arnal, J. W. I. Stratton, E. A. Rojas-Nastrucci, M. F. Córdoba-Erazo, *et al.*, "A 2.45 GHz Phased Array Antenna Unit Cell Fabricated Using 3-D Multi-Layer Direct Digital Manufacturing," *IEEE Transactions on Microwave Theory and Techniques*, vol. 63, pp. 4382-4394, 2015.

[43] N. Arnal, T. Ketterl, Y. Vega, J. Stratton, C. Perkowski, P. Deffenbaugh, *et al.*, "3D multi-layer additive manufacturing of a 2.45 GHz RF front end," in *Microwave Symposium (IMS), 2015 IEEE MTT-S International*, 2015, pp. 1-4.

[44] E. A. Rojas-Nastrucci, R. Ramirez, D. Hawatmeh, D. Lan, J. Wang, and T. Weller, "Laser enhanced direct print additive manufacturing for mm-wave components and packaging," in *2017 International Conference on Electromagnetics in Advanced Applications (ICEAA)*, 2017, pp. 1531-1534.

[45] E. A. Rojas-Nastrucci, H. Tsang, P. I. Deffenbaugh, R. A. Ramirez, D. Hawatmeh, A. Ross, *et al.*, "Characterization and Modeling of K-Band Coplanar Waveguides Digitally Manufactured Using Pulsed Picosecond Laser Machining of Thick-Film Conductive Paste," *IEEE Transactions on Microwave Theory and Techniques*, 2017.

[46] E. A. Rojas-Nastrucci, R. A. Ramirez, and T. M. Weller, "Direct Digital Manufacturing of mm-Wave Vertical Interconnects," presented at the Wireless and Microwave Technology Conference (WAMICON), 2018.

[47] I. Ju, I. b. Yom, and K. K. Ryu, "Design and verification of SMT MMIC package using a 20 GHz LNA, a 40 GHz LNA and a 40GHz digital attenuator," in *2013 IEEE 22nd Conference on Electrical Performance of Electronic Packaging and Systems*, 2013, pp. 255-258.

[48] H. C. Huang, A. Ezzeddine, A. Darwish, B. Hsu, J. Williams, and S. Peak, "Ku-band MMIC's in low-cost, SMT compatible packages," in *2002 IEEE MTT-S International Microwave Symposium Digest (Cat. No.02CH37278)*, 2002, pp. 27-30 vol.1.

[49] T. Lu, J. Kulick, J. Lannon, G. Bernstein, and P. Fay, "Heterogeneous microwave and millimeter-wave system integration using quilt packaging," in *2016 IEEE MTT-S International Microwave Symposium (IMS)*, 2016, pp. 1-4.

[50] M. Imagawa, S. Fujita, T. Satoh, T. Tokumitsu, and Y. Hasegawa, "Cost effective Wafer-Level Chip Size Package technology and application for high speed wireless communications," in *2009 European Microwave Integrated Circuits Conference (EuMIC)*, 2009, pp. 49-52.

[51] B. Zheng, J. R. Cubillo, G. Katti, C. Jin, R. Rajoo, and K. C. Chan, "Study on low-cost QFN packages for high-frequency applications," in *2012 IEEE 14th Electronics Packaging Technology Conference (EPTC)*, 2012, pp. 401-406.

[52] M. C. Hsieh, S. Lin, I. Hsu, C. Y. Chen, and N. Cho, "Fine pitch high bandwidth flip chip package-on-package development," in *2017 21st European Microelectronics and Packaging Conference (EMPC) & Exhibition*, 2017, pp. 1-5.

[53] M. L. Wu, S. Y. Chiou, and Y. M. Hwang, "Empirical Equations for Optimization Conditions in Thermal Compression Bonding of Copper Pillar Flip Chip Packages," *IEEE Transactions on Components, Packaging and Manufacturing Technology*, pp. 1-5, 2018.

www.manaraa.com

[54] S. G. Mehta, L. E. Milner, and M. E. Parker, "A 70 GHz chip to printed circuit board interconnect using Kapton flexible substrate," in *2016 IEEE 2nd Australian Microwave Symposium (AMS)*, 2016, pp. 9-10.

[55] B. K. Tehrani, B. S. Cook, and M. M. Tentzeris, "Inkjet-printed 3D interconnects for millimeter-wave system-on-package solutions," in *2016 IEEE MTT-S International Microwave Symposium (IMS)*, 2016, pp. 1-4.

[56] B. K. Tehrani, J. Bito, B. S. Cook, and M. M. Tentzeris, "Fully inkjet-printed multilayer microstrip and T-resonator structures for the RF characterization of printable materials and interconnects," in *2014 IEEE MTT-S International Microwave Symposium (IMS2014)*, 2014, pp. 1-4.

[57] S. Pavlidis, B. Wright, and J. Papapolymerou, "3-D printed substrates for MMIC packaging," in *2017 IEEE Radio and Wireless Symposium (RWS)*, 2017, pp. 79-82.

[58] R. A. Ramirez, D. Lan, J. Wang, and T. M. Weller, "MMIC packaging and on-chip low-loss lateral interconnection using additive manufacturing and laser machining," in *2017 IEEE MTT-S International Microwave Symposium (IMS)*, 2017, pp. 38-40.

[59] B. K. Tehrani, B. S. Cook, and M. M. Tentzeris, "Post-process fabrication of multilayer mm-wave on-package antennas with inkjet printing," in *2015 IEEE International Symposium on Antennas and Propagation & USNC/URSI National Radio Science Meeting*, 2015, pp. 607-608.

[60] S. Mandal, S. K. Mandal, and A. K. Mal, "On-chip antennas using standard CMOS technology: A brief overview," in *2017 International Conference on Innovations in Electronics, Signal Processing and Communication (IESC)*, 2017, pp. 74-78.

[61] B. K. Tehrani and M. M. Tentzeris, "Substrate-independent system-on-package antenna integration with inkjet printing," in *2016 IEEE International Symposium on Antennas and Propagation (APSURSI)*, 2016, pp. 827-828.

[62] Y. Yao, H. Yu, J. Yu, and X. Chen, "Design of dual-band compact ceramic chip antenna for terminal applications," in *2017 11th European Conference on Antennas and Propagation (EUCAP)*, 2017, pp. 1980-1983.

[63] M. I. M. Ghazali, J. A. Byford, S. Karuppuswami, A. Kaur, J. Lennon, and P. Chahal, "3D Printed Out-of-Plane Antennas for Use on High Density Boards," in *2017 IEEE 67th Electronic Components and Technology Conference (ECTC)*, 2017, pp. 1835-1842.

[64] J. L. Volakis, C. C. Chen, and K. Fujimoto, *Small Antennas : Miniaturization Techniques & Applications* vol. 1. USA, 2010.

[65] J. Frolik, "Deciwavelength-scale fade mitigation," in *The 8th European Conference on Antennas and Propagation (EuCAP 2014)*, 2014, pp. 1026-1028.

[66] R. A. Ramirez, D. Lugo, T. M. Weller, M. Golmohamadi, and J. Frolik, "Additive manufactured tripolar antenna system for link improvement in high multipath environments," in *2017 IEEE International Symposium on Antennas and Propagation & USNC/URSI National Radio Science Meeting*, 2017, pp. 2539-2540.

[67] N.A. (2017). *Nscrypt, micro-dispensing*. Available: www.nscrypt.com/micro-dispensing/

www.manaraa.com

[68] R. A. Ramirez, M. Golmohamadi, J. Frolik, and T. M. Weller, "3D printed on-package tripolar antennas for mitigating harsh channel conditions," in *2017 IEEE Radio and Wireless Symposium (RWS)*, 2017, pp. 62-64.

[69] N. P. Lawrence, C. Fumeaux, and D. Abbott, "Planar Triorthogonal Diversity Slot Antenna," *IEEE Transactions on Antennas and Propagation,* vol. 65, pp. 1416-1421, 2017.

[70] S. M. Mikki and Y. M. M. Antar, "On Cross Correlation in Antenna Arrays With Applications to Spatial Diversity and MIMO Systems," *IEEE Transactions on Antennas and Propagation,* vol. 63, pp. 1798-1810, 2015.

[71] K. R. Jha and S. K. Sharma, "Combination of MIMO Antennas for Handheld Devices [Wireless Corner]," *IEEE Antennas and Propagation Magazine,* vol. 60, pp. 118-131, 2018.

[72] J. Frolik, T. M. Weller, S. DiStasi, and J. Cooper, "A Compact Reverberation Chamber for Hyper-Rayleigh Channel Emulation," *IEEE Transactions on Antennas and Propagation,* vol. 57, pp. 3962-3968, 2009.

[73] E. Genender, C. L. Holloway, K. A. Remley, J. M. Ladbury, G. Koepke, and H. Garbe, "Simulating the Multipath Channel With a Reverberation Chamber: Application to Bit Error Rate Measurements," *IEEE Transactions on Electromagnetic Compatibility,* vol. 52, pp. 766-777, 2010.

[74] C. Xiaoming and P. S. Kildal, "Accuracy of antenna input reflection coefficient and mismatch factor measured in reverberation chamber," in *2009 3rd European Conference on Antennas and Propagation*, 2009, pp. 2678-2681.

[75] N. Wisitpongphan, G. Ferrari, S. Panichpapiboon, J. S. Parikh, and O. K. Tonguz, "QoS provisioning using BER-based routing in ad hoc wireless networks," in *2005 IEEE 61st Vehicular Technology Conference*, 2005, pp. 2483-2487 Vol. 4.

[76] T. Yélémou, J. Ledy, B. Hilt, A. M. Poussard, and P. Meseure, "Performance comparison of BER-based routing protocols under realistic conditions," in *2011 IEEE 36th Conference on Local Computer Networks*, 2011, pp. 259-262.

[77] T. P. Ketterl, "A 2.45 GHz Phased Array Antenna Unit Cell Fabricated Using 3-D Multi-Layer Direct Digital Manufacturing," *IEEE Trans. Microw. Theory Techn.*, vol. 63, No. 12, pp. 4382-4394, Dec. 2015.

[78] M. F. Cordoba-Erazo and T. M. Weller, "Noncontact Electrical Characterization of Printed Resistors Using Microwave Microscopy," *Instrumentation and Measurement, IEEE Transactions on,* vol. 64, pp. 509-515, 2015.

[79] A. Vera López, E. A. Rojas-Nastrucci, M. Córdoba-Erazo, T. Weller, and J. Papapolymerou, "Ka-Band Characterization and RF Design of Acrylonitrile Butadiene Styrene (ABS)," presented at the 2015 IEEE MTT-S International Microwave Symposium (IMS), 2015.

[80] A. L. Vera-López, E. A. Rojas-Nastrucci, M. Córdoba-Erazo, T. Weller, and J. Papapolymerou, "Ka-band characterization and RF design of Acrynolitrile Butadiene Styrene (ABS)," in *2015 IEEE MTT-S International Microwave Symposium*, 2015, pp. 1-4.

www.manaraa.com

[81] M. F. Córdoba-Erazo, E. A. Rojas-Nastrucci, and T. Weller, "Simultaneous RF electrical conductivity and topography mapping of smooth and rough conductive traces using microwave microscopy to identify localized variations," in *2015 IEEE 16th Annual Wireless and Microwave Technology Conference (WAMICON)*, 2015, pp. 1-4.

[82] J. Castro, E. A. Rojas-Nastrucci, A. Ross, T. M. Weller, and J. Wang, "Fabrication, Modeling, and Application of Ceramic-Thermoplastic Composites for Fused Deposition Modeling of Microwave Components," *IEEE Transactions on Microwave Theory and Techniques*, vol. 65, pp. 2073-2084, 2017.

[83] R. A. Ramirez, D. Lan, E. A. Rojas-Nastrucci, and T. Weller, "Laser Assisted Additive Manufacturing of CPW mm-Wave Interdigital Capacitors," presented at the 2018 IEEE MTT-S International Microwave Symposium (IMS), 2018.

[84] W. Hongwei, W. Yunling, L. Yu, and Y. Wensheng, "3D antenna for UHF RFID tags with near omni-direction," in *Antennas, Propagation and EM Theory, 2008. ISAPE 2008. 8th International Symposium on*, 2008, pp. 118-121.

[85] R. A. Ramirez, E. A. Rojas-Nastrucci, and T. M. Weller, "3D tag with improved read range for UHF RFID applications using Additive Manufacturing," in *Wireless and Microwave Technology Conference (WAMICON), 2015 IEEE 16th Annual*, 2015, pp. 1-4.

[86] T. Phatarachaisakul, T. Pumpoung, C. Phongcharoenpanich, and S. Kosulvit, "Tag antenna using printed dipole with H-slot for UHF RFID applications," in *Electrical Engineering Congress (iEECON), 2014 International*, 2014, pp. 1-4.

[87] H. Yejun and Z. Huaxia, "A new UHF anti-metal RFID tag antenna design with open-circuited stub feed," in *Communications (ICC), 2013 IEEE International Conference on*, 2013, p. 5809.

[88] S. Genovesi and A. Monorchio, "Low-Profile Three-Arm Folded Dipole Antenna for UHF Band RFID Tags Mountable on Metallic Objects," *Antennas and Wireless Propagation Letters, IEEE*, vol. 9, pp. 1225-1228, 2010.

[89] A. E. Abdulhadi and R. Abhari, "Passive UHF RFID printed monopole tag antenna for identification of metallic objects," in *Antennas and Propagation Society International Symposium (APSURSI), 2012 IEEE*, 2012, pp. 1-2.

[90] S. R. Best, "The Significance of Ground-Plane Size and Antenna Location in Establishing the Performance of Ground-Plane-Dependent Antennas," *Antennas and Propagation Magazine, IEEE*, vol. 51, pp. 29-43, 2009.

[91] W. Strauss, S. Kraus, M. Hartmann, C. Grabowski, and J. Bernhard, "Read range measurements of UHF RFID transponders in mobile anechoic chamber," in *RFID, 2009 IEEE International Conference on*, 2009, pp. 48-55.

[92] K. H. Lee, J. S. Lee, G. Kim, J. Yeo, B. H. Moon, J. Yang, *et al.*, "Design of a UHF RFID metal tag for long reading range using a cavity structure," in *2008 Asia-Pacific Microwave Conference*, 2008, pp. 1-4.

[93] R. A. Ramirez, E. A. Rojas-Nastrucci, and T. M. Weller, "UHF RFID Tags for On- and Off-Metal Applications Fabricated Using Additive Manufacturing," *IEEE Antennas and Wireless Propagation Letters*, vol. 16, pp. 1635-1638, 2017.

www.manaraa.com

[94] H. D. Chen and Y. H. Tsao, "Low-Profile PIFA Array Antennas for UHF Band RFID Tags Mountable on Metallic Objects," *IEEE Transactions on Antennas and Propagation,* vol. 58, pp. 1087-1092, 2010.

[95] E. S. Yang and H. W. Son, "Dual-polarised metal-mountable UHF RFID tag antenna for polarisation diversity," *Electronics Letters,* vol. 52, pp. 496-498, 2016.

[96] A. K. H. Obsiye, H. E. AbdEl-Raouf, and R. El-Islam, "Design of a compact planar inverted-F antenna (PIFA) for RFID applications," in *RF and Microwave Conference, 2008. RFM 2008. IEEE International*, 2008, pp. 277-278.

www.manaraa.com

APPENDIX A: COPYRIGHT PERMISSIONS

A.1. Permissions for Chapter 1

5/14/2018 RightsLink® by Copyright Clearance Center

Copyright Clearance Center RightsLink®

Home | Create Account | Help

IEEE Requesting permission to reuse content from an IEEE publication

Title:	Laser enhanced direct print additive manufacturing for mm-wave components and packaging
Conference Proceedings:	Electromagnetics in Advanced Applications (ICEAA), 2017 International Conference on
Author:	Eduardo A. Rojas-Nastrucci
Publisher:	IEEE
Date:	Sept. 2017

Copyright © 2017, IEEE

LOGIN

If you're a copyright.com user, you can login to RightsLink using your copyright.com credentials.
Already a RightsLink user or want to learn more?

Thesis / Dissertation Reuse

The IEEE does not require individuals working on a thesis to obtain a formal reuse license, however, you may print out this statement to be used as a permission grant:

Requirements to be followed when using any portion (e.g., figure, graph, table, or textual material) of an IEEE copyrighted paper in a thesis:

1) In the case of textual material (e.g., using short quotes or referring to the work within these papers) users must give full credit to the original source (author, paper, publication) followed by the IEEE copyright line © 2011 IEEE.
2) In the case of illustrations or tabular material, we require that the copyright line © [Year of original publication] IEEE appear prominently with each reprinted figure and/or table.
3) If a substantial portion of the original paper is to be used, and if you are not the senior author, also obtain the senior author's approval.

Requirements to be followed when using an entire IEEE copyrighted paper in a thesis:

1) The following IEEE copyright/ credit notice should be placed prominently in the references: © [year of original publication] IEEE. Reprinted, with permission, from [author names, paper title, IEEE publication title, and month/year of publication]
2) Only the accepted version of an IEEE copyrighted paper can be used when posting the paper or your thesis on-line.
3) In placing the thesis on the author's university website, please display the following message in a prominent place on the website: In reference to IEEE copyrighted material which is used with permission in this thesis, the IEEE does not endorse any of [university/educational entity's name goes here]'s products or services. Internal or personal use of this material is permitted. If interested in reprinting/republishing IEEE copyrighted material for advertising or promotional purposes or for creating new collective works for resale or redistribution, please go to http://www.ieee.org/publications_standards/publications/rights/rights_link.html to learn how to obtain a License from RightsLink.

If applicable, University Microfilms and/or ProQuest Library, or the Archives of Canada may supply single copies of the dissertation.

BACK | CLOSE WINDOW

Copyright © 2018 Copyright Clearance Center, Inc. All Rights Reserved. Privacy statement. Terms and Conditions.
Comments? We would like to hear from you. E-mail us at customercare@copyright.com

www.manaraa.com

A.2. Permissions for Chapter 2

5/16/2018 Rightslink® by Copyright Clearance Center

Copyright Clearance Center RightsLink®

Home | Create Account | Help

IEEE Requesting permission to reuse content from an IEEE publication

Title: Low-Loss 3-D Multilayer Transmission Lines and Interconnects Fabricated by Additive Manufacturing Technologies
Author: Fan Cai
Publication: Microwave Theory and Techniques, IEEE Transactions on
Publisher: IEEE
Date: Oct. 2016
Copyright © 2016, IEEE

LOGIN
If you're a copyright.com user, you can login to RightsLink using your copyright.com credentials.
Already a RightsLink user or want to learn more?

Thesis / Dissertation Reuse

The IEEE does not require individuals working on a thesis to obtain a formal reuse license, however, you may print out this statement to be used as a permission grant:

Requirements to be followed when using any portion (e.g., figure, graph, table, or textual material) of an IEEE copyrighted paper in a thesis:

1) In the case of textual material (e.g., using short quotes or referring to the work within these papers) users must give full credit to the original source (author, paper, publication) followed by the IEEE copyright line © 2011 IEEE.
2) In the case of illustrations or tabular material, we require that the copyright line © [Year of original publication] IEEE appear prominently with each reprinted figure and/or table.
3) If a substantial portion of the original paper is to be used, and if you are not the senior author, also obtain the senior author's approval.

Requirements to be followed when using an entire IEEE copyrighted paper in a thesis:

1) The following IEEE copyright/ credit notice should be placed prominently in the references: © [year of original publication] IEEE. Reprinted, with permission, from [author names, paper title, IEEE publication title, and month/year of publication]
2) Only the accepted version of an IEEE copyrighted paper can be used when posting the paper or your thesis on-line.
3) In placing the thesis on the author's university website, please display the following message in a prominent place on the website: In reference to IEEE copyrighted material which is used with permission in this thesis, the IEEE does not endorse any of [university/educational entity's name goes here]'s products or services. Internal or personal use of this material is permitted. If interested in reprinting/republishing IEEE copyrighted material for advertising or promotional purposes or for creating new collective works for resale or redistribution, please go to http://www.ieee.org/publications_standards/publications/rights/rights_link.html to learn how to obtain a License from RightsLink.

If applicable, University Microfilms and/or ProQuest Library, or the Archives of Canada may supply single copies of the dissertation.

BACK | CLOSE WINDOW

Copyright © 2018 Copyright Clearance Center, Inc. All Rights Reserved. Privacy statement. Terms and Conditions.
Comments? We would like to hear from you. E-mail us at customercare@copyright.com

www.manaraa.com

Copyright Clearance Center RightsLink®

Home | Create Account | Help

IEEE Requesting permission to reuse content from an IEEE publication

Title: High-Performance RF Devices and Components on Flexible Cellulose Substrate by Vertically Integrated Additive Manufacturing Technologies
Author: Chiara Mariotti
Publication: Microwave Theory and Techniques, IEEE Transactions on
Publisher: IEEE
Date: Jan. 2017
Copyright © 2017, IEEE

LOGIN
If you're a copyright.com user, you can login to RightsLink using your copyright.com credentials.
Already a RightsLink user or want to learn more?

Thesis / Dissertation Reuse

The IEEE does not require individuals working on a thesis to obtain a formal reuse license, however, you may print out this statement to be used as a permission grant:

Requirements to be followed when using any portion (e.g., figure, graph, table, or textual material) of an IEEE copyrighted paper in a thesis:

1) In the case of textual material (e.g., using short quotes or referring to the work within these papers) users must give full credit to the original source (author, paper, publication) followed by the IEEE copyright line © 2011 IEEE.
2) In the case of illustrations or tabular material, we require that the copyright line © [Year of original publication] IEEE appear prominently with each reprinted figure and/or table.
3) If a substantial portion of the original paper is to be used, and if you are not the senior author, also obtain the senior author's approval.

Requirements to be followed when using an entire IEEE copyrighted paper in a thesis:

1) The following IEEE copyright/ credit notice should be placed prominently in the references: © [year of original publication] IEEE. Reprinted, with permission, from [author names, paper title, IEEE publication title, and month/year of publication]
2) Only the accepted version of an IEEE copyrighted paper can be used when posting the paper or your thesis on-line.
3) In placing the thesis on the author's university website, please display the following message in a prominent place on the website: In reference to IEEE copyrighted material which is used with permission in this thesis, the IEEE does not endorse any of [university/educational entity's name goes here]'s products or services. Internal or personal use of this material is permitted. If interested in reprinting/republishing IEEE copyrighted material for advertising or promotional purposes or for creating new collective works for resale or redistribution, please go to http://www.ieee.org/publications_standards/publications/rights/rights_link.html to learn how to obtain a License from RightsLink.

If applicable, University Microfilms and/or ProQuest Library, or the Archives of Canada may supply single copies of the dissertation.

BACK | CLOSE WINDOW

Copyright © 2018 Copyright Clearance Center, Inc. All Rights Reserved. Privacy statement. Terms and Conditions.
Comments? We would like to hear from you. E-mail us at customercare@copyright.com

المنارة للاستشارات
www.manaraa.com

Copyright Clearance Center RightsLink®

Home | Create Account | Help

IEEE Requesting permission to reuse content from an IEEE publication

Title: Propagation Characteristics and Modeling of Meshed Ground Coplanar Waveguide
Author: Eduardo A. Rojas-Nastrucci
Publication: Microwave Theory and Techniques, IEEE Transactions on
Publisher: IEEE
Date: Nov. 2016
Copyright © 2016, IEEE

LOGIN
If you're a copyright.com user, you can login to RightsLink using your copyright.com credentials.
Already a RightsLink user or want to learn more?

Thesis / Dissertation Reuse

The IEEE does not require individuals working on a thesis to obtain a formal reuse license, however, you may print out this statement to be used as a permission grant:

Requirements to be followed when using any portion (e.g., figure, graph, table, or textual material) of an IEEE copyrighted paper in a thesis:

1) In the case of textual material (e.g., using short quotes or referring to the work within these papers) users must give full credit to the original source (author, paper, publication) followed by the IEEE copyright line © 2011 IEEE.
2) In the case of illustrations or tabular material, we require that the copyright line © [Year of original publication] IEEE appear prominently with each reprinted figure and/or table.
3) If a substantial portion of the original paper is to be used, and if you are not the senior author, also obtain the senior author's approval.

Requirements to be followed when using an entire IEEE copyrighted paper in a thesis:

1) The following IEEE copyright/ credit notice should be placed prominently in the references: © [year of original publication] IEEE. Reprinted, with permission, from [author names, paper title, IEEE publication title, and month/year of publication]
2) Only the accepted version of an IEEE copyrighted paper can be used when posting the paper or your thesis on-line.
3) In placing the thesis on the author's university website, please display the following message in a prominent place on the website: In reference to IEEE copyrighted material which is used with permission in this thesis, the IEEE does not endorse any of [university/educational entity's name goes here]'s products or services. Internal or personal use of this material is permitted. If interested in reprinting/republishing IEEE copyrighted material for advertising or promotional purposes or for creating new collective works for resale or redistribution, please go to http://www.ieee.org/publications_standards/publications/rights/rights_link.html to learn how to obtain a License from RightsLink.

If applicable, University Microfilms and/or ProQuest Library, or the Archives of Canada may supply single copies of the dissertation.

BACK | CLOSE WINDOW

Copyright © 2018 Copyright Clearance Center, Inc. All Rights Reserved. Privacy statement. Terms and Conditions.
Comments? We would like to hear from you. E-mail us at customercare@copyright.com

www.manaraa.com

Copyright Clearance Center RightsLink®

Home | Create Account | Help

IEEE Requesting permission to reuse content from an IEEE publication

Title: Characterization and Modeling of K-Band Coplanar Waveguides Digitally Manufactured Using Pulsed Picosecond Laser Machining of Thick-Film Conductive Paste
Author: Eduardo A. Rojas-Nastrucci
Publication: Microwave Theory and Techniques, IEEE Transactions on
Publisher: IEEE
Date: Sept. 2017
Copyright © 2017, IEEE

LOGIN
If you're a copyright.com user, you can login to RightsLink using your copyright.com credentials.
Already a RightsLink user or want to learn more?

Thesis / Dissertation Reuse

The IEEE does not require individuals working on a thesis to obtain a formal reuse license, however, you may print out this statement to be used as a permission grant:

Requirements to be followed when using any portion (e.g., figure, graph, table, or textual material) of an IEEE copyrighted paper in a thesis:

1) In the case of textual material (e.g., using short quotes or referring to the work within these papers) users must give full credit to the original source (author, paper, publication) followed by the IEEE copyright line © 2011 IEEE.
2) In the case of illustrations or tabular material, we require that the copyright line © [Year of original publication] IEEE appear prominently with each reprinted figure and/or table.
3) If a substantial portion of the original paper is to be used, and if you are not the senior author, also obtain the senior author's approval.

Requirements to be followed when using an entire IEEE copyrighted paper in a thesis:

1) The following IEEE copyright/ credit notice should be placed prominently in the references: © [year of original publication] IEEE. Reprinted, with permission, from [author names, paper title, IEEE publication title, and month/year of publication]
2) Only the accepted version of an IEEE copyrighted paper can be used when posting the paper or your thesis on-line.
3) In placing the thesis on the author's university website, please display the following message in a prominent place on the website: In reference to IEEE copyrighted material which is used with permission in this thesis, the IEEE does not endorse any of [university/educational entity's name goes here]'s products or services. Internal or personal use of this material is permitted. If interested in reprinting/republishing IEEE copyrighted material for advertising or promotional purposes or for creating new collective works for resale or redistribution, please go to http://www.ieee.org/publications_standards/publications/rights/rights_link.html to learn how to obtain a License from RightsLink.

If applicable, University Microfilms and/or ProQuest Library, or the Archives of Canada may supply single copies of the dissertation.

BACK | CLOSE WINDOW

Copyright © 2018 Copyright Clearance Center, Inc. All Rights Reserved. Privacy statement. Terms and Conditions.
Comments? We would like to hear from you. E-mail us at customercare@copyright.com

www.manaraa.com

Copyright Clearance Center RightsLink®

Home | Create Account | Help

IEEE Requesting permission to reuse content from an IEEE publication

Title: Design and verification of SMT MMIC package using a 20 GHz LNA, a 40 GHz LNA and a 40GHz digital attenuator
Conference Proceedings: Electrical Performance of Electronic Packaging and Systems (EPEPS), 2013 IEEE 22nd Conference on
Author: Inkwon Ju
Publisher: IEEE
Date: Oct. 2013
Copyright © 2013, IEEE

LOGIN
If you're a copyright.com user, you can login to RightsLink using your copyright.com credentials.
Already a RightsLink user or want to learn more?

Thesis / Dissertation Reuse

The IEEE does not require individuals working on a thesis to obtain a formal reuse license, however, you may print out this statement to be used as a permission grant:

Requirements to be followed when using any portion (e.g., figure, graph, table, or textual material) of an IEEE copyrighted paper in a thesis:

1) In the case of textual material (e.g., using short quotes or referring to the work within these papers) users must give full credit to the original source (author, paper, publication) followed by the IEEE copyright line © 2011 IEEE.
2) In the case of illustrations or tabular material, we require that the copyright line © [Year of original publication] IEEE appear prominently with each reprinted figure and/or table.
3) If a substantial portion of the original paper is to be used, and if you are not the senior author, also obtain the senior author's approval.

Requirements to be followed when using an entire IEEE copyrighted paper in a thesis:

1) The following IEEE copyright/ credit notice should be placed prominently in the references: © [year of original publication] IEEE. Reprinted, with permission, from [author names, paper title, IEEE publication title, and month/year of publication]
2) Only the accepted version of an IEEE copyrighted paper can be used when posting the paper or your thesis on-line.
3) In placing the thesis on the author's university website, please display the following message in a prominent place on the website: In reference to IEEE copyrighted material which is used with permission in this thesis, the IEEE does not endorse any of [university/educational entity's name goes here]'s products or services. Internal or personal use of this material is permitted. If interested in reprinting/republishing IEEE copyrighted material for advertising or promotional purposes or for creating new collective works for resale or redistribution, please go to http://www.ieee.org/publications_standards/publications/rights/rights_link.html to learn how to obtain a License from RightsLink.

If applicable, University Microfilms and/or ProQuest Library, or the Archives of Canada may supply single copies of the dissertation.

BACK | CLOSE WINDOW

Copyright © 2018 Copyright Clearance Center, Inc. All Rights Reserved. Privacy statement. Terms and Conditions.
Comments? We would like to hear from you. E-mail us at customercare@copyright.com

www.manaraa.com

Copyright Clearance Center RightsLink®

Home | Create Account | Help

IEEE Requesting permission to reuse content from an IEEE publication

Title: 3-D printed substrates for MMIC packaging
Conference Proceedings: Radio and Wireless Symposium (RWS), 2017 IEEE
Author: Spyridon Pavlidis
Publisher: IEEE
Date: Jan. 2017
Copyright © 2017, IEEE

LOGIN
If you're a copyright.com user, you can login to RightsLink using your copyright.com credentials.
Already a RightsLink user or want to learn more?

Thesis / Dissertation Reuse

The IEEE does not require individuals working on a thesis to obtain a formal reuse license, however, you may print out this statement to be used as a permission grant:

Requirements to be followed when using any portion (e.g., figure, graph, table, or textual material) of an IEEE copyrighted paper in a thesis:

1) In the case of textual material (e.g., using short quotes or referring to the work within these papers) users must give full credit to the original source (author, paper, publication) followed by the IEEE copyright line © 2011 IEEE.
2) In the case of illustrations or tabular material, we require that the copyright line © [Year of original publication] IEEE appear prominently with each reprinted figure and/or table.
3) If a substantial portion of the original paper is to be used, and if you are not the senior author, also obtain the senior author's approval.

Requirements to be followed when using an entire IEEE copyrighted paper in a thesis:

1) The following IEEE copyright/ credit notice should be placed prominently in the references: © [year of original publication] IEEE. Reprinted, with permission, from [author names, paper title, IEEE publication title, and month/year of publication]
2) Only the accepted version of an IEEE copyrighted paper can be used when posting the paper or your thesis on-line.
3) In placing the thesis on the author's university website, please display the following message in a prominent place on the website: In reference to IEEE copyrighted material which is used with permission in this thesis, the IEEE does not endorse any of [university/educational entity's name goes here]'s products or services. Internal or personal use of this material is permitted. If interested in reprinting/republishing IEEE copyrighted material for advertising or promotional purposes or for creating new collective works for resale or redistribution, please go to http://www.ieee.org/publications_standards/publications/rights/rights_link.html to learn how to obtain a License from RightsLink.

If applicable, University Microfilms and/or ProQuest Library, or the Archives of Canada may supply single copies of the dissertation.

BACK | CLOSE WINDOW

Copyright © 2018 Copyright Clearance Center, Inc. All Rights Reserved. Privacy statement, Terms and Conditions.
Comments? We would like to hear from you. E-mail us at customercare@copyright.com

www.manaraa.com

Title: 3D Printed Out-of-Plane Antennas for Use on High Density Boards

Conference Proceedings: Electronic Components and Technology Conference (ECTC), 2017 IEEE 67th

Author: Mohd Ifwat Mohd Ghazali

Publisher: IEEE

Date: May 2017

Copyright © 2017, IEEE

LOGIN
If you're a copyright.com user, you can login to RightsLink using your copyright.com credentials.
Already a RightsLink user or want to learn more?

Thesis / Dissertation Reuse

The IEEE does not require individuals working on a thesis to obtain a formal reuse license, however, you may print out this statement to be used as a permission grant:

Requirements to be followed when using any portion (e.g., figure, graph, table, or textual material) of an IEEE copyrighted paper in a thesis:

1) In the case of textual material (e.g., using short quotes or referring to the work within these papers) users must give full credit to the original source (author, paper, publication) followed by the IEEE copyright line © 2011 IEEE.
2) In the case of illustrations or tabular material, we require that the copyright line © [Year of original publication] IEEE appear prominently with each reprinted figure and/or table.
3) If a substantial portion of the original paper is to be used, and if you are not the senior author, also obtain the senior author's approval.

Requirements to be followed when using an entire IEEE copyrighted paper in a thesis:

1) The following IEEE copyright/ credit notice should be placed prominently in the references: © [year of original publication] IEEE. Reprinted, with permission, from [author names, paper title, IEEE publication title, and month/year of publication]
2) Only the accepted version of an IEEE copyrighted paper can be used when posting the paper or your thesis on-line.
3) In placing the thesis on the author's university website, please display the following message in a prominent place on the website: In reference to IEEE copyrighted material which is used with permission in this thesis, the IEEE does not endorse any of [university/educational entity's name goes here]'s products or services. Internal or personal use of this material is permitted. If interested in reprinting/republishing IEEE copyrighted material for advertising or promotional purposes or for creating new collective works for resale or redistribution, please go to http://www.ieee.org/publications_standards/publications/rights/rights_link.html to learn how to obtain a License from RightsLink.

If applicable, University Microfilms and/or ProQuest Library, or the Archives of Canada may supply single copies of the dissertation.

BACK CLOSE WINDOW

Copyright © 2018 Copyright Clearance Center, Inc. All Rights Reserved. Privacy statement. Terms and Conditions.
Comments? We would like to hear from you. E-mail us at customercare@copyright.com

www.manaraa.com

Copyright Clearance Center RightsLink®

Home | Create Account | Help

IEEE Requesting permission to reuse content from an IEEE publication

Title: Substrate-independent system-on-package antenna integration with inkjet printing
Conference Proceedings: Antennas and Propagation (APSURSI), 2016 IEEE International Symposium on
Author: Bijan K. Tehrani
Publisher: IEEE
Date: June 2016
Copyright © 2016, IEEE

LOGIN
If you're a copyright.com user, you can login to RightsLink using your copyright.com credentials.
Already a RightsLink user or want to learn more?

Thesis / Dissertation Reuse

The IEEE does not require individuals working on a thesis to obtain a formal reuse license, however, you may print out this statement to be used as a permission grant:

Requirements to be followed when using any portion (e.g., figure, graph, table, or textual material) of an IEEE copyrighted paper in a thesis:

1) In the case of textual material (e.g., using short quotes or referring to the work within these papers) users must give full credit to the original source (author, paper, publication) followed by the IEEE copyright line © 2011 IEEE.
2) In the case of illustrations or tabular material, we require that the copyright line © [Year of original publication] IEEE appear prominently with each reprinted figure and/or table.
3) If a substantial portion of the original paper is to be used, and if you are not the senior author, also obtain the senior author's approval.

Requirements to be followed when using an entire IEEE copyrighted paper in a thesis:

1) The following IEEE copyright/ credit notice should be placed prominently in the references: © [year of original publication] IEEE. Reprinted, with permission, from [author names, paper title, IEEE publication title, and month/year of publication]
2) Only the accepted version of an IEEE copyrighted paper can be used when posting the paper or your thesis on-line.
3) In placing the thesis on the author's university website, please display the following message in a prominent place on the website: In reference to IEEE copyrighted material which is used with permission in this thesis, the IEEE does not endorse any of [university/educational entity's name goes here]'s products or services. Internal or personal use of this material is permitted. If interested in reprinting/republishing IEEE copyrighted material for advertising or promotional purposes or for creating new collective works for resale or redistribution, please go to http://www.ieee.org/publications_standards/publications/rights/rights_link.html to learn how to obtain a License from RightsLink.

If applicable, University Microfilms and/or ProQuest Library, or the Archives of Canada may supply single copies of the dissertation.

BACK | CLOSE WINDOW

Copyright © 2018 Copyright Clearance Center, Inc. All Rights Reserved. Privacy statement. Terms and Conditions.
Comments? We would like to hear from you. E-mail us at customercare@copyright.com

www.manaraa.com

Copyright Clearance Center RightsLink®

Home | Create Account | Help

IEEE Requesting permission to reuse content from an IEEE publication

Title: A case for considering hyper-Rayleigh fading channels
Author: Jeff Frolik
Publication: Wireless Communications, IEEE Transactions on
Publisher: IEEE
Date: April 2007
Copyright © 2007, IEEE

LOGIN
If you're a copyright.com user, you can login to RightsLink using your copyright.com credentials.
Already a RightsLink user or want to learn more?

Thesis / Dissertation Reuse

The IEEE does not require individuals working on a thesis to obtain a formal reuse license, however, you may print out this statement to be used as a permission grant:

Requirements to be followed when using any portion (e.g., figure, graph, table, or textual material) of an IEEE copyrighted paper in a thesis:

1) In the case of textual material (e.g., using short quotes or referring to the work within these papers) users must give full credit to the original source (author, paper, publication) followed by the IEEE copyright line © 2011 IEEE.
2) In the case of illustrations or tabular material, we require that the copyright line © [Year of original publication] IEEE appear prominently with each reprinted figure and/or table.
3) If a substantial portion of the original paper is to be used, and if you are not the senior author, also obtain the senior author's approval.

Requirements to be followed when using an entire IEEE copyrighted paper in a thesis:

1) The following IEEE copyright/ credit notice should be placed prominently in the references: © [year of original publication] IEEE. Reprinted, with permission, from [author names, paper title, IEEE publication title, and month/year of publication]
2) Only the accepted version of an IEEE copyrighted paper can be used when posting the paper or your thesis on-line.
3) In placing the thesis on the author's university website, please display the following message in a prominent place on the website: In reference to IEEE copyrighted material which is used with permission in this thesis, the IEEE does not endorse any of [university/educational entity's name goes here]'s products or services. Internal or personal use of this material is permitted. If interested in reprinting/republishing IEEE copyrighted material for advertising or promotional purposes or for creating new collective works for resale or redistribution, please go to http://www.ieee.org/publications_standards/publications/rights/rights_link.html to learn how to obtain a License from RightsLink.

If applicable, University Microfilms and/or ProQuest Library, or the Archives of Canada may supply single copies of the dissertation.

BACK | CLOSE WINDOW

Copyright © 2018 Copyright Clearance Center, Inc. All Rights Reserved. Privacy statement. Terms and Conditions.
Comments? We would like to hear from you. E-mail us at customercare@copyright.com

www.manaraa.com

Copyright Clearance Center RightsLink®

Home | Create Account | Help

IEEE Requesting permission to reuse content from an IEEE publication

Title: Depolarization in three dimensions: Theoretical formulations and empirical results

Conference Proceedings: Wireless and Microwave Technology Conference (WAMICON), 2016 IEEE 17th Annual

Author: Marcia Golmohamadi

Publisher: IEEE

Date: April 2016

Copyright © 2016, IEEE

LOGIN

If you're a copyright.com user, you can login to RightsLink using your copyright.com credentials.

Already a RightsLink user or want to learn more?

Thesis / Dissertation Reuse

The IEEE does not require individuals working on a thesis to obtain a formal reuse license, however, you may print out this statement to be used as a permission grant:

Requirements to be followed when using any portion (e.g., figure, graph, table, or textual material) of an IEEE copyrighted paper in a thesis:

1) In the case of textual material (e.g., using short quotes or referring to the work within these papers) users must give full credit to the original source (author, paper, publication) followed by the IEEE copyright line © 2011 IEEE.
2) In the case of illustrations or tabular material, we require that the copyright line © [Year of original publication] IEEE appear prominently with each reprinted figure and/or table.
3) If a substantial portion of the original paper is to be used, and if you are not the senior author, also obtain the senior author's approval.

Requirements to be followed when using an entire IEEE copyrighted paper in a thesis:

1) The following IEEE copyright/ credit notice should be placed prominently in the references: © [year of original publication] IEEE. Reprinted, with permission, from [author names, paper title, IEEE publication title, and month/year of publication]
2) Only the accepted version of an IEEE copyrighted paper can be used when posting the paper or your thesis on-line.
3) In placing the thesis on the author's university website, please display the following message in a prominent place on the website: In reference to IEEE copyrighted material which is used with permission in this thesis, the IEEE does not endorse any of [university/educational entity's name goes here]'s products or services. Internal or personal use of this material is permitted. If interested in reprinting/republishing IEEE copyrighted material for advertising or promotional purposes or for creating new collective works for resale or redistribution, please go to http://www.ieee.org/publications_standards/publications/rights/rights_link.html to learn how to obtain a License from RightsLink.

If applicable, University Microfilms and/or ProQuest Library, or the Archives of Canada may supply single copies of the dissertation.

BACK | CLOSE WINDOW

Copyright © 2018 Copyright Clearance Center, Inc. All Rights Reserved. Privacy statement. Terms and Conditions.
Comments? We would like to hear from you. E-mail us at customercare@copyright.com

www.manaraa.com

Copyright Clearance Center RightsLink®

Home | Create Account | Help

IEEE Requesting permission to reuse content from an IEEE publication

Title: Mitigating severe channel effects using tripolar antenna diversity
Conference Proceedings: Antennas and Propagation (EuCAP), 2015 9th European Conference on
Author: Jeff Frolik
Publisher: IEEE
Date: April 2015
Copyright © 2015, IEEE

LOGIN
If you're a copyright.com user, you can login to RightsLink using your copyright.com credentials.
Already a RightsLink user or want to learn more?

Thesis / Dissertation Reuse

The IEEE does not require individuals working on a thesis to obtain a formal reuse license, however, you may print out this statement to be used as a permission grant:

Requirements to be followed when using any portion (e.g., figure, graph, table, or textual material) of an IEEE copyrighted paper in a thesis:

1) In the case of textual material (e.g., using short quotes or referring to the work within these papers) users must give full credit to the original source (author, paper, publication) followed by the IEEE copyright line © 2011 IEEE.
2) In the case of illustrations or tabular material, we require that the copyright line © [Year of original publication] IEEE appear prominently with each reprinted figure and/or table.
3) If a substantial portion of the original paper is to be used, and if you are not the senior author, also obtain the senior author's approval.

Requirements to be followed when using an entire IEEE copyrighted paper in a thesis:

1) The following IEEE copyright/ credit notice should be placed prominently in the references: © [year of original publication] IEEE. Reprinted, with permission, from [author names, paper title, IEEE publication title, and month/year of publication]
2) Only the accepted version of an IEEE copyrighted paper can be used when posting the paper or your thesis on-line.
3) In placing the thesis on the author's university website, please display the following message in a prominent place on the website: In reference to IEEE copyrighted material which is used with permission in this thesis, the IEEE does not endorse any of [university/educational entity's name goes here]'s products or services. Internal or personal use of this material is permitted. If interested in reprinting/republishing IEEE copyrighted material for advertising or promotional purposes or for creating new collective works for resale or redistribution, please go to http://www.ieee.org/publications_standards/publications/rights/rights_link.html to learn how to obtain a License from RightsLink.

If applicable, University Microfilms and/or ProQuest Library, or the Archives of Canada may supply single copies of the dissertation.

BACK | CLOSE WINDOW

Copyright © 2018 Copyright Clearance Center, Inc. All Rights Reserved. Privacy statement. Terms and Conditions.
Comments? We would like to hear from you. E-mail us at customercare@copyright.com

www.manaraa.com

Copyright Clearance Center RightsLink®

Home | Create Account | Help

IEEE Requesting permission to reuse content from an IEEE publication

Title: MMIC packaging and on-chip low-loss lateral interconnection using additive manufacturing and laser machining
Conference Proceedings: Microwave Symposium (IMS), 2017 IEEE MTT-S International
Author: Ramiro A. Ramirez
Publisher: IEEE
Date: June 2017
Copyright © 2017, IEEE

LOGIN
If you're a copyright.com user, you can login to RightsLink using your copyright.com credentials. Already a RightsLink user or want to learn more?

Thesis / Dissertation Reuse

The IEEE does not require individuals working on a thesis to obtain a formal reuse license, however, you may print out this statement to be used as a permission grant:

Requirements to be followed when using any portion (e.g., figure, graph, table, or textual material) of an IEEE copyrighted paper in a thesis:

1) In the case of textual material (e.g., using short quotes or referring to the work within these papers) users must give full credit to the original source (author, paper, publication) followed by the IEEE copyright line © 2011 IEEE.
2) In the case of illustrations or tabular material, we require that the copyright line © [Year of original publication] IEEE appear prominently with each reprinted figure and/or table.
3) If a substantial portion of the original paper is to be used, and if you are not the senior author, also obtain the senior author's approval.

Requirements to be followed when using an entire IEEE copyrighted paper in a thesis:

1) The following IEEE copyright/ credit notice should be placed prominently in the references: © [year of original publication] IEEE. Reprinted, with permission, from [author names, paper title, IEEE publication title, and month/year of publication]
2) Only the accepted version of an IEEE copyrighted paper can be used when posting the paper or your thesis on-line.
3) In placing the thesis on the author's university website, please display the following message in a prominent place on the website: In reference to IEEE copyrighted material which is used with permission in this thesis, the IEEE does not endorse any of [university/educational entity's name goes here]'s products or services. Internal or personal use of this material is permitted. If interested in reprinting/republishing IEEE copyrighted material for advertising or promotional purposes or for creating new collective works for resale or redistribution, please go to http://www.ieee.org/publications_standards/publications/rights/rights_link.html to learn how to obtain a License from RightsLink.

If applicable, University Microfilms and/or ProQuest Library, or the Archives of Canada may supply single copies of the dissertation.

BACK | CLOSE WINDOW

Copyright © 2018 Copyright Clearance Center, Inc. All Rights Reserved. Privacy statement. Terms and Conditions.
Comments? We would like to hear from you. E-mail us at customercare@copyright.com

www.manaraa.com

A.3. Permissions for Chapter 3

5/14/2018 Rightslink® by Copyright Clearance Center

Copyright Clearance Center RightsLink®

Home | Create Account | Help

IEEE Requesting permission to reuse content from an IEEE publication

Title:	3D printed on-package tripolar antennas for mitigating harsh channel conditions
Conference Proceedings:	Radio and Wireless Symposium (RWS), 2017 IEEE
Author:	Ramiro A. Ramirez
Publisher:	IEEE
Date:	Jan. 2017

Copyright © 2017, IEEE

LOGIN

If you're a copyright.com user, you can login to RightsLink using your copyright.com credentials.

Already a RightsLink user or want to learn more?

Thesis / Dissertation Reuse

The IEEE does not require individuals working on a thesis to obtain a formal reuse license, however, you may print out this statement to be used as a permission grant:

Requirements to be followed when using any portion (e.g., figure, graph, table, or textual material) of an IEEE copyrighted paper in a thesis:

1) In the case of textual material (e.g., using short quotes or referring to the work within these papers) users must give full credit to the original source (author, paper, publication) followed by the IEEE copyright line © 2011 IEEE.
2) In the case of illustrations or tabular material, we require that the copyright line © [Year of original publication] IEEE appear prominently with each reprinted figure and/or table.
3) If a substantial portion of the original paper is to be used, and if you are not the senior author, also obtain the senior author's approval.

Requirements to be followed when using an entire IEEE copyrighted paper in a thesis:

1) The following IEEE copyright/ credit notice should be placed prominently in the references: © [year of original publication] IEEE. Reprinted, with permission, from [author names, paper title, IEEE publication title, and month/year of publication]
2) Only the accepted version of an IEEE copyrighted paper can be used when posting the paper or your thesis on-line.
3) In placing the thesis on the author's university website, please display the following message in a prominent place on the website: In reference to IEEE copyrighted material which is used with permission in this thesis, the IEEE does not endorse any of [university/educational entity's name goes here]'s products or services. Internal or personal use of this material is permitted. If interested in reprinting/republishing IEEE copyrighted material for advertising or promotional purposes or for creating new collective works for resale or redistribution, please go to http://www.ieee.org/publications_standards/publications/rights/rights_link.html to learn how to obtain a License from RightsLink.

If applicable, University Microfilms and/or ProQuest Library, or the Archives of Canada may supply single copies of the dissertation.

BACK | CLOSE WINDOW

Copyright © 2018 Copyright Clearance Center, Inc. All Rights Reserved. Privacy statement. Terms and Conditions.
Comments? We would like to hear from you. E-mail us at customercare@copyright.com

www.manaraa.com

Copyright Clearance Center RightsLink®

Home | Create Account | Help

IEEE Requesting permission to reuse content from an IEEE publication

Title: Additive manufactured tripolar antenna system for link improvement in high multipath environments
Conference Proceedings: Antennas and Propagation & USNC/URSI National Radio Science Meeting, 2017 IEEE International Symposium on
Author: Ramiro A. Ramirez
Publisher: IEEE
Date: July 2017
Copyright © 2017, IEEE

LOGIN
If you're a copyright.com user, you can login to RightsLink using your copyright.com credentials.
Already a RightsLink user or want to learn more?

Thesis / Dissertation Reuse

The IEEE does not require individuals working on a thesis to obtain a formal reuse license, however, you may print out this statement to be used as a permission grant:

Requirements to be followed when using any portion (e.g., figure, graph, table, or textual material) of an IEEE copyrighted paper in a thesis:

1) In the case of textual material (e.g., using short quotes or referring to the work within these papers) users must give full credit to the original source (author, paper, publication) followed by the IEEE copyright line © 2011 IEEE.
2) In the case of illustrations or tabular material, we require that the copyright line © [Year of original publication] IEEE appear prominently with each reprinted figure and/or table.
3) If a substantial portion of the original paper is to be used, and if you are not the senior author, also obtain the senior author's approval.

Requirements to be followed when using an entire IEEE copyrighted paper in a thesis:

1) The following IEEE copyright/ credit notice should be placed prominently in the references: © [year of original publication] IEEE. Reprinted, with permission, from [author names, paper title, IEEE publication title, and month/year of publication]
2) Only the accepted version of an IEEE copyrighted paper can be used when posting the paper or your thesis on-line.
3) In placing the thesis on the author's university website, please display the following message in a prominent place on the website: In reference to IEEE copyrighted material which is used with permission in this thesis, the IEEE does not endorse any of [university/educational entity's name goes here]'s products or services. Internal or personal use of this material is permitted. If interested in reprinting/republishing IEEE copyrighted material for advertising or promotional purposes or for creating new collective works for resale or redistribution, please go to http://www.ieee.org/publications_standards/publications/rights/rights_link.html to learn how to obtain a License from RightsLink.

If applicable, University Microfilms and/or ProQuest Library, or the Archives of Canada may supply single copies of the dissertation.

BACK | CLOSE WINDOW

Copyright © 2018 Copyright Clearance Center, Inc. All Rights Reserved. Privacy statement. Terms and Conditions.
Comments? We would like to hear from you. E-mail us at customercare@copyright.com

www.manaraa.com

A.4. Permissions for Chapter 4

5/14/2018 Rightslink® by Copyright Clearance Center

Copyright Clearance Center RightsLink®

Home | Create Account | Help

IEEE Requesting permission to reuse content from an IEEE publication

Title: MMIC packaging and on-chip low-loss lateral interconnection using additive manufacturing and laser machining
Conference Proceedings: Microwave Symposium (IMS), 2017 IEEE MTT-S International
Author: Ramiro A. Ramirez
Publisher: IEEE
Date: June 2017
Copyright © 2017, IEEE

LOGIN
If you're a copyright.com user, you can login to RightsLink using your copyright.com credentials.
Already a RightsLink user or want to learn more?

Thesis / Dissertation Reuse

The IEEE does not require individuals working on a thesis to obtain a formal reuse license, however, you may print out this statement to be used as a permission grant:

Requirements to be followed when using any portion (e.g., figure, graph, table, or textual material) of an IEEE copyrighted paper in a thesis:

1) In the case of textual material (e.g., using short quotes or referring to the work within these papers) users must give full credit to the original source (author, paper, publication) followed by the IEEE copyright line © 2011 IEEE.
2) In the case of illustrations or tabular material, we require that the copyright line © [Year of original publication] IEEE appear prominently with each reprinted figure and/or table.
3) If a substantial portion of the original paper is to be used, and if you are not the senior author, also obtain the senior author's approval.

Requirements to be followed when using an entire IEEE copyrighted paper in a thesis:

1) The following IEEE copyright/ credit notice should be placed prominently in the references: © [year of original publication] IEEE. Reprinted, with permission, from [author names, paper title, IEEE publication title, and month/year of publication]
2) Only the accepted version of an IEEE copyrighted paper can be used when posting the paper or your thesis on-line.
3) In placing the thesis on the author's university website, please display the following message in a prominent place on the website: In reference to IEEE copyrighted material which is used with permission in this thesis, the IEEE does not endorse any of [university/educational entity's name goes here]'s products or services. Internal or personal use of this material is permitted. If interested in reprinting/republishing IEEE copyrighted material for advertising or promotional purposes or for creating new collective works for resale or redistribution, please go to http://www.ieee.org/publications_standards/publications/rights/rights_link.html to learn how to obtain a License from RightsLink.

If applicable, University Microfilms and/or ProQuest Library, or the Archives of Canada may supply single copies of the dissertation.

BACK | CLOSE WINDOW

Copyright © 2018 Copyright Clearance Center, Inc. All Rights Reserved. Privacy statement. Terms and Conditions.
Comments? We would like to hear from you. E-mail us at customercare@copyright.com

www.manaraa.com

Copyright Clearance Center RightsLink®

Home | Create Account | Help

IEEE Requesting permission to reuse content from an IEEE publication

Title: Laser enhanced direct print additive manufacturing for mm-wave components and packaging
Conference Proceedings: Electromagnetics in Advanced Applications (ICEAA), 2017 International Conference on
Author: Eduardo A. Rojas-Nastrucci
Publisher: IEEE
Date: Sept. 2017
Copyright © 2017, IEEE

LOGIN
If you're a copyright.com user, you can login to RightsLink using your copyright.com credentials. Already a RightsLink user or want to learn more?

Thesis / Dissertation Reuse

The IEEE does not require individuals working on a thesis to obtain a formal reuse license, however, you may print out this statement to be used as a permission grant:

Requirements to be followed when using any portion (e.g., figure, graph, table, or textual material) of an IEEE copyrighted paper in a thesis:

1) In the case of textual material (e.g., using short quotes or referring to the work within these papers) users must give full credit to the original source (author, paper, publication) followed by the IEEE copyright line © 2011 IEEE.
2) In the case of illustrations or tabular material, we require that the copyright line © [Year of original publication] IEEE appear prominently with each reprinted figure and/or table.
3) If a substantial portion of the original paper is to be used, and if you are not the senior author, also obtain the senior author's approval.

Requirements to be followed when using an entire IEEE copyrighted paper in a thesis:

1) The following IEEE copyright/ credit notice should be placed prominently in the references: © [year of original publication] IEEE. Reprinted, with permission, from [author names, paper title, IEEE publication title, and month/year of publication]
2) Only the accepted version of an IEEE copyrighted paper can be used when posting the paper or your thesis on-line.
3) In placing the thesis on the author's university website, please display the following message in a prominent place on the website: In reference to IEEE copyrighted material which is used with permission in this thesis, the IEEE does not endorse any of [university/educational entity's name goes here]'s products or services. Internal or personal use of this material is permitted. If interested in reprinting/republishing IEEE copyrighted material for advertising or promotional purposes or for creating new collective works for resale or redistribution, please go to http://www.ieee.org/publications_standards/publications/rights/rights_link.html to learn how to obtain a License from RightsLink.

If applicable, University Microfilms and/or ProQuest Library, or the Archives of Canada may supply single copies of the dissertation.

BACK | CLOSE WINDOW

Copyright © 2018 Copyright Clearance Center, Inc. All Rights Reserved. Privacy statement. Terms and Conditions.
Comments? We would like to hear from you. E-mail us at customercare@copyright.com

www.manaraa.com

A.5. Permissions for Chapter 6

5/14/2018 Rightslink® by Copyright Clearance Center

Copyright Clearance Center RightsLink®

Home | Create Account | Help

IEEE Requesting permission to reuse content from an IEEE publication

Title: UHF RFID Tags for On-/Off-Metal Applications Fabricated Using Additive Manufacturing
Author: Ramiro A. Ramirez
Publication: IEEE Antennas and Wireless Propagation Letters
Publisher: IEEE
Date: 2017
Copyright © 2017, IEEE

LOGIN
If you're a copyright.com user, you can login to RightsLink using your copyright.com credentials.
Already a RightsLink user or want to learn more?

Thesis / Dissertation Reuse

The IEEE does not require individuals working on a thesis to obtain a formal reuse license, however, you may print out this statement to be used as a permission grant:

Requirements to be followed when using any portion (e.g., figure, graph, table, or textual material) of an IEEE copyrighted paper in a thesis:

1) In the case of textual material (e.g., using short quotes or referring to the work within these papers) users must give full credit to the original source (author, paper, publication) followed by the IEEE copyright line © 2011 IEEE.
2) In the case of illustrations or tabular material, we require that the copyright line © [Year of original publication] IEEE appear prominently with each reprinted figure and/or table.
3) If a substantial portion of the original paper is to be used, and if you are not the senior author, also obtain the senior author's approval.

Requirements to be followed when using an entire IEEE copyrighted paper in a thesis:

1) The following IEEE copyright/ credit notice should be placed prominently in the references: © [year of original publication] IEEE. Reprinted, with permission, from [author names, paper title, IEEE publication title, and month/year of publication]
2) Only the accepted version of an IEEE copyrighted paper can be used when posting the paper or your thesis on-line.
3) In placing the thesis on the author's university website, please display the following message in a prominent place on the website: In reference to IEEE copyrighted material which is used with permission in this thesis, the IEEE does not endorse any of [university/educational entity's name goes here]'s products or services. Internal or personal use of this material is permitted. If interested in reprinting/republishing IEEE copyrighted material for advertising or promotional purposes or for creating new collective works for resale or redistribution, please go to http://www.ieee.org/publications_standards/publications/rights/rights_link.html to learn how to obtain a License from RightsLink.

If applicable, University Microfilms and/or ProQuest Library, or the Archives of Canada may supply single copies of the dissertation.

BACK | CLOSE WINDOW

Copyright © 2018 Copyright Clearance Center, Inc. All Rights Reserved. Privacy statement. Terms and Conditions.
Comments? We would like to hear from you. E-mail us at customercare@copyright.com

www.manaraa.com

ABOUT THE AUTHOR

Ramiro A. Ramirez-Hernandez earned his B.S. in Electrical Engineering from "Universidad de Carabobo", Valencia, Venezuela, in 2009. From 2010 to 2013, he worked as a Project Engineer for a private consultant company in Venezuela.

In 2013 he joined the Wireless and Microwave Information Systems (WAMI) group at the University of South Florida, Tampa, FL, earning the M.S.E.E in 2015, his doctoral research is focused on additive manufacturing, RFID systems, and antenna system design for high clutter channels.

www.manaraa.com